

# **Silver nanoparticle effects on simple stream food webs and ecosystem processes: Periphyton-grazer system**

THÈSE No 6699 (2015)

PRÉSENTÉE LE 9 JUILLET 2015

À LA FACULTÉ DE L'ENVIRONNEMENT NATUREL, ARCHITECTURAL ET CONSTRUIT  
LABORATOIRE DE TOXICOLOGIE DE L'ENVIRONNEMENT  
PROGRAMME DOCTORAL EN GÉNIE CIVIL ET ENVIRONNEMENT

ÉCOLE POLYTECHNIQUE FÉDÉRALE DE LAUSANNE

POUR L'OBTENTION DU GRADE DE DOCTEUR ÈS SCIENCES

PAR

**Carmen Omayra GIL ALLUÉ**

acceptée sur proposition du jury :

Prof. U. von Gunten, président du jury  
Prof. K. Schirmer, Dr R. Behra, directrices de thèse  
Prof. V. Slaveykova, rapporteuse  
Prof. M. Bundschuh, rapporteur  
Prof. R. Bernier-Latmani, rapporteuse



ÉCOLE POLYTECHNIQUE  
FÉDÉRALE DE LAUSANNE

Suisse  
2015



## Summary

With the global nanotechnology market growing rapidly, nanomaterials are being increasingly released into aquatic environments, where they can undergo modifications and sedimentation, which will put benthic organisms at risk. Of particular interest is the study of nanomaterial effects on periphyton, a community of auto- and heterotrophic microorganisms embedded in an extracellular polymer matrix that covers submerged surfaces in aquatic ecosystems. Although periphyton assumes important functions in ecosystems, like primary production, little information is available on its sensitivity to nanomaterials and how these might be transferred to higher trophic levels in food webs.

In the present thesis, effects of short- and long-term exposures to citrate-coated silver nanoparticles (AgNP, 35 nm) and silver ions (Ag<sup>+</sup>, dosed as AgNO<sub>3</sub>) were assessed on periphyton in microcosm studies for periods between 2 hours and 21 days. After exposure, primary production, secondary production, photosynthetic yield, microbial respiration and potential extracellular enzyme activity were measured. Moreover, addition of an aquatic snail, *Physa acuta*, feeding on periphyton allowed the assessment of effects of AgNP on an aquatic herbivore and trophic transfer efficiency. Contaminated (AgNP and AgNO<sub>3</sub>) and uncontaminated periphyton was offered to snails in a 5-day experiment to determine silver uptake and the mortality, feeding rate and reproduction of the snails.

Our findings show that all endpoints measured in periphyton were affected by both AgNP and AgNO<sub>3</sub> during short-term exposure, but AgNO<sub>3</sub> was more toxic on a total silver mass basis than AgNP. Concentrations causing a 50% reduction in the different endpoints (EC<sub>50</sub>) ranged from 17 to 83 µM AgNP and from 2 to 4 µM AgNO<sub>3</sub>. Exposure of periphyton in the presence of silver ion ligands to complex Ag<sup>+</sup> (ca. 1% of total silver in AgNP suspensions) prevented AgNP toxicity to most endpoints, confirming that the observed toxic effects were caused by the bioavailable Ag<sup>+</sup>. An exception was the extracellular enzyme leucine aminopeptidase, which was directly affected by AgNP.

Concentrations of AgNP and AgNO<sub>3</sub> that caused low toxicity during short-term exposure also caused effects on periphyton functions upon long-term exposure, with algae and bacteria being differently affected. Periphyton exposed to 10 µM AgNP for 21 days showed a 63% decrease in primary production and a 246% increase in bacterial secondary production per unit of total periphyton biomass. The community composition exposed to AgNP or AgNO<sub>3</sub> differed from that of the control and also from each other. Furthermore, AgNP-exposed communities were more tolerant to subsequent AgNP exposure.

Trophic transfer of silver from contaminated periphyton to snails occurred efficiently, independently of the silver form. Feeding rate of snails on AgNO<sub>3</sub>-exposed communities was 50% lower than on controls, and disturbance of digestion was evident upon feeding on both AgNP- and AgNO<sub>3</sub>-exposed communities. No changes in the mortality or egg production of the snails were observed. However, the hatching success of eggs from snails that fed on

contaminated periphyton was reduced by more than 79%, and 28-day old embryos showed malformations.

Overall, this study clearly identified damaging effects of AgNP on periphyton, with consequent indirect impacts on a consumer, trophic relationships and stream ecosystem processes.

**Keywords**

Silver nanoparticles, aquatic community, microcosm, primary production, trophic transfer, periphyton, gastropod.

## Résumé

Avec le développement des nanotechnologies, le risque de contamination des milieux aquatiques par les nanoparticules est de plus en plus important, perturbant ainsi les communautés benthiques dans ces écosystèmes. Parmi ces communautés, le périphyton est un ensemble de microorganismes auto- et hétérotrophes, inclus dans une matrice d'exopolymères et fixés sur un support solide immergés dans l'eau. En dépit du fait que le périphyton joue un rôle essentiel dans les cours d'eau, peu d'informations sont disponibles sur sa sensibilité aux nanoparticules ainsi que sur les effets sur la chaîne trophique.

Dans cette thèse, les effets des expositions à court- et long-terme aux nanoparticules d'argent (AgNP, 35nm) et à l'argent ionique ( $\text{Ag}^+$ , ajouté sous forme d' $\text{AgNO}_3$ ) sur le périphyton ont été déterminés dans des microcosmes entre deux heures et 21 jours. La production primaire et secondaire, l'efficacité photosynthétique, la respiration microbienne ainsi que des activités enzymatiques extracellulaires ont été mesurées. En outre, nous avons étudié les effets des AgNP sur les organismes brouteurs aquatiques ainsi que sur les transferts trophiques en incluant un escargot d'eau douce, *Physa acuta*. Pour cela, les escargots se sont nourris pendant 5 jours sur du périphyton contaminé par AgNP ou  $\text{AgNO}_3$ . Ensuite, l'assimilation de l'argent par les escargots ainsi que leurs mortalité, comportement alimentaire et reproduction ont été déterminés.

Nos résultats ont montré que toutes les fonctions, mesurées après l'exposition à court-terme du périphyton aux AgNP et  $\text{AgNO}_3$ , ont été affectées, avec une toxicité plus élevée d' $\text{AgNO}_3$ . Les concentrations d'argent induisant 50% de réduction des différents paramètres variaient entre 17 et 83  $\mu\text{M}$  d'AgNP et entre 2 et 4  $\mu\text{M}$  d' $\text{AgNO}_3$ . L'addition d'un ligand chélateur des ions d'argent libres a indiqué qu'à l'exception de la leucine aminopeptidase, la toxicité des AgNP a été causée par l' $\text{Ag}^+$  dissous à partir des nanoparticules.

L'exposition à long-terme du périphyton à de faibles concentrations d'AgNP et  $\text{AgNO}_3$  a perturbé les fonctions bactériennes et algales différemment. Par exemple, dans le périphyton exposé pendant 21 jours à 10  $\mu\text{M}$  d'AgNP, la production primaire a été réduite de 63% alors que la production secondaire a augmenté de 246%. En outre, la diversité des communautés microbienne des périphyton exposés aux AgNP et  $\text{AgNO}_3$  ont été différentes de celles du contrôle mais aussi entre elles. Enfin, les communautés exposées aux AgNP sont devenues plus tolérantes à ce polluant en comparaison au contrôle.

Le transfert d'argent à partir du périphyton contaminé aux escargots a été observé quelque soit la forme de l'argent testé. Le taux de consommation par *P. acuta* de périphyton contaminé avec  $\text{AgNO}_3$  a été réduit de 50% en comparaison au contrôle. De plus, une perturbation du système digestif a été observée après la consommation du périphyton contaminé par AgNP ou  $\text{AgNO}_3$ . Par ailleurs, aucun effet n'a été observé sur la mortalité des escargots ou leur production d'œuf. Cependant, le taux d'éclosion des œufs produits par les escargots qui se sont nourris avec du périphyton contaminé a été réduit de 79% et les embryons ont montré des malformations.

D'une manière générale, ce travail a clairement démontré des effets négatifs des AgNP sur le périphyton avec des conséquences sur un organisme brouteur du périphyton ainsi que sur les relations trophiques et les processus écologiques dans les cours d'eau.

**Mots clés**

Nanoparticules d'argent, communauté aquatique, microcosmes, production primaire, transfert trophique, périphyton, gastéropode.

# Contents

<b>Summary .....</b>	<b>I</b>
<b>Résumé.....</b>	<b>III</b>
 <b>Chapter 1. General introduction .....</b>	 <b>1</b>
1.1 Introduction.....	1
1.2. Fate of silver nanoparticles in the aquatic ecosystem and bioavailability .....	1
1.3 Toxicity of silver nanoparticles to algae and bacteria.....	3
1.4 Toxicity of silver nanoparticles to microbial communities.....	5
1.5 Toxicity to invertebrates .....	6
1.6 Trophic transfer of nanomaterials .....	7
1.7 Scope of the thesis.....	7
 <b>Chapter 2. Effects of silver nanoparticles on the functions of stream periphyton after short-term exposures.....</b>	 <b>9</b>
2.1 Introduction.....	9
2.2 Materials and Methods .....	10
Materials.....	10
Characterization of nanoparticles.....	11
Periphyton colonization.....	12
Exposure experiments .....	12
Response variables.....	12
2.3 Results .....	14
Nanoparticle characterization.....	14
Short-term effects of AgNP and AgNO <sub>3</sub> .....	15
2.4 Discussion.....	16
Environmental implications .....	18
2.5 Figures and tables.....	19
 <b>Chapter 3. Silver nanoparticle uptake and effects on the function and community structure of stream periphyton during long-term exposures .....</b>	 <b>23</b>
3.1 Introduction.....	23
3.2 Materials and methods.....	24
Characterization of silver exposure.....	24
Periphyton colonization and silver exposure .....	25
Effects of AgNP and AgNO <sub>3</sub> on periphyton during long-term exposure (Experiment 1) .....	26
Assessment of pollution-induced community tolerance of periphyton communities after long-term exposure to AgNP and AgNO <sub>3</sub> (Experiment 2) .....	26

Silver distribution in medium and periphyton.....	26
Biological functions of periphyton .....	27
Periphyton community analysis .....	29
Data analysis.....	30
3.3 Results.....	31
Silver nanoparticle characterization.....	31
Silver distribution in periphyton .....	31
Effects of AgNP and AgNO <sub>3</sub> on biological functions of periphyton .....	32
Effects on the periphyton community structure.....	33
Assessment of pollution induced community tolerance to AgNP, AgNO <sub>3</sub> and CuSO <sub>4</sub> ...	34
3.4 Discussion .....	34
Environmental implications .....	37
3.5 Figures and tables .....	38
<b>Chapter 4. Trophic transfer of silver nanoparticles from stream periphyton to the aquatic snail <i>Physa acuta</i> .....</b>	<b>43</b>
4.1 Introduction.....	43
4.2 Materials and methods.....	44
Silver nanoparticles.....	44
Snail culture .....	45
Periphyton colonization and silver loading.....	45
Feeding experiments with <i>Physa acuta</i> .....	45
Trophic transfer of silver.....	45
Biological parameters .....	46
4.3 Results.....	47
Trophic transfer of silver to <i>Physa acuta</i> .....	47
Effects of diet exposure to silver on survival, feeding behavior and reproduction of <i>Physa acuta</i> .....	48
4.4 Discussion .....	49
Environmental implications .....	51
4.5 Figures and tables .....	52
<b>Chapter 5. Outlook .....</b>	<b>55</b>
5.1 Interaction of silver nanoparticles with extracellular enzymes of periphyton.....	55
5.2 Pollution-induced community tolerance in periphyton upon exposure to silver nanoparticles.....	56
5.3 Early life stage and multigeneration toxicity studies with silver nanoparticles and <i>Physa acuta</i> .....	57



<b>Appendix A. Supporting information of Chapter 2.....</b>	<b>59</b>
<b>Appendix B. Supporting information of Chapter 3 .....</b>	<b>67</b>
<b>Appendix C. Supporting information of Chapter 4 .....</b>	<b>81</b>
 <b>References .....</b>	 <b>83</b>
<b>Acknowledgements.....</b>	<b>95</b>
<b>Curriculum Vitae .....</b>	<b>99</b>



## List of figures

<b>Figure 2.1.</b> Comparison of $\zeta$ -potential and particle diameters measured by DLS in 12.5 and 100 $\mu\text{M}$ AgNP suspensions of fresh and conditioned exposure medium for 2 and 20 hours in the absence or presence of the $\text{Ag}^+$ ligand DMPS .....	19
<b>Figure 2.2.</b> Proportion of dissolved Ag(I) in AgNP suspensions as determined by ultracentrifugation and ICP-MS .....	19
<b>Figure 2.3.</b> Effects of AgNP and $\text{AgNO}_3$ on photosynthesis, respiration, and the activity of extracellular enzymes $\beta$ -glucosidase and leucine aminopeptidase .....	20
<b>Figure 2.4.</b> Effects of 10 $\mu\text{M}$ $\text{AgNO}_3$ and 100 $\mu\text{M}$ AgNP on photosynthesis, respiration, and the activity of extracellular enzymes $\beta$ -glucosidase and leucine aminopeptidase, with and without the addition of 25 $\mu\text{M}$ DMPS .....	21
<b>Figure 3.1.</b> Comparison of $\zeta$ -potential and particle diameters measured by DLS in 1 and 10 $\mu\text{M}$ AgNP suspensions of fresh and conditioned exposure medium for 0, 24 and 72 hours .....	38
<b>Figure 3.2.</b> Effects of AgNP and $\text{AgNO}_3$ to periphyton after 21 days of exposure on ash-free dry mass, photosynthetic yield, respiration, primary production, secondary production, and the activity of extracellular enzymes $\beta$ -glucosidase, alkaline phosphatase and leucine aminopeptidase .....	39
<b>Figure 3.3.</b> Community-level physiological profile as determined by substrate-induced respiration, after 21 days of exposure to 0.1, 1 and 10 $\mu\text{M}$ AgNP, or 0.1 $\mu\text{M}$ $\text{AgNO}_3$ .....	40
<b>Figure 3.4.</b> Principal component analysis of the content of marker pigments in periphyton of experiment 2, after 21 days of exposure to 10 $\mu\text{M}$ AgNP and 0.1 $\mu\text{M}$ $\text{AgNO}_3$ .....	41
<b>Figure 3.5.</b> Principal component analysis of the community structure of periphyton, as determined by denaturing gradient gel electrophoresis with conserved 18S and 16S rDNA fragments, after 21 days of exposure to 10 $\mu\text{M}$ AgNP and 0.1 $\mu\text{M}$ $\text{AgNO}_3$ in experiment 2 .....	41
<b>Figure 4.1.</b> Feeding and defecation rates of snails upon feeding on AgNP- and $\text{AgNO}_3$ -preexposed periphyton .....	52
<b>Figure 4.2.</b> Development of snail embryos after 28 days of incubation in fresh PERIQUIL after the end of the experiment .....	53
<b>Figure A.1.</b> Ratios of fluorescence at 470, 520 and 645 nm to fluorescence at 665 nm of control periphyton suspensions for each of the six independently colonized communities used in toxicity tests .....	60
<b>Figure A.2.</b> Particle diameter distributions as measured by DLS of 12.5 and 100 $\mu\text{M}$ AgNP suspensions in fresh and conditioned medium after 2 and 20 hours of exposure, and in the presence or absence of the $\text{Ag}^+$ ion ligand DMPS .....	62

<b>Figure A.3.</b> UV-Vis spectra of AgNP suspensions in fresh and conditioned medium after 2 and 20 hours of exposure and in the presence or absence of the Ag <sup>+</sup> ion ligand DMPS .....	63
<b>Figure A.4.</b> Silver recovery with the ultracentrifugation and ultrafiltration method in fresh and conditioned medium in the absence and presence of DMPS .....	63
<b>Figure A.5.</b> Activities of $\beta$ -glucosidase (GLU), alkaline phosphatase and leucine aminopeptidase in whole periphyton suspensions and filtrates containing the periphyton EPS matrix, and effects of AgNP and AgNO <sub>3</sub> on GLU activity present in the periphyton EPS matrix .....	64
<b>Figure B.1.</b> Diagram of the timeline of measurements and medium exchanges in experiments 1 and 2 .....	69
<b>Figure B.2.</b> Diagram of the periphyton fractionation procedure for the quantification of silver distribution .....	70
<b>Figure B.3.</b> Complementary characterization of silver nanoparticles .....	71
<b>Figure B.4.</b> Effects of 0.1, 1 and 10 $\mu$ M AgNP and 0.1 $\mu$ M AgNO <sub>3</sub> after 7 days of exposure in experiment 1 on the ash-free dry mass, photosynthetic yield, respiration, and extracellular enzymatic activity of $\beta$ -glucosidase, alkaline phosphatase and leucine aminopeptidase .....	73
<b>Figure B.5.</b> Community-level physiological profile as determined by substrate-induced respiration (SIR), after 7 days of exposure to 0.1, 1 and 10 $\mu$ M AgNP, or 0.1 $\mu$ M AgNO <sub>3</sub> .....	74
<b>Figure B.6.</b> Comparison of the response of biological functions to 21-day exposures to 10 $\mu$ M AgNP and 0.1 $\mu$ M AgNO <sub>3</sub> between experiments 1 and 2, for photosynthetic yield, respiration, primary production and secondary production .....	75
<b>Figure B7.</b> Chlorophyll a content in periphyton across the treatments in experiments 1 and 2 .....	76
<b>Figure B.8.</b> Principal component analysis of the content of marker pigments in periphyton of experiment 2, after 21 days of exposure to 10 $\mu$ M AgNP and 0.1 $\mu$ M AgNO <sub>3</sub> .....	78
<b>Figure B.9.</b> Principal component analysis of the community structure of periphyton, as determined by denaturing gradient gel electrophoresis with conserved 18S and 16S rDNA fragments, after 21 days of exposure to 10 $\mu$ M AgNP and 0.1 $\mu$ M AgNO <sub>3</sub> in experiment 1 .....	78
<b>Figure B.10.</b> Concentration-response curves obtained from short-term bioassays to assess the pollution-induced community tolerance of periphyton pre-exposed during 21 days to 10 $\mu$ M AgNP and 0.1 $\mu$ M AgNO <sub>3</sub> , compared to non-preexposed control periphyton .....	79
<b>Figure C.1.</b> Biomass of periphyton as the total ash-free dry mass in the microcosm at day 0 and day 5, in absence and presence of snails .....	81

## List of tables

<b>Table 2.1.</b> EC <sub>50</sub> values for photosynthesis, respiration and extracellular enzymatic activities of periphyton calculated from individual experiments with independently colonized communities .....	20
<b>Table 3.1.</b> Distribution of total silver in different fractions of periphyton and in exposure medium after 21 days of exposure in both experiments .....	38
<b>Table 3.2.</b> EC <sub>50</sub> values from photosynthesis, respiration, and primary and secondary production from 2-hour bioassays data in experiment 2 for the assessment of pollution-induced community tolerance .....	42
<b>Table 4.1.</b> Total silver concentrations in periphyton, snails and feces as determined by ICP-MS .....	52
<b>Table 4.2.</b> Reproduction output and hatching success of snails upon feeding on AgNP- and AgNO <sub>3</sub> -preexposed periphyton .....	52
<b>Table A.1.</b> Composition of exposure medium .....	59
<b>Table A.2.</b> Total activities of $\beta$ -glucosidase, alkaline phosphatase and leucine aminopeptidase of control periphyton suspensions for each of three independent experiments .....	60
<b>Table A.3.</b> Particle diameter characterization by nanoparticle tracking analysis and dynamic light scattering .....	61
<b>Table A.4.</b> Speciation of silver at the range of AgNO <sub>3</sub> concentrations tested in exposure medium .....	63
<b>Table A.5.</b> EC <sub>50</sub> values of AgNP and AgNO <sub>3</sub> for photosynthesis, respiration, and activity of $\beta$ -glucosidase based on total silver in AgNP suspensions, AgNP, or as a function of dissolved Ag <sup>+</sup> .....	65
<b>Table B.1.</b> Composition of the exposure medium PERIQUIL .....	67
<b>Table B.2.</b> Water chemistry of exposure medium samples from all microcosms, sampled weekly after medium exchanges during the 21-day exposure in experiment 2 .....	68
<b>Table B.3.</b> Speciation of silver in the range of AgNO <sub>3</sub> concentrations tested in exposure medium .....	72
<b>Table B.4.</b> Measurements of biomass accrual and biological function responses in control periphyton over the duration of long-term exposures in experiment 1 .....	72
<b>Table B.5.</b> Relative content of quantified pigments in periphyton across the treatments in experiments 1 and 2 .....	77
<b>Table C.1.</b> Estimation of the range of silver assimilation efficiency (AE) in snails over the five-day feeding experiment by two methods .....	81
<b>Table C.2.</b> Total silver concentrations in exposure medium, and exopolysaccharide matrix (EPS) of periphyton, as determined by ICP-MS .....	82



# Chapter 1. General introduction

## 1.1 Introduction

Silver is one of the most toxic metals in its ionic form (Ratte 1999) and has been mined since ancient times for its use as antimicrobial agent (Franke 2007), but also for ornamental and industrial applications. In the last decade, silver nanoparticles (AgNP) have been manufactured in large quantities by industry due to their enhanced properties compared to the corresponding bulk material (Kirchner et al. 2005, Wijnhoven et al. 2009), which emerge from their size in the nanoscale and the large specific surface area (Auffan et al. 2009). Nanoparticles are by definition particles with at least two dimensions in the range of 1 to 100 nm (ISO 2008). AgNP are mostly synthesized by the controlled reduction of a silver salt, and the addition of a coating to improve colloidal stability (Tan & Cheong 2013).

Along with increasing efforts in research and technological innovation, the release of nanomaterials into the environment is expected (Gottschalk et al. 2009). There is evidence that microbial and benthic organisms are put at risk when AgNP enter the aquatic environment, due to sedimentation of particles (Cleveland et al. 2012, Lowry et al. 2012) and the high toxicity of silver ions ( $\text{Ag}^+$ ), especially to microorganisms, which can dissolve from AgNP (Ratte 1999). AgNP have shown to be toxic to single species of microorganisms and invertebrates (Baun et al. 2008, Navarro et al. 2008a), and a limited number of studies have focused on microbial communities and benthic invertebrates (Bernot & Brandenburg 2013, Colman et al. 2012, Das et al. 2012, Pradhan et al. 2011).

Periphyton, as a benthic microorganism assemblage consisting mainly of algal and bacterial communities forming biofilms, is therefore susceptible to be affected by AgNP. These harmful effects would ultimately result in the disturbance of key ecosystem processes for which periphyton is responsible in the aquatic environment, like primary production (Minshall 1978, Wetzel 1963). Primary production is the production of biomass from inorganic sources, mainly through photosynthesis, and represents the point of entry of energy in ecosystems. Furthermore, periphyton is known to efficiently accumulate metals (Bradac et al. 2009b, Ramelow et al. 1987). Silver that accumulates in periphyton could be transferred to organisms feeding on it, causing a propagation of effects (Croteau et al. 2011b). Macroinvertebrates feeding on periphyton, like aquatic snails, also represent an important link in the trophic chain, between the primary producers and higher organisms like fish. Therefore, the investigation of the effects of AgNP to periphyton and the trophic transfer to higher levels is of great importance in the assessment of the impacts of AgNP in the aquatic environment.

## 1.2. Fate of silver nanoparticles in the aquatic ecosystem and bioavailability

AgNP contained in consumer products are likely to be released and reach the aquatic environment (Benn & Westerhoff 2008, Farkas et al. 2011, Kaegi et al. 2010). However, the detection and quantification of AgNP in the environment (and nanomaterials in general) is currently limited by the performance of analytical methods in complex matrices (Gallego-Urrea

et al. 2011, Schaumann et al. 2015). Meanwhile, environmental concentrations can be estimated with models. Recently, AgNP concentrations in surface waters were estimated to fall in the picogram to nanogram range and in the microgram per kg and year range in sediments (Sun et al. 2014). Measured environmental concentrations of dissolved silver are also typically found in the picomolar range, but can reach nanomolar concentrations in mining areas (Lanceleur et al. 2011, Tappin et al. 2010).

When they reach the aquatic environment, AgNP can undergo transformations that will influence their fate and bioavailability to aquatic organisms. The most important processes are agglomeration and aggregation, redox reactions and changes in silver speciation (Behra et al. 2013, Fabrega et al. 2011a, Levard et al. 2012, Luoma et al. 2014). Colloidal stability of AgNP in the aquatic environment will depend both on the particle characteristics and the environmental conditions. Particle characteristics such as size and surface properties are determined during manufacture. AgNP are often synthesized by the controlled reduction of silver ions ( $\text{Ag}^+$ ) to metallic silver ( $\text{Ag}^0$ ). Coatings are added to the surface of AgNP to maintain the colloidal stability, and consist of molecules that confer particles electrostatic (*i.e.*, positive or negative charge) or steric stability (Tan & Cheong 2013).

The main environmental factors affecting stability of AgNP in the aquatic environment are pH, ionic strength, and dissolved organic carbon (DOC) (Bae et al. 2010, Cumberland & Lead 2009, Dasari & Hwang 2010, El Badawy et al. 2011, Piccapietra et al. 2012b). A higher pH can cause a neutralization of the particle surface of negatively charged particles, which eliminates the electrostatic forces that maintain colloidal stability (Sigg et al. 2014). Moderate ionic strength in natural waters is known to cause colloids to agglomerate (Chinnapongse et al. 2011, Piccapietra et al. 2012b). The concentration of divalent cations in surface waters, and of  $\text{Ca}^{2+}$  in particular, has been observed to play an important role in AgNP agglomeration (Piccapietra et al. 2012b, Topuz et al. 2014). AgNP can remain stable in fresh waters with low values of ionic strength, but might agglomerate in more nutrient-rich waters and estuaries. AgNP agglomerates are susceptible to deposit in the sediments, where they can be available to benthic organisms and filter-feeders, which can take up aggregates more efficiently than small AgNP (Lowry et al. 2012, Ward & Kach 2009). Differently, organic matter can form aggregates with AgNP, which, depending on the density, will stabilize particles in the water column, but can also cause deposition or sorption to sediments and biofilms (Topuz et al. 2014). Furthermore, the exopolysaccharides present in the outer surface of microbial cells and in the biofilm matrices (EPS) can limit the mobility of AgNP by causing particle aggregation, and of dissolved  $\text{Ag}^+$  by complexation and reduction (Choi et al. 2010, Dimkpa et al. 2011, Kroll et al. 2014, Miao et al. 2009, Peulen & Wilkinson 2011).

Dissolution of AgNP can occur when  $\text{Ag}^0$  is oxidized to  $\text{Ag}^+$  on the surface of AgNP. Oxidation has been observed to increase in environmental conditions of low pH and presence of strong ligands (El Badawy et al. 2010, Gondikas et al. 2012, Liu & Hurt 2010, Odzak et al. 2014). However, particle characteristics, such as size and coating, can also influence the magnitude of dissolution (Dobias & Bernier-Latmani 2013, Odzak et al. 2014). Dissolved  $\text{Ag}^+$  are expected to interact with sulfur and chloride, forming soluble silver chloride species (*i.e.*,  $\text{AgCl}_2^-$  and



AgCl<sup>0</sup>(aq)) and solid silver sulfide (i.e., Ag<sub>2</sub>S(s)) (Behra et al. 2013, Bell & Kramer 1999). Recently, it was also reported that AgNP can rapidly undergo sulfidation to Ag<sub>2</sub>S(s) in the presence of metal sulfides in surface waters (Thalmann et al. 2014), as well as in wastewater (Kaegi et al. 2011). These changes in silver speciation might reduce the bioavailability of dissolved Ag(I) due to poor water solubility of silver sulfide (Levard et al. 2013) and limited uptake of silver chloride species by some organisms (Lee et al. 2004). Furthermore, reduction of Ag<sup>+</sup> to nanosized Ag<sup>0</sup> is also expected to occur in the presence of fulvic acids and sunlight (Adegboyega et al. 2013).

### 1.3 Toxicity of silver nanoparticles to algae and bacteria

Since one of the main applications of AgNP is as an antimicrobial agent, microbes like algae and bacteria, which are the main constituents of the periphyton community, are expected to be targets for AgNP toxicity in the environment. Most studies on the effects of AgNP on microorganisms are focused on pathogenic bacteria due to their medical relevance, and only a small fraction has been carried out with microorganisms with environmental relevance. Half maximal effective concentrations (EC<sub>50</sub>) for algal photosynthesis and growth and bacterial viability typically fall in the range of 0.1 to 1 mg/L, except for resistant bacterial strains (Choi & Hu 2008, Griffitt et al. 2008, Ivask et al. 2013, Navarro et al. 2008b, Samberg et al. 2011).

Toxicity of AgNP and other metallic nanomaterials can be caused directly by nanoparticles, or indirectly by dissolved metal ions. Direct toxicity is caused by the intrinsic properties of AgNP, and it has been evaluated in some studies by investigating the influence of relevant particle characteristics, *e.g.*, size, shape and surface charge. Size may be the most critical characteristic of AgNP, since it confers particles with enhanced reactivity due to the large surface exposed in relation to the volume of the particle. Indeed, toxicity has been observed to correlate with size of AgNP. Smaller sized AgNP (i.e., smaller than 5 or 10 nm) showed higher toxicity to algae and bacteria, and it has been reported that size can influence the dissolution rate (Dobias & Bernier-Latmani 2013, Ivask et al. 2014) or the attachment efficiency to the cell surface (Choi & Hu 2008, Morones et al. 2005, Sotiriou & Pratsinis 2010). Geometry of AgNP can also play a role, and Pal et al. (2007) reported significant differences in the cytotoxic potential of spherical AgNP, nanorods and truncated triangular nanoplates on *E. coli*. In these two cases, differences in toxicity are probably caused by different Ag<sup>+</sup> dissolution rates among particles with different shapes. As a last example, surface charge (i.e., zeta potential) can determine the particle stability and the affinity to other molecules, such as the ones composing the outer surface of organisms. El Badawy et al. (2011) found positively charged AgNP to be more toxic than negatively charged ones, probably due to the negatively charged bacterial surfaces acting as an “electrostatic barrier”.

Although there is not a demonstrated mechanism of toxicity of AgNP (Fabrega et al. 2011a), one important effect in microorganisms is their ability to disturb biological membranes, as supported by the evidence from studies with *E. coli* (Pal et al. 2007, Samberg et al. 2011, Sondi & Salopek-Sondi 2004) and *Staphylococcus aureus* (Mirzajani et al. 2011, Potara et al. 2011, Samberg

et al. 2011). Membrane disruption alters the ability to regulate the intracellular chemistry and, therefore, the normal functioning of the cell. Similarly, AgNP can interact with proteins such as enzymes, which can result in the loss of their function (Wigginton et al. 2010).

The cell wall of microorganisms is expected to be a barrier to the internalization of AgNP, due to small pore sizes and complexation potential to its surface (Macfie et al. 1994, Prasad et al. 1998). AgNP have been reported to be internalized in *E. coli* (Morones et al. 2005, Pal et al. 2007, Sondi & Salopek-Sondi 2004) and *Pseudomonas putida* cells (Fabrega et al. 2009). However, it is possible that internalization occurred only after disruption of the cell membranes in these studies. Once they are present in the intracellular medium, AgNP can release  $\text{Ag}^+$ , which can interact with proteins, interfering with the normal functioning of the cell (Choi & Hu 2008, Dimkpa et al. 2011, Holt & Bard 2005, Xiu et al. 2011). Algae have been reported to be able to secrete binding polypeptides that act as a detoxification mechanism against internalized metal ions (Le Faucheur et al. 2005, Scheidegger et al. 2012), but so far this mechanism has not been studied regarding AgNP.

Apart from effects directly caused by the nanoparticle, indirect effects through the dissolved ions can also occur. Dissolution of  $\text{Ag}^+$  from AgNP at the organism interface, and rapid uptake of  $\text{Ag}^+$  through Cu(I) transporters, results in a more efficient  $\text{Ag}^+$  delivery to the cell than uptake of  $\text{Ag}^+$  from the aqueous medium (Fabrega et al. 2009, Leclerc & Wilkinson 2013, Pal et al. 2007, Solioz & Odermatt 1995). Binding sites on the cell wall surface do not seem to reduce the  $\text{Ag}^+$  toxicity significantly, as reported by Piccapietra et al. (2012a), who found that the uptake rate of  $\text{Ag}^+$  is reduced initially due to the presence of cell wall but no significant long-term effects on uptake are expected. A study with metal oxide nanoparticles showed an association of these particles with the cell wall of the alga *Thalassiosira weissflogii*, while metal ions were found in the intracellular compartment in association with organelles (Bielmyer-Fraser et al. 2014).

In some studies, the toxic effects reported on microorganisms can be explained by the release of  $\text{Ag}^+$  from AgNP, ruling out a nanosize-inherent effect (Xiu et al. 2012). AgNP showed no toxic effects to *E. coli* in an experiment under anoxic conditions that prevented  $\text{Ag}^+$  dissolution, and in the presence of silver ligands that reduce the bioavailability of  $\text{Ag}^+$  (Xiu et al. 2011). Similarly, Navarro et al. (2008b) showed that photosynthetic activity of the alga *Chlamydomonas reinhardtii* was decreased after exposure to AgNP, but complexation of  $\text{Ag}^+$  with a silver ligand eliminated the toxic effects. AgNP dissolution is proposed to have occurred before the uptake, releasing  $\text{Ag}^+$  that are rapidly taken up by the algae. Miao et al. (2009) had similar observations in their studies with *T. weissflogii*, and also suggest that exopolymeric substances can affect the dissolution and dispersion of AgNP. In this study, the toxicity of the AgNP suspension was abolished after the addition of glutathione as a silver ligand. However, in a later study with lower glutathione to total silver ratios (Miao et al. 2010) toxicity was still present, suggesting that enhanced dissolution occurs at the particle-algal interface, probably facilitated by metabolic products like  $\text{H}_2\text{O}_2$  (He et al. 2012, Leclerc & Wilkinson 2013).

## 1.4 Toxicity of silver nanoparticles to microbial communities

In general, the knowledge on the toxicity of AgNP to aquatic organisms is still very scarce and mainly focused on the direct toxicity of the chemical to individual species (Fabrega et al. 2011a). However, by assessing effects on communities, important knowledge on indirect effects that arise from the interactions among species can be gathered (Clements & Rohr 2009). In microbial communities, species can interact with each other through, e.g., competition or mutualistic relationships (Neely & Wetzel 1995, Scott et al. 2008). These interactions can be disturbed due to differences in species sensitivities, when particular species in the community are affected or eliminated by a chemical. The consequences of structural changes can be positive or negative for other components of the community, depending on their relationship, e.g., reduction of competition or disturbance of mutualism. The removal of sensitive species from a community can lead to an increased tolerance of the community to the stressor. This concept has been described in ecotoxicology as pollution-induced community tolerance (PICT) (Blanck et al. 1988). The associated loss of diversity can imply an increased vulnerability to other stressors. While functions of the community can persist even if some species are removed due to functional redundancy, a loss of functions might occur (Hooper et al. 2005). Therefore, by assessing the community as a whole, information on relevant ecosystems processes driven by microbial communities, i.e. primary production, nutrient cycling, can be investigated.

Studies on the effects of AgNP on microbial communities are still limited in number. AgNP inhibited the growth, respiration and enzymatic activity of bacterioplankton (Colman et al. 2012, Das et al. 2012). In sediments, AgNP have been shown to cause the inhibition of substrate degradation capacity of bacterial communities (Echavarri-Bravo et al. 2015). Pradhan et al. (2011) observed a decrease in biomass and biodiversity in the bacterial and fungal communities of a leaf litter decomposing community after long-term exposure to AgNP. A first study on periphyton revealed that AgNP inhibited the growth of the biofilm and caused changes in the algal community (González et al. 2014).

In the present thesis, the effects of AgNP on periphyton are investigated. In the last decades, periphyton has been the subject of ecotoxicological studies dealing with a variety of chemicals because of its ecological relevance. Still, very little is known about silver toxicity to periphyton. Soldo and Behra (2000) reported a strong inhibition of photosynthetic activity of periphyton by Ag<sup>+</sup>. Other field and microcosm studies have as well shown the sensitivity of periphyton to other metals (Tlili et al. 2010). Accumulation of metals has been reported to occur very fast in periphytic organisms, and closely reflect changes in environmental concentrations (Bradac et al. 2009b, Meylan et al. 2003). Barranget et al. (2003) observed changes in the substrate degradation capacity after exposure to copper and Fechner et al. (2010) reported inhibition of the extracellular enzymatic activity ( $\beta$ -glucosidase), both of which can have effects on the nutrient cycling in the ecosystem. Guasch et al. (2002) reported a more significant change in the periphytic community structure than in its function after chronic exposure to copper. Several studies have evidenced structural changes in the periphyton community upon chronic exposure

that correlated with the tolerance to the stressor (Blanck 2002, Navarro et al. 2008c, Soldo & Behra 2000).

### 1.5 Toxicity to invertebrates

Most studies on the effects of AgNP on invertebrates are based on the model organism *Daphnia magna*, due to its ecotoxicological and ecological relevance. *D. magna* is a filter feeder, a group of organisms that can be particularly put at risk due to their feeding habits (Griffitt et al. 2008). Filter feeders have been reported to ingest AgNP more efficiently than dissolved Ag(I) (Zhao & Wang 2010), particularly when the particle size was 50 nm or less (Zhao & Wang 2012). Median lethal concentrations (LC<sub>50</sub>) after short-term exposures to AgNP range from 4 to 30 µg L<sup>-1</sup> (Griffitt et al. 2008, Hoheisel et al. 2012, Ivask et al. 2013). In some studies, the toxic effects correlated with the dissolution of Ag<sup>+</sup> from AgNP, suggesting no specific particle effects (Newton et al. 2013, Seitz et al. 2015). However, proteomic analysis of *D. magna* suggest that toxicity mechanisms for AgNP and Ag<sup>+</sup> are different (Rainville et al. 2014). Long-term exposures to AgNP have been reported to cause lower growth and reproduction (Römer et al. 2011, Zhao & Wang 2011). Although there are no studies on multigenerational effects with AgNP, exposure of *D. magna* to TiO<sub>2</sub> nanoparticles in the long term has been reported to cause an increased sensitivity over several generations (Bundschuh et al. 2012, Jacobasch et al. 2014).

Other studies on the toxicity of AgNP to filter-feeders show that the bivalves *Mytilus edulis* and *Crassostrea virginica* efficiently take up polystyrene NP agglomerates larger than 100 nm, which showed a higher retention time in gut than particles of micrometer size (Ward & Kach 2009). This finding shows a particle selectivity based on size by filter-feeders. Once ingested, AgNP agglomerates are transported to the digestive gland, where they have been reported to cause cytotoxicity in *Mytilus* spp. (Canesi et al. 2012) and DNA damage in *Elliptio complanata* (Gagné et al. 2013). Furthermore, AgNP adversely affected the embryonic development of *C. virginica*, and a metallothionein induction was measured in the embryos (Ringwood et al. 2010).

In the case of sediment-dwelling organisms, individuals of the nematode *Caenorhabditis elegans* feeding on AgNP-contaminated sediment showed a reduction on length growth and maternal transfer to eggs (Meyer et al. 2010). A sediment-associated polychaete, *Nereis diversicolor*, accumulated AgNP and Ag<sup>+</sup> from contaminated sediment similarly, but more DNA damage was observed in the AgNP treatment (Cong et al. 2014). In another study, AgNP were observed to be internalized in gut epithelium of the polychaete (García-Alonso et al. 2011).

In the case of periphyton-grazing organisms, no evidence of particle size selectivity has been found (Oliver et al. 2014). The aquatic snail *Lymnaea stagnalis* efficiently accumulated silver upon AgNP and Ag<sup>+</sup> exposures (Croteau et al. 2011b). LC<sub>50</sub> values of short-term exposures to AgNP were 48.10 and 2.18 µg L<sup>-1</sup> for the aquatic snails *Lymnaea luteola* and *Physa acuta*, respectively. AgNP have been observed to cause a disturbance of digestion and increased oxidative stress levels and DNA damage in digestive gland cells of *Lymnaea* spp. (Ali et al. 2014, Croteau et al. 2011b). Interestingly, AgNP has been reported to cause a behavioral response in snails similar to predator cues (Bernot & Brandenburg 2013, Justice & Bernot 2014).

Furthermore, the reproductive output of *Physa acuta* was reduced by exposures to AgNP over 28 days to concentrations ranging from 0.01 to 1  $\mu\text{g L}^{-1}$  (Bernot & Brandenburg 2013). These studies indicate a high sensitivity of aquatic snails to AgNP.

## 1.6 Trophic transfer of nanomaterials

The study of trophic transfer of nanomaterials is important to discern the potential fate in the food web, the propagation of effects in higher organisms, and the consequences for predator-prey relationships (Clements & Rohr 2009, Evans-White & Lamberti 2009). Furthermore, dietborne exposure of consumers to AgNP is expected to be a more important uptake route than waterborne exposure in the environment (García-Alonso et al. 2011, Garnier-Laplace et al. 1992, Zhao & Wang 2010).

Biofilms may be an important point of entry in the food web, since the particles were transferred to upper trophic levels (snails). Ferry et al. (2009) observed in a mesocosm study that benthic organisms (i.e. clams and biofilms) efficiently accumulated gold nanoparticles, which make them potential sinks for nanomaterials in the environment. Studies have shown the trophic transfer of quantum dots from bacteria and protozoa to different consumers (Bouldin et al. 2008, Holbrook et al. 2008, Werlin et al. 2011). Croteau et al. (2011a) reported dietary uptake of zinc originated from dissolution of zinc oxide nanoparticles in snails feeding on a population of preexposed diatoms. Another study with AgNP (Croteau et al. 2011b) showed that AgNP can have effects on the trophic transfer, since the feeding rate of snails on diatoms was reduced. Additionally, bioaccumulation is expected to happen in higher trophic levels due to poor depuration. Terhaar et al. (1977) reported the trophic transfer of  $\text{Ag}^+$  in a simplified food web composed by algae, daphnids, mussels and fish. However, biomagnification did not occur. A first study showed no evidence of the biomagnification of AgNP in aquatic food webs (Yoo-iam et al. 2014).

## 1.7 Scope of the thesis

There is still a lack of information on the risk that AgNP may pose to aquatic communities and food webs. In order to contribute to these knowledge gaps, in this study, the effects of both AgNP and  $\text{AgNO}_3$  (added as a source of  $\text{Ag}^+$  ions) to a simplified system consisting of a periphyton community and a grazer snail were assessed. In the periphyton community, the algal and bacterial communities (autotrophic and heterotrophic fractions, respectively) were studied. These two communities are responsible for the ecosystem functions of primary production and nutrient cycling. Additionally, the interdependent algal and bacterial metabolisms bring the opportunity to assess the effects of AgNP also on species interactions. Finally, the trophic transfer of silver and the subsequent toxic effects of AgNP were studied in a grazer, the aquatic snail *Physa acuta*, feeding on the periphytic community. These questions are addressed in the chapters of the present thesis.

In Chapter 2, the effects of AgNP and  $\text{AgNO}_3$  on the autotrophic and heterotrophic communities in periphyton were investigated after short-term exposures. An overview of the

response of the communities was obtained by assessing effects on the photosynthetic yield of autotrophs, the respiration potential of the periphyton community, and activities extracellular enzymes, which play a role in nutrient acquisition by periphyton. Additionally, the role of dissolved Ag(I) was assessed through experiments with a silver ion ligand in order to complex the dissolved Ag(I) in AgNP suspensions.

In Chapter 3, the effects of long-term exposure to AgNP and AgNO<sub>3</sub> on biological functions and community structure of periphyton were assessed. In addition of further investigating the effects of AgNP and AgNO<sub>3</sub> over longer exposure times, which also integrate the effects of species interactions, the community structure of periphyton was examined by techniques targeting the autotrophic and heterotrophic components of the periphyton.

In Chapter 4, the potential of trophic transfer of silver from periphyton to *P. acuta* upon introduction of AgNP and AgNO<sub>3</sub> in the system was assessed. Effects of AgNP and AgNO<sub>3</sub> on the trophic relationship between periphyton and snails were investigated through the feeding behavior of snails. Furthermore, effects of the dietary exposure to AgNP and AgNO<sub>3</sub> were examined through the reproductive output of the snails.

In Chapter 5, research questions emerging from this thesis are discussed.

## Chapter 2. Silver nanoparticle effects on stream periphyton during short-term exposures

*Carmen Gil-Allué, Kristin Schirmer, Ahmed Tlili, Mark O. Gessner, and Renata Behra.*

*Published in Environmental Science & Technology, 2015, 49 (2), pp 1165–1172.*

Silver nanoparticles (AgNP) are increasingly used as antimicrobials in consumer products. Subsequently released into aquatic environments, they are likely to come in contact with microbial communities like periphyton, which plays a key role as a primary producer in stream ecosystems. At present, however, very little is known about the effects of nanoparticles on processes mediated by periphyton communities. We assessed the effects of citrate-coated silver nanoparticles and silver ions (dosed as AgNO<sub>3</sub>) on five functional parameters reflecting community and ecosystem-level processes in periphyton: photosynthetic yield, respiration potential, and the activity of three extracellular enzymes. After 2-hour exposures in experimental microcosms, AgNP and AgNO<sub>3</sub> inhibited respiration and photosynthesis of periphyton and the activities of two of the three extracellular enzymes. Addition of a chelating ligand that complexes free silver ions indicated that, in most cases, toxicity of AgNP suspensions was caused by Ag(I) dissolved from the particles. However, these suspensions inhibited an extracellular enzyme (leucine aminopeptidase), indicating a specific toxicity of AgNP independent of the dissolved Ag(I). Our results show that silver nanoparticles and silver ions have potential to disrupt basic metabolic functions and enzymatic resource acquisition of stream periphyton.

### 2.1 Introduction

Silver nanoparticles (AgNP) are currently one of the most widely used nanomaterials in consumer products, due to the well-known antimicrobial properties of silver (Franke 2007). The release of AgNP into the environment during the life cycle of manufactured goods has been estimated by means of models and empirical studies, as in the case of AgNP-treated façades (Gottschalk et al. 2013, Kaegi et al. 2010). These studies have revealed that AgNP can be released into the environment in amounts that potentially pose a risk to aquatic ecosystems. However, AgNP reaching the environment are subject to modifications (Levard et al. 2012), which can increase (e.g. dissolution) or decrease (e.g. sulfidation) their toxic potential (Levard et al. 2013). The relative importance of these processes greatly depends on local water chemistry (Colman et al. 2012).

Toxic effects of AgNP to microorganisms attributed to their nano-specific properties, such as bacterial membrane disruption upon physical contact, have been reported (Sondi & Salopek-

Sondi 2004), however, the exact mechanisms remain unknown. More often, effects appear to be caused by dissolved  $\text{Ag}^+$  ions or other dissolved oxidized silver species, such as  $\text{AgCl}_n$  (aq) and  $\text{AgOH}$  (aq), collectively denominated here as dissolved  $\text{Ag(I)}$  (Navarro et al. 2008a).  $\text{Ag}^+$  ions can remain in solution as a residue of nanoparticle synthesis, or they dissolve when the surface of AgNP is oxidized. Therefore, a suitable  $\text{Ag}^+$  ion control is necessary in ecotoxicological studies. The determinant role of  $\text{Ag}^+$  ions in causing toxicity to algae is suggested by the lack of negative effects observed in the presence of silver ligands (Navarro et al. 2008b), and by the insensitivity of bacteria under anaerobic conditions when the oxidative dissolution of AgNP is suppressed (Xiu et al. 2012). The high toxicity of  $\text{Ag}^+$  ions to aquatic organisms (Ratte 1999) is probably due to the high affinity of  $\text{Ag}^+$  for thiol groups, which causes the ion to interact strongly with membranes and enzymes, affecting essential physiological processes such as photosynthesis, respiration and other enzymatically driven processes (Holt & Bard 2005, Pillai et al. 2014).

Investigations into the fate of nanomaterials in aquatic environments suggest that benthic organisms encounter nanomaterials when they agglomerate and settle at the bottom of water bodies (Ferry et al. 2009). Accordingly, the biomass and diversity of bacterioplankton, marine bacterial biofilms and microbes associated with leaf litter in streams has been found to be reduced following exposure to AgNP (Das et al. 2012, Doiron et al. 2012, Fabrega et al. 2011b, Pradhan et al. 2011). Overall, however, very little is known about the effects of AgNP on benthic microbial communities. An important microbial community in stream ecosystems is periphyton (Minshall 1978), which consists of autotrophic and heterotrophic communities, mainly algae and bacteria, embedded in a polymer matrix and forming a biofilm on hard surfaces (Blenkinsopp & Lock 1994). Periphyton has long been used in both ecological and ecotoxicological studies because it plays a fundamental role in assuring primary production in shallow waters (Uehlinger et al. 2000), and because it has proved useful as an indicator of chemical pollution in aquatic ecosystems (Sabater et al. 2007). Yet, to our knowledge, studies on the effects of AgNP on natural periphyton communities have not been reported to date, and significant knowledge gaps exist also on the effects of nanomaterials to aquatic microbial communities, with scarce studies published so far (Battin et al. 2009, Das et al. 2012).

In the present study, we aimed to assess responses of periphyton affected by 2-hour exposures to AgNP, and  $\text{AgNO}_3$  as a source of silver ions. A silver ion ligand was used to differentiate between effects caused by AgNP and by the dissolved  $\text{Ag}^+$  ions. The response parameters chosen to assess the functioning of periphyton were the photosynthetic yield of autotrophs, the respiration potential of the periphyton community, and activities of three extracellular enzymes:  $\beta$ -glucosidase (GLU), alkaline phosphatase (AP), and leucine aminopeptidase (LAP). These enzymes were chosen for their role in nutrient acquisition by periphyton.

## **2.2 Materials and Methods**

### **Materials**

Citrate-coated AgNP were purchased from NanoSys GmbH (Wolfhalden, Switzerland;



fabrication date: October 2011) as an aqueous suspension with a nominal silver concentration of 1 g L<sup>-1</sup> or 9.27 mM. Concentrations of AgNP are expressed as the molar concentration of total silver, unless stated otherwise. To ensure stability of AgNP and control silver speciation during exposure experiments, all AgNP suspensions and AgNO<sub>3</sub> solutions were prepared in defined, reconstituted fresh water. The composition of the exposure medium (Table A.1 in Appendix A) was modified from Le Faucheur et al. (2005) by reducing the calcium concentration to prevent particle agglomeration (Piccapietra et al. 2012b), and by adding silicates to adequate the medium to diatoms present in periphyton. AgNO<sub>3</sub>, exposure medium components, 2,3-dimercaptopropanesulfonate (DMPS), and substrate analogues for the three extracellular enzymes (i.e. 4-methylumbelliferyl- $\beta$ -D-glucopyranoside, L-leucine-7-amido-4-methylcoumarin hydrochloride and 4-methylumbelliferyl phosphate disodium salt) were purchased from Sigma-Aldrich (Buchs SG, Switzerland). HNO<sub>3</sub> (65%, Suprapur) was purchased from Merck (Darmstadt, Germany). All solutions containing silver were stored in the dark to prevent light-induced chemical reactions. Working solutions of DMPS were prepared shortly before use and kept on ice, while the DMPS powder was stored at 4 °C under an argon atmosphere to minimize oxidation. All reusable materials were soaked for at least 24 hours in 0.03 M HNO<sub>3</sub>, and rinsed with deionized nanopure water (18  $\Omega$ , Milli-Q) before use.

### **Characterization of nanoparticles**

AgNP diluted in nanopure water (100  $\mu$ M) were characterized prior to exposure experiments. In addition, AgNP suspensions of 12.5 and 100  $\mu$ M prepared in either fresh or conditioned exposure medium were also characterized. Conditioned exposure medium was obtained by incubating periphyton in fresh medium under exposure conditions (2 hours at 15 °C in the dark) and then removing the periphyton before adding AgNP. The hydrodynamic diameter of AgNP in the suspensions was measured by dynamic light scattering (DLS) using a Zetasizer (Nano ZS, Malvern Instruments Ltd, Worcestershire, UK) and by nanoparticle tracking analysis (NTA) using a NanoSight LM10 (NanoSight Ltd., Wiltshire, UK). The  $\zeta$ -potential of the AgNP suspensions was measured using the Zetasizer. Results of size and  $\zeta$ -potential measurements are reported here as the average of the three technical replicates and the corresponding standard deviation. The optical properties of AgNP suspensions were determined by recording UV-Vis spectra in the 350-700 nm range using a spectrophotometer (UVIKON 930, Kontron Instruments, Basel, Switzerland). Dissolved Ag(I) present in the AgNP suspensions was determined after ultracentrifugation for 3 hours at 146000  $\times$  g (Centrikon T2070, Kontron Instruments, Basel, Switzerland) to remove AgNP larger than 5 nm, and by centrifugal ultrafiltration for 30 min at 3220  $\times$  g (Megafuge 1.0R, Thermo Scientific Inc., Waltham, MA, USA) using Ultracel 3k Centrifugal Filter Devices (Amicon Millipore) with a molecular cut-off of 3 kDa (pore size < 2 nm) (Piccapietra et al. 2012a). The speciation of silver in the exposure medium was estimated by using the free software Visual MINTEQ v3.0 Beta (<http://www2.lwr.kth.se/English/OurSoftware/vminteq>).

To quantify total silver in samples containing AgNP, an acid digestion was performed in an

ultraCLAVE 4 microwave digestion system (MLS GmbH, Leutkirch, Germany). One mL of sample was pipetted into a Teflon tube and acidified with 4 mL of 65 % HNO<sub>3</sub>. The digestion program ran for 24 min with a maximum temperature of 200 °C and a maximum pressure of 100 bar. The digests were diluted 50 times with nanopure water before total silver was quantified by measuring the isotope <sup>109</sup>Ag on an Element 2 High Resolution Sector Field ICP-MS (Thermo Scientific Inc.). A certified reference for water with a known silver concentration (National Water Research Institute, Burlington, Canada) was analyzed to assure the accuracy of the measurements.

### **Periphyton colonization**

Glass slides were colonized by periphyton exposed to a natural inoculum from Chriesbach, a small peri-urban stream in Dübendorf, Switzerland. Water from the stream was pumped to indoor flow-through channels made of Plexiglas (880 x 110 mm), where 40 pairs of microscope slides (76 x 26 mm) were vertically placed side by side in four longitudinal slots cut in the bottom of the channels (Navarro et al. 2007). The water flow was kept constant at 1 cm s<sup>-1</sup>. Light conditions consisted of a 12-hour light/dark photoperiod under BioSun fluorescent tubes (MLT Moderne Licht-Technik AG, Wettingen, Switzerland). The colonized slides were sampled after 4 weeks and placed in exposure medium to acclimatize the periphyton to the experimental conditions for 30 minutes before exposure to AgNP or AgNO<sub>3</sub>.

### **Exposure experiments**

Six colonized slides were placed in polystyrene microcosms (180 x 134 x 60 mm; Semadeni AG, Ostermundigen, Switzerland) filled with 300 mL of exposure medium. Silver was added as AgNP (12.5, 25, 50, 100 and 200 µM) or AgNO<sub>3</sub> (1.25, 2.5, 5, 10 and 25 µM). The microcosms were placed on a Three-Dimensional Orbital Shaker (Edmund Bühler GmbH, Hechingen, Germany) rotating at 20 rpm with a vertical angle of 5° to mimic turbulent flow across the periphyton surface. Periphyton was exposed in the dark at 15 °C to avoid photoreduction of Ag(I). One microcosm with six slides was prepared in each experiment per treatment, and experiments were repeated three times with newly colonized periphyton communities. After 2 hours, periphyton was scraped off the slides with a polystyrene spatula. The pooled samples of the six slides from a given microcosm were homogeneously suspended in 30 mL of exposure medium and these suspensions were used for all measurements.

In a second set of experiments conducted under identical exposure conditions, periphyton was exposed to 100 µM AgNP and 10 µM AgNO<sub>3</sub> in the presence or absence of 25 µM DMPS. DMPS has two thiol groups, which have a high affinity to Ag<sup>+</sup> ions (Mason & Jenkins 1995). Before exposing periphyton in these experiments, media containing AgNP or AgNO<sub>3</sub> were pre-equilibrated with DMPS for 15 min to ensure the complete complexation of Ag<sup>+</sup> ions.

### **Response variables**

Photosynthesis was assessed by measuring the quantum yield of photosystem II with a portable

fluorometer (PHYTO-PAM; Heinz Walz GmbH, Effeltrich, Germany). Suspensions were allowed to acclimate to ambient light conditions for 15 min before taking measurements. The quantum yield was calculated as  $(F_m - F_t)/F_m$ , where  $F_t$  is the instantaneous fluorescence measured immediately after a saturating light pulse and  $F_m$  is the basal fluorescence (Schreiber 1998). Fluorescence data for four excitation wavelengths (470, 520, 645, 665 nm) were used as proxies to assess the ratios of autotrophic groups in periphyton communities based on the absorption and emission spectra of different photosynthetic pigments. Readings were arcsine square root transformed and normalized to the fluorescence measured at an excitation wavelength of 665 nm, which mainly corresponds to chlorophyll a, and were compared across all control periphyton suspensions to assess the similarity of independently colonized periphyton. The fluorometry-based community composition of periphyton before exposure to silver was generally similar, with one of the six tested communities differing in its fluorescence at 470 and 645 nm (Tukey's test,  $p < 0.001$ ) (Figure A.1).

Respiration potential was measured according to Tlili et al. (2011) by using the MicroResp™ approach, a colorimetric method based on CO<sub>2</sub> production in a closed microplate system. Periphyton suspensions of 500 µL were transferred to the wells of a microplate (Nunc™ DeepWell, Thermo Scientific Inc.), and 25 mM glucose was added as a carbon source to maximize respiration. Microplates were air-tight sealed, pairing the wells with a second detection plate that contained a pH indicator embedded in agar with a maximum absorbance at 572 nm. The diffusion of CO<sub>2</sub> in the detection gel causes the pH to decrease due to the formation of carbonic acid, which in turn leads to a shift in the absorbance wavelength. Absorbance of the detection gels was measured at 572 nm on a Tecan Infinite 200 PRO microplate reader (Tecan Trading AG, Männedorf, Switzerland) before and after incubation for 18 hours at 25 °C in the dark. Four analytical replicates were prepared and measured. The average change in absorbance was normalized to the ash-free dry mass (AFDM) of the periphyton.

AFDM of the periphyton was determined by filtering three 1-mL aliquots of the suspensions through pre-weighed glass fiber filters (GF/F, 25 mm diameter, 0.7 µm average pore size; Whatman Ltd., Maidstone, UK), drying the filters for 24 hours at 105 °C, weighing them to the nearest 0.01 mg, combusting the organic matter for 1 hour at 480 °C in a muffle furnace (LE 1/11, Nabertherm GmbH, Lilienthal, Germany), and re-weighing the filters.

Potential activities of three enzymes were assayed by means of fluorescent substrate analogues following a slightly modified protocol of Romaní et al. (2004). β-Glucosidase (GLU) hydrolyses β-1,4 bonds of carbohydrates to provide cells with an organic carbon source, alkaline phosphatase (AP) is responsible for the hydrolysis of phosphate esters, and leucine aminopeptidase (LAP) cleaves peptides and supplies cells with a nitrogen source. One-mL aliquots of the periphyton suspensions were incubated at saturating concentrations of the substrate analogues (1 mM) at 25 °C in the dark. The enzymatic reactions were stopped after 40 min by adding 1 mL of 1 M glycine buffer (pH 10.55) and centrifuging the periphyton suspensions for 10 min at 24000 × g (Microcentrifuge 2417R, Eppendorf, Hamburg, Germany). Aliquots of the supernatant (200 µL) were transferred to a black 96-well microplate (Greiner-

Bio-One GmbH, Frickenhausen, Germany) to measure fluorescence. The emission and excitation wavelengths were 366 and 442 nm, respectively, for substrates containing 4-methylumbelliferyl as the fluorophore. The respective wavelengths for substrates containing 7-amido-4-methylcoumarin were 340 and 436 nm. The fluorescence data were converted to concentrations of cleaved substrate analogues based on a calibration curve obtained by measuring fluorescence of fluorophores at concentrations ranging from 0 to 5  $\mu\text{M}$  ( $R^2 = 0.99$ ). The extracellular enzymatic activities of control periphyton differed up to tenfold among the different communities used in independent experiments (Table A.2), reflecting considerable natural variability.

Extracellular enzyme activities in the loosely bound extracellular polymer matrix (EPS) of the periphyton and in the medium were assessed by filtering the periphyton suspension (0.2  $\mu\text{m}$ , Chromafil Xtra PES-20/25, Macherey-Nagel GmbH, Düren, Germany) and determining enzymatic activities in the filtrates.

Toxicity parameters and statistical significance were assessed using SigmaPlot for Windows version 12.0 (Systat Software Inc., San Jose, CA, USA). Effects of AgNP and AgNO<sub>3</sub> on functional parameters are expressed as values relative to the controls. The corresponding concentration-response curves were fitted to a logistic equation to derive the concentrations causing 50% inhibition relative to the controls ( $\text{EC}_{50}$ ):

$$\text{Activity (\%)} = 100\% / [1 + ([\text{Ag}] / \text{EC}_{50})^{-H}]$$

where  $[\text{Ag}]$  is the concentration of AgNP or AgNO<sub>3</sub> in the treatment and  $H$  is the Hill slope of the curve.

Student's  $t$ -test was used to test the significance of the difference between the  $\text{EC}_{50}$  values of AgNP and AgNO<sub>3</sub> for a certain parameter. Dunnett's test was used for the multiple comparisons among the different treatments in the experiment with the silver ligand to assess the prevention of effects by the ligand.

## 2.3 Results

### Nanoparticle characterization

AgNP in 100  $\mu\text{M}$  dilutions of the stock suspension in nanopure water had an average diameter of  $35 \pm 1$  nm and a  $\zeta$ -potential of  $-32 \pm 1$  mV. A slight agglomeration of particles was observed with increasing exposure time, the presence of exudates in the conditioned medium and in the presence of DMPS. The average particle diameter in fresh exposure medium was  $30 \pm 1$  and  $56 \pm 3$  nm for 12.5  $\mu\text{M}$  and 100  $\mu\text{M}$  AgNP suspensions, respectively (Figure 2.1), increasing to  $50 \pm 1$  nm and  $116 \pm 1$  nm in conditioned medium. Addition of 25  $\mu\text{M}$  DMPS increased the average particle diameters to between  $67 \pm 1$  nm and  $126 \pm 2$  nm. AgNP in fresh exposure medium at concentrations of 12.5 and 100  $\mu\text{M}$  had a  $\zeta$ -potential of  $-5 \pm 1$  and  $-12 \pm 3$  mV, respectively (Figure 2.1). More negative charges were measured in conditioned exposure medium,  $-13 \pm 2$  and  $-18 \pm 1$  mV, and in the presence of DMPS,  $-16 \pm 1$  and  $-26 \pm 1$  mV. Similar particle sizes in AgNP suspensions were determined by NTA (Table A.3). AgNP size distributions are shown in Figure A.2.

The UV-Vis spectra of all AgNP suspensions showed the characteristic plasmon resonance peaks in the 405–447 nm range (Figure A.1) that are indicative of AgNP presence (Piccapietra et al. 2012b). A pronounced shoulder was present in the spectra of AgNP in conditioned medium and DMPS addition widened the absorbance distribution. Both characteristics indicate agglomeration of AgNP.

The fraction of dissolved Ag(I) in AgNP suspensions was similar across AgNP concentrations, media and exposure times, as determined by ultracentrifugation (Figure 2.2). The highest level of dissolved Ag(I) measured in fresh medium was 3 % in a 12.5  $\mu\text{M}$  AgNP suspension after 20 hours. The presence of DMPS increased the proportion of dissolved Ag(I) to up to 45 % and 14 % for 12.5 and 100  $\mu\text{M}$  AgNP suspensions, respectively. Similar results were obtained with the centrifugal ultrafiltration method, however, this method resulted in very low recoveries when DMPS was present (Figure A.4). Calculations of the speciation of dissolved Ag(I) revealed that 96 to 97% was present as  $\text{Ag}^+$  ions in both the AgNP and  $\text{AgNO}_3$  treatments (Table A.4).

### Short-term effects of AgNP and $\text{AgNO}_3$

Photosynthetic yield of periphyton decreased with increasing concentrations of AgNP and  $\text{AgNO}_3$  (Figure 2.3A). Average  $\text{EC}_{50}$  values over independent experiments were estimated at  $83 \pm 3$   $\mu\text{M}$  AgNP and  $3.5 \pm 0.2$   $\mu\text{M}$   $\text{AgNO}_3$  (Table 2.1). Similarly, the respiration potential of periphyton was also inhibited by increasing concentrations of AgNP and  $\text{AgNO}_3$  (Figure 2.3B), with  $\text{EC}_{50}$  values of  $22 \pm 3$   $\mu\text{M}$  AgNP and  $4.1 \pm 0.3$   $\mu\text{M}$   $\text{AgNO}_3$  (Table 2.1). Based on these values,  $\text{AgNO}_3$  was 28 times more toxic to photosynthesis than AgNP (Student's *t*-test;  $p < 0.001$ ), while the difference was only 6 fold for respiration ( $p < 0.05$ ).

Effects on LAP and GLU were similar to those on photosynthesis and respiration in that the activities of these two enzymes decreased with increasing concentration of AgNP and  $\text{AgNO}_3$  (Figure 2.3C,D). In contrast, AP activity was not significantly affected and  $\text{EC}_{50}$  values could not be derived.  $\text{EC}_{50}$  values for GLU averaged over the three independent experiments were  $17 \pm 6$   $\mu\text{M}$  for AgNP and  $2.4 \pm 0.5$   $\mu\text{M}$  for  $\text{AgNO}_3$ . In the case of LAP,  $\text{EC}_{50}$  values were  $23 \pm 3$   $\mu\text{M}$  for AgNP and  $2.0 \pm 0.3$   $\mu\text{M}$  for  $\text{AgNO}_3$ .  $\text{AgNO}_3$  was 13 and 7 times more effective than AgNP at reducing the activity of GLU and LAP, respectively ( $p < 0.05$ ).

Filtrates of periphyton suspensions containing the soluble and loosely bound EPS fractions passing a 0.2- $\mu\text{m}$  pore-size filter showed GLU activities very similar to those of the whole suspensions (Figure A.5A). In contrast, activities of LAP and AP in the EPS fraction were negligible (Figure A.5A). At the highest concentrations tested, AgNP (100  $\mu\text{M}$ ) and  $\text{AgNO}_3$  (1  $\mu\text{M}$ ) completely suppressed GLU activity in the filtrate (Figure A.5B).

Addition of the  $\text{Ag}^+$  ligand DMPS at a concentration of 25  $\mu\text{M}$  strongly prevented the toxicity of AgNP and  $\text{AgNO}_3$  to photosynthesis, respiration and extracellular enzyme activities in almost all cases (Figure 2.4). Specifically, virtually complete inhibition of photosynthesis at silver concentrations of 100  $\mu\text{M}$  AgNP and 10  $\mu\text{M}$   $\text{AgNO}_3$  was almost completely prevented by DMPS (90 % of the photosynthetic yield shown by the controls). Similarly, DMPS fully prevented the more than 50% reduction in respiration caused by AgNP and  $\text{AgNO}_3$  (Figure 2.4). Furthermore,

the activity of GLU, reduced to 42 % by AgNP and to 15 % by AgNO<sub>3</sub>, was nearly completely recovered in the presence of DMPS (Figure 2.4). Finally, DMPS partly also restored the activity of LAP, which AgNO<sub>3</sub> decreased to 5 % of the control value, but the ligand was unable to prevent the complete inhibition of LAP caused by AgNP. DMPS did not cause effects on the functions at the concentration tested.

## 2.4 Discussion

Most ecotoxicological assessments of silver nanoparticle effects have been carried out on single species of microorganisms (Bernhardt et al. 2010), and limited information on microbial communities relevant for ecosystem processes is available. To capture functional responses of stream periphyton communities to AgNP and AgNO<sub>3</sub> in the present study, we chose respiration and three extracellular enzymatic activities as integrative variables reflecting responses of the whole periphyton community, and used photosynthesis to more specifically target processes driven by the autotrophic organisms in the periphyton.

Both AgNP and AgNO<sub>3</sub> inhibited four of the five response variables tested, following standard concentration-response relationships. The exception was the activity of AP, which was either inhibited or stimulated at different exposure concentrations. The EC<sub>50</sub> values calculated for photosynthesis, respiration, GLU and LAP suggest that the toxicity of AgNO<sub>3</sub> was significantly higher than that of AgNP. Although to our knowledge no previous studies have tested for AgNP effects on periphyton, the photosynthetic yield of periphyton is known to be highly sensitive to dissolved Ag(I) (Soldo & Behra 2000), and photosynthesis of a free-swimming model alga (*C. reinhardtii*) has been found to be more strongly affected by AgNO<sub>3</sub> than by AgNP (Navarro et al. 2008b). Similarly, in accordance with a previous study on freshwater plankton and sediment communities (Colman et al. 2012), microbial respiration was more sensitive to AgNO<sub>3</sub> than to AgNP. In the same study, LAP activity declined after exposure to AgNP and AgNO<sub>3</sub>, whereas AP activity was inhibited by AgNO<sub>3</sub> and stimulated by AgNP. These results contrast with the concentration-response relationship observed for AP in freshwater bacterioplankton exposed to AgNP and AgNO<sub>3</sub> at concentrations similar to those in our experiment (Das et al. 2012). This discrepancy among studies could be caused by differences in microbial communities or AgNP characteristics or by differences in AgNP stability during the experiments due to variation in water chemistry and other environmental conditions. Therefore, understanding the importance of these influencing factors and the mechanisms behind the effects they cause is crucial to making rational predictions about AgNP toxicity on periphyton in other circumstances.

Ag<sup>+</sup> ions are known to disrupt photosynthesis, respiration and other enzymatically driven processes (Holt & Bard 2005, Pillai et al. 2014), but it is unclear whether the mechanisms causing negative effects involve internalization of AgNP by algal, bacterial or other cells. Extracellular enzymes, however, can make direct contact with AgNP so that negative effects on enzymatic activity can result from two types of mechanisms: inhibition of the enzyme or inhibition of enzyme secretion. In the present study, the complete inhibition of GLU activity observed in

filtrates demonstrates that both AgNP and AgNO<sub>3</sub> caused direct enzyme inhibition. However, this observation does not preclude the possibility that the secretion of newly synthesized GLU is inhibited as well.

Experiments were carried out with DMPS, an effective heavy metal ligand (Rooney 2007), to distinguish between an inherent toxic effect of AgNP and increased silver dissolution caused by direct contact of AgNP with organisms and their metabolic products (He et al. 2012). The two thiol groups of DMPS complex Ag<sup>+</sup> and can thereby neutralize toxicity of the silver ion. Other Ag<sup>+</sup> ligands containing thiol groups, like cysteine, have been successfully used to prevent AgNO<sub>3</sub> and AgNP toxicity, showing the importance of Ag<sup>+</sup> in mediating AgNP toxicity (Navarro et al. 2008b). Likewise, in the present study, DMPS completely prevented the negative effects caused by AgNO<sub>3</sub> and AgNP on respiration, and nearly prevented the inhibition of photosynthesis, thus pointing to dissolved Ag<sup>+</sup> as the primary toxic agent. The prevention of AgNP toxicity by DMPS also ruled out confounding effects from the citrate coating.

In the case of GLU, AgNP toxicity was alleviated but not completely prevented by DMPS. This could indicate inhibition of the enzyme by AgNP without the action of dissolved Ag<sup>+</sup>. Alternatively, the effect might be linked to increased dissolution of AgNP in the presence of DMPS (up to 14% for 100 µM AgNP). This finding is in agreement with the increased dissolution of Ag<sup>+</sup> from AgNP which other studies have found to be induced by high concentrations of cysteine (Gondikas et al. 2012). However, though DMPS (25 µM) was still clearly in excess of Ag<sup>+</sup> when 14% of the AgNP silver was dissolved, it cannot be ruled out that the dissolution of Ag(I) from AgNP at the AgNP-periphyton interface by metabolic products such as H<sub>2</sub>O<sub>2</sub> (He et al. 2012) caused residual toxicity even in the presence of DMPS.

No preventive effects of DMPS on the toxicity of AgNP were noted in the case of LAP. In contrast to the results on the other enzymes, this outcome suggests a specific particle effect, which could be caused by physical interactions of AgNP and LAP resulting in a modification of enzyme structure or obstruction of the enzyme's reaction center. The fact that toxic effects of AgNO<sub>3</sub> to LAP were only partially prevented could point to a residual inhibitory potential of DMPS-Ag complexes to this enzyme.

Since Ag<sup>+</sup> ions were identified as the primary toxic agent in most cases, the extent of the enhanced dissolution of Ag<sup>+</sup> ions from AgNP by periphyton was assessed. Concentration-response curves for the effects of AgNP on photosynthetic yield, respiration and GLU activity were plotted as a function of the measured dissolved silver fraction instead of total Ag, and EC<sub>50</sub> values were derived accordingly. Since organisms rapidly take up Ag<sup>+</sup> ions, dissolution measurements in media could only be carried out in the absence of periphyton (Piccapietra et al. 2012a). AgNP suspensions contained 1.5 % Ag<sup>+</sup> during measurements of photosynthetic yield and 3 % when measuring respiration, because periphyton was incubated for an additional 18 hours to measure CO<sub>2</sub> release in the respiration assay. If the presence of periphyton did not enhance the dissolution of Ag<sup>+</sup> ions from AgNP, the EC<sub>50</sub> values obtained should match the ones for AgNO<sub>3</sub>. However, EC<sub>50</sub> values for AgNP were smaller than for AgNO<sub>3</sub> (Table A.5), implying an increased dissolution of AgNP in the presence of periphyton, which was not detectable when

AgNP were exposed to periphyton exudates alone. Despite the presence of EPS, AgNP smaller than 50 nm can diffuse into bacterial biofilms (Peulen & Wilkinson 2011), where close contact with organisms facilitates AgNP oxidation.

### **Environmental implications**

While environmental concentrations are expected to be lower than in this study (Gottschalk et al. 2013) and the varying composition of natural waters will affect the extent and nature of the effects of AgNP (Colman et al. 2012, Das et al. 2014), the potential implications of the effects of AgNP and dissolved Ag(I) observed in the present study are manifold. The impacts on benthic primary production, which is the most important role of periphyton in stream ecosystems (Wetzel 1963), and the reduced organic carbon uptake by cells due to GLU inhibition, would lead to a reduction of biomass production of both autotrophic and heterotrophic periphyton components. Inhibition of LAP may limit nitrogen acquisition of cells as well, with indirect repercussions on photosynthetic efficiency (Berges et al. 1996) and ultimately primary production as well. Nutrient cycling could also be affected. Complementary investigations designed to determine AgNP effects over extended exposure times are needed to assess more comprehensively the impacts of AgNP at the ecosystem level, integrating the effects of changes in periphyton community structure and species interactions (Colman et al. 2014). Furthermore, it would be important to assess the trophic transfer of AgNP, and its effects, in stream food webs (Ferry et al. 2009), because periphyton is an important resource for consumers while acting as a likely trap of sedimenting nanoparticles.



## 2.5 Figures and tables

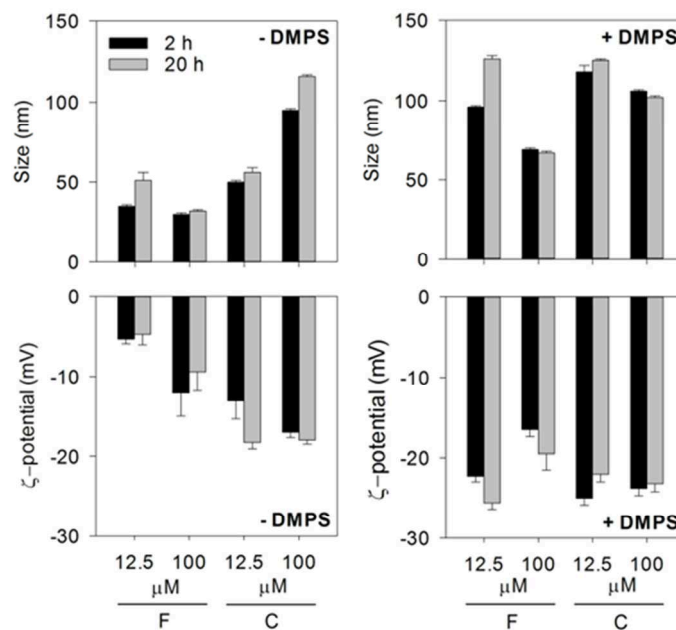


**Figure 2.1.** Comparison of  $\zeta$ -potential and particle diameters measured by DLS in 12.5 and 100  $\mu\text{M}$  AgNP suspensions of fresh (F) and conditioned (C) exposure medium for 2 (black bars) and 20 (grey bars) hours in the absence or presence of the  $\text{Ag}^+$  ligand DMPS. Error bars correspond to standard deviations of three analytical replicates. 100  $\mu\text{M}$  dilutions in nanopure water of the stock AgNP suspension had an average diameter of  $35 \pm 1$  nm and a  $\zeta$ -potential of  $-32 \pm 1$  mV.

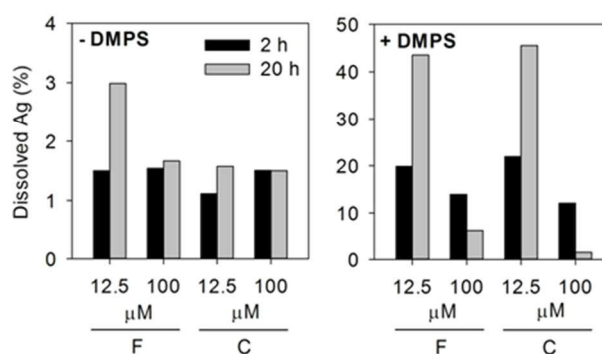


**Figure 2.2.** Proportion of dissolved Ag(I) in AgNP suspensions as determined by ultracentrifugation and ICP-MS. Measurements were made in fresh (F) and conditioned (C) exposure medium after 2 and 20 hours in the absence or presence of the  $\text{Ag}^+$  ligand DMPS.

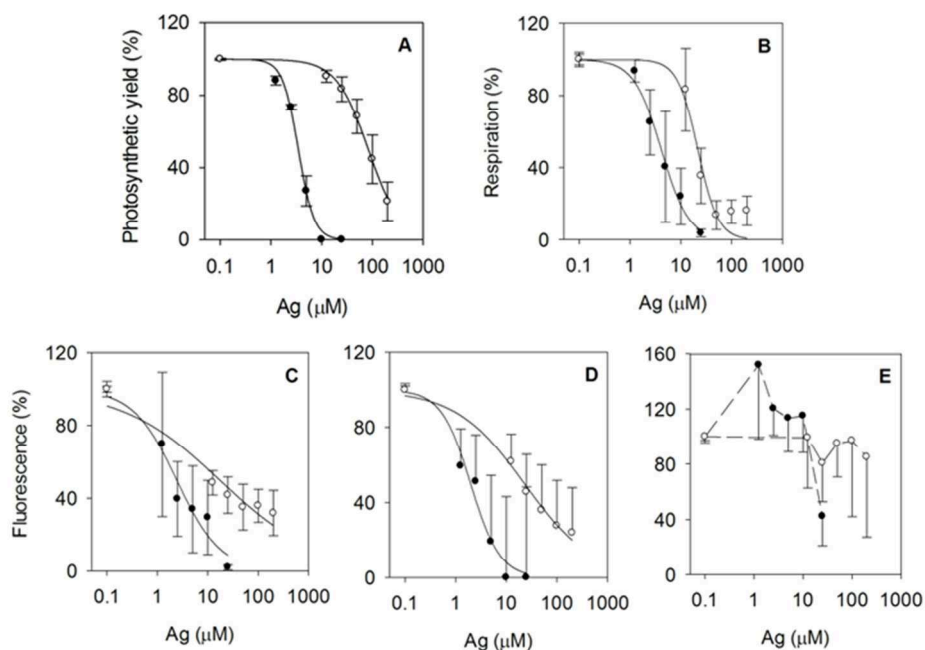


**Figure 2.3.** Effects of AgNP (○) and AgNO<sub>3</sub> (●) on photosynthesis (A), respiration (B), and the activity of extracellular enzymes  $\beta$ -glucosidase (C), leucine aminopeptidase (D) and alkaline phosphatase (E). All parameters were measured after 2 hours of exposure. Solid lines represent fits to four-parameter logistic models used to derive EC<sub>50</sub> values from three independent experiments. Error bars correspond to standard errors calculated across three independent experiments with newly colonized periphyton communities.

**Table 2.1.** EC<sub>50</sub> values for photosynthesis, respiration and extracellular enzymatic activities of periphyton calculated from individual experiments with independently colonized communities. Standard errors are based on three analytical replicates for photosynthetic yield and enzymatic activities, and four replicates for respiration. ND indicates unsuitable data to estimate an EC<sub>50</sub>. This was invariably the case for alkaline phosphatase. Average EC<sub>50</sub> values calculated across the average values of the three experiments are also shown.

Experiment	EC <sub>50</sub> (μM)			
	Photosynthetic yield	Respiration	GLU	LAP
AgNP 1	96 ± 8	32 ± 5	7 ± 1.7	13 ± 1
AgNP 2	115 ± 6	32 ± 5	10 ± 1	10 ± 1
AgNP 3	44 ± 2	10 ± 5	ND	12 ± 1
AgNO <sub>3</sub> 1	3.9 ± 0.2	ND	0.7 ± 0.1	1.3 ± 0.4
AgNO <sub>3</sub> 2	3.4 ± 0.2	2.7 ± 0.1	0.9 ± 0.1	1.0 ± 0.8
AgNO <sub>3</sub> 3	3.2 ± 0.1	2.1 ± 0.1	5.4 ± 1.8	40 ± 9
Average AgNP	83 ± 3	22 ± 3	17 ± 6	23 ± 3
Average AgNO <sub>3</sub>	3.5 ± 0.2	4.1 ± 0.3	2.4 ± 0.5	2.0 ± 0.3

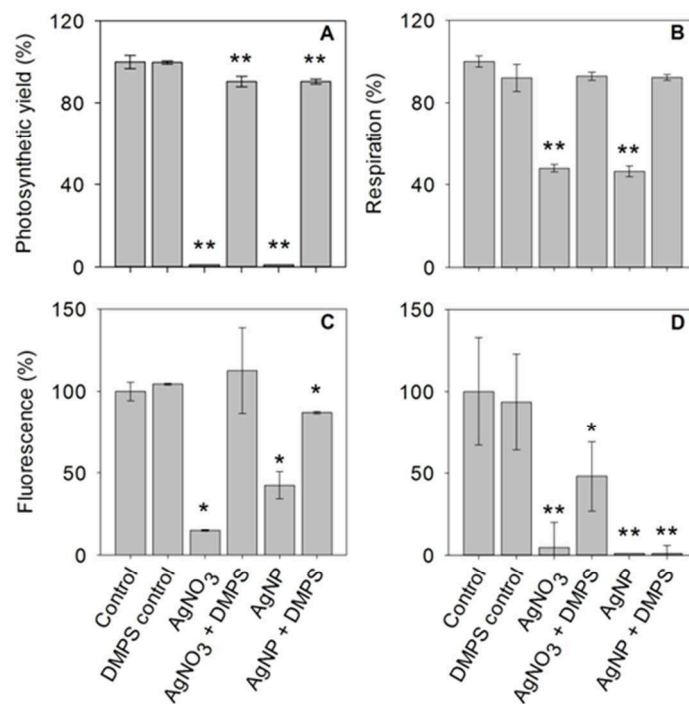


**Figure 2.4.** Effects of 10  $\mu\text{M}$   $\text{AgNO}_3$  and 100  $\mu\text{M}$  AgNP on photosynthesis (A), respiration (B), and the activity of extracellular enzymes  $\beta$ -glucosidase (C) and leucine aminopeptidase (D), with and without the addition of 25  $\mu\text{M}$  DMPS. Standard deviations correspond to three analytical replicates. Statistically significant differences between treatments and controls were assessed with Dunnett's test (\*  $p < 0.05$ , \*\*  $p < 0.001$ ).



## Chapter 3. Silver nanoparticle uptake and effects on the function and community structure of stream periphyton during long-term exposures

*Carmen Gil-Allué, Kristin Schirmer, Ahmed Tlili, Mark O. Gessner, and Renata Behra.  
In preparation.*

Silver nanoparticles (AgNP) released from consumer products and applications are susceptible to reach the environment. Although one of the main uses of AgNP is as an antimicrobial, very little is known on their impacts on microbial communities and microbially driven ecosystem processes. Periphyton is a microbial community that importantly contributes to primary production in aquatic ecosystems. In the present study, the uptake and distribution of AgNP and AgNO<sub>3</sub> in periphyton and their effects on biological functions and community structure were investigated. Periphyton was exposed to 0.1, 1 and 10 µM AgNP and 0.1 µM AgNO<sub>3</sub> in microcosms for up to 21 days. At the end of the exposure, 84 to 98 % of the total silver introduced in the microcosm was strongly associated with periphyton. Biological functions were mostly affected by the highest AgNP concentration (10 µM), which caused a decrease of the primary production that contrasted with an increase of the secondary production and biomass accrual. A change in the community structure of autotrophs and heterotrophs occurred after 21 days of exposure to 10 µM AgNP, which was associated with an increased tolerance to AgNP. Overall, our results show that periphyton efficiently accumulated AgNP, which caused toxic effects leading to the disturbance of the species interactions in the periphyton community.

### 3.1 Introduction

During the last decades, applications of silver nanoparticles (AgNP) mainly based on silver's well-known antibacterial properties (Franke 2007) have been developed by industry due to their enhanced properties compared to the corresponding bulk material (Kirchner et al. 2005, Wijnhoven et al. 2009). Along with increasing efforts in research and technological innovation, the use of nanomaterials is expected to increase in the next years (Gottschalk et al. 2009).

The release of AgNP from consumer products into aquatic environments has already been reported (Kägi et al. 2010, Farkas et al. 2011). The behavior of AgNP in aquatic systems will be determined by water chemistry, and agglomeration is likely to occur due to e.g. interactions with divalent cations and dissolved organic carbon (DOC) (Bae et al. 2010, Behra et al. 2013, Piccapietra et al. 2012b). When AgNP agglomerate and deposit in the sediments, benthic organisms like periphyton are put at risk. Ferry et al. (2009) assessed the fate of gold nanoparticles -used as a model of nanomaterial because of its low dissolution- in mesocosms and observed that the nanomaterial particularly accumulated in periphyton and other benthic

organisms. Fate studies of AgNP in mesocosms have confirmed their association with the benthic compartment and related biota (Cleveland et al. 2012, Lowry et al. 2012).

Microbial communities have an important role in ecosystem processes (Battin et al. 2003). In particular, periphyton is an important primary producer in fresh water ecosystems (Minshall 1978, Wetzel 1963). Periphyton is composed of autotrophic and heterotrophic organisms, namely algae and bacteria, which interact with each other through their metabolic products (Haack & Gordon 1982). The interactions among species in a community can influence the effects of stressors (Clements et al. 2012), which can in turn disrupt interspecies relationships (Scott et al. 2008). Periphyton has been used for decades in the monitoring of metal pollution (Ramelow et al. 1987), since metals can accumulate rapidly in periphyton organisms and closely reflect changes in environmental metal concentrations (Meylan et al. 2004, Bradac et al. 2009).

In a previous study, we reported that periphyton was adversely affected by short-term exposure to AgNP (12.5-200  $\mu$ M) (Gil-Allué et al. 2015), but long-term effects on functions and community structure, which integrate species interactions in the community, are still unknown. Knowledge on the effects of long-term exposure to AgNP on aquatic microbial communities is also limited, with only a few studies focusing on heterotrophic communities involved in nutrient cycling. Reduced community functions and changes in community structure upon long-term exposure to AgNP has been observed in bacterial and fungal communities of a leaf litter decomposition system (Pradhan et al. 2011), as well as in bacterial communities in the water column and sediments (Colman et al. 2012, Das et al. 2012).

The aim of the present study was to assess the effects of long-term exposure to AgNP and dissolved  $\text{Ag}^+$  ions on biological functions and community structure of periphyton. A set of functional parameters targeting the autotrophic and heterotrophic components of the community were assessed to capture the responses of autotrophs, heterotrophs, and periphyton community as a whole. Community structure of periphyton was examined by techniques targeting the autotrophic and heterotrophic components of the periphyton. Furthermore, based on the PICT concept (Blanck et al. 1988), which predicts an increased tolerance of communities to chemicals that have caused structural changes, we also examined the tolerance of periphyton after long-term experiments.

## **3.2 Materials and methods**

### **Characterization of silver exposure**

Citrate-coated AgNP were purchased from NanoSys GmbH (Wolfhalden, Switzerland) as an aqueous suspension with a nominal silver concentration of 9.27 mM, expressed as the molar concentration of total silver. A 100- $\mu$ M suspension of the AgNP stock in nanopure water showed an average size of  $35 \pm 1$  nm and a  $\zeta$ -potential of  $-32 \pm 1$  mV (Gil-Allué et al. 2015). All AgNP suspensions and  $\text{AgNO}_3$  solutions were prepared in a defined reconstituted fresh water medium (PERIQUIL) (Stewart et al. 2015), used to minimize AgNP agglomeration and control silver speciation during the experiments. The composition of PERIQUIL is showed in Table B.1 in Appendix B. The water chemistry was monitored in fresh, as well as in conditioned

PERIQUIL once per week after renewal during the exposure experiments (Table B.2). Conditioned PERIQUIL is the exposure medium where periphyton had been incubated for three days, after which it was renewed with fresh PERIQUIL. All chemicals were purchased from Sigma-Aldrich (Buchs SG, Switzerland) unless otherwise stated.

Characterization of 1 and 10  $\mu\text{M}$  AgNP suspensions was done under exposure conditions in either fresh or conditioned PERIQUIL to assess the effects of excreted biomolecules from periphyton on the AgNP stability, as described in Gil-Allué et al. (2015). Size of AgNP in the suspensions was measured as the hydrodynamic diameter by dynamic light scattering (DLS) using a Zetasizer (Nano ZS, Malvern Instruments Ltd, Worcestershire, UK) and by nanoparticle tracking analysis (NTA) using a NanoSight LM10 (NanoSight Ltd., Wiltshire, UK). The  $\zeta$ -potential of the AgNP suspensions was measured using the Zetasizer. Particle diameter and  $\zeta$ -potential are reported as the mean of three replicate measurements and the corresponding standard deviation. The optical properties of the 10  $\mu\text{M}$  AgNP suspensions were determined by recording UV-Vis spectra in the 350-700 nm range using a spectrophotometer (UVIKON 930, Kontron Instruments, Basel, Switzerland). Dissolved Ag(I) present in the AgNP suspensions was determined by centrifugal ultrafiltration for 30 min at  $3220 \times g$  (Megafuge 1.0R, Thermo Scientific Inc., Waltham, MA, USA) using Amicon Ultra-15 centrifugal filter units (Merck Millipore, Darmstadt, Germany) with Ultracel-3 membrane of a molecular cut-off of 3 kDa, with an estimated pore size of  $< 2$  nm (Piccapietra et al. 2012a). The speciation of silver in PERIQUIL was estimated by using the free software Visual MINTEQ v3.0 Beta (<http://vminteq.lwr.kth.se/>). Total silver in samples containing AgNP was quantified by ICP-MS after an acidic digestion. Briefly, one mL of liquid sample or a known amount of lyophilized biomass, was placed into a Teflon tube and acidified with 4 mL of 65 %  $\text{HNO}_3$  (Merck, Darmstadt, Germany). Samples were digested in an ultraCLAVE 4 microwave digestion system (MLS GmbH, Leutkirch, Germany) during 24 min with a maximum temperature of 200 °C and a maximum pressure of 100 bar. The digests were diluted 50 times with nanopure water before total silver quantification on an Element 2 High Resolution Sector Field ICP-MS (Thermo Scientific Inc.). The accuracy of the measurements was ensured with a certified reference for water with a known silver concentration (National Water Research Institute, Burlington, Canada).

### **Periphyton colonization and silver exposure**

Periphyton was colonized on glass slides (76 x 26 mm) in indoor flow-through channels fed with stream water as described in Gil-Allué et al. (2015). The colonized slides were sampled after 4 weeks and submerged in PERIQUIL to acclimatize the periphyton to the experimental conditions for 24 hours before exposure to AgNP or  $\text{AgNO}_3$ . For the silver exposure, colonized slides were placed in polystyrene microcosms (180 x 134 x 60 mm; Semadeni AG, Ostermundigen, Switzerland) filled with 300 mL of PERIQUIL. This exposure medium was renewed every three days to maintain optimal concentrations of nutrients, and water chemistry was analyzed in the removed medium. Periphyton was exposed at 15 °C and 12-hour light/dark photoperiod with a photosynthetically active radiation (PAR) intensity of 60  $\mu\text{mol photons m}^{-2}$

s<sup>-1</sup> under BioSun fluorescent tubes (MLT Moderne Licht-Technik AG, Wettingen, Switzerland), and tridimensional rotation at 20 rpm with a vertical angle of 5° to mimic turbulent flow across the periphyton surface (Three-Dimensional Orbital Shaker, Edmund Bühler GmbH, Hechingen, Germany). Experiments were carried out twice (experiments 1 and 2) to examine the response variability between independently colonized periphyton communities. A diagram with the timeline of the experiments is shown in Figure B.1.

### **Effects of AgNP and AgNO<sub>3</sub> on periphyton during long-term exposure (Experiment 1)**

In the first experiment, the effects of AgNP on the biological functions of periphyton after a long-term exposure were assessed. Periphyton was exposed to AgNP (0.1, 1 and 10 µM) or AgNO<sub>3</sub> (0.1 µM) by placing six colonized slides in three microcosms per treatment and time point. Silver concentrations were selected based on a previous study, indicating less than 20 % inhibition of photosynthetic yield and respiration after 2 hours of exposure to 12.5 µM AgNP and 0.1 µM AgNO<sub>3</sub> (Gil-Allué et al. 2015). After 7 and 21 days of exposure, periphyton was scraped off the slides with a polystyrene spatula. The pooled samples of the six slides from a given microcosm were homogeneously suspended in 50 mL of PERIQUIL and these suspensions were used for quantification of silver distribution in periphyton and measurement of effects of silver on biological functions and community structure.

### **Assessment of pollution-induced community tolerance of periphyton communities after long-term exposure to AgNP and AgNO<sub>3</sub> (Experiment 2)**

Experiment 2 was carried out to investigate the effects of long-term exposure to AgNP and AgNO<sub>3</sub> on the development of (co-)tolerance to AgNP, AgNO<sub>3</sub> and CuSO<sub>4</sub>. Six microcosms per treatment with eight colonized slides each were used to expose periphyton to 10 µM AgNP and 0.1 µM AgNO<sub>3</sub>. After 21 days, the slides from two microcosms were scraped and pooled into 200 mL PERIQUIL. A total of three suspensions per treatment were obtained as biological replicates to be used for all the measurements. The silver distribution, biological functions, and community structure of periphyton were assessed at the end of the exposure. Tolerance towards AgNP, AgNO<sub>3</sub>, and CuSO<sub>4</sub> was assessed in short-term toxicity tests to quantify the sensitivity of various functional endpoints. Aliquots of 10 mL of periphyton suspension of comparable biomass (OD<sub>700nm</sub> = 0.7), were transferred to 15 mL centrifugation tubes, where exposure to several concentrations of AgNP (12.5, 25, 50, 100 and 200 µM), AgNO<sub>3</sub> (1.25, 2.5, 5, 10 and 25 µM) or CuSO<sub>4</sub> (12.5, 25, 50, 100 and 200 µM) took place during 2 hours at 15 °C and in the light. At the end of the 2-hour exposure, the response of AgNP- and AgNO<sub>3</sub>-preexposed, and control periphyton was measured for selected endpoints: photosynthetic yield, respiration, primary production and secondary production. The comparison of sensitivities among the periphyton communities was done based on the EC<sub>50</sub> values for a certain chemical and end point.

### **Silver distribution in medium and periphyton**

Silver was quantified in medium and periphyton suspensions after 21 days of exposure to



assess the distribution of silver in periphyton during both experiments. Total silver in medium at the end of the exposure was quantified in a 1-mL aliquot from each microcosm by ICP-MS after acidic digestion. A volume of 10 mL of periphyton suspension from each biological replicate was centrifuged for 10 minutes at  $1880 \times g$  to separate different periphyton fractions (Stewart et al. 2015). A diagram of the fractionation process is shown in Figure B.2. The soluble fraction of the EPS was collected from the supernatant after the first centrifugation. The periphyton pellet was washed with 10 mL of 25  $\mu\text{M}$  DMPS to complex the strongly sorbed  $\text{Ag}^+$  ions, based on the high affinity of the two thiol groups in DMPS to  $\text{Ag}^+$  ions (Mason & Jenkins 1995). After centrifugation, the supernatant was collected in a new 15-mL centrifugation tube, and the pellet was resuspended in 10 mL of PERIQUIL as an additional washing step. The non-DMPS-exchangeable silver fraction in the pellet after the last centrifugation step represents the fraction of total silver either strongly associated or internalized in the biomass. Total silver in the supernatant samples was quantified in 1-mL aliquots by ICP-MS after acidic digestion. Periphyton pellets were lyophilized and weighed before acidic digestion and ICP-MS quantification of total silver.

### Biological functions of periphyton

Photosynthesis was assessed by measuring the quantum yield of photosystem II with a portable fluorometer (PHYTO-PAM; Heinz Walz GmbH, Effeltrich, Germany). Suspensions were allowed to acclimate to ambient light conditions for 15 min before taking measurements. The quantum yield ( $\phi$ ) was calculated as:

$$\phi = (F_m - F_t) / F_m$$

where  $F_m$  is the basal fluorescence and  $F_t$  is the instantaneous fluorescence (Schreiber 1998).

Respiration potential was measured by using the MicroResp approach (Tlili et al. 2011), a colorimetric method based on the diffusion of  $\text{CO}_2$  produced from respiration into a detection gel, which causes a decrease in pH and a change of absorbance at 572 nm. Respiration from 500  $\mu\text{L}$  of periphyton suspensions contained in a microplate (Nunc™ DeepWell, Thermo Scientific Inc.) was induced by adding 25 mM glucose as a carbon source. Absorbance of the MicroResp detection gels was measured at 572 nm on a Tecan Infinite 200 PRO microplate reader (Tecan Trading AG, Männedorf, Switzerland) before and after incubation for 18 hours at 25 °C in the dark. Four analytical replicates were prepared and measured. The average change in absorbance was normalized to the ash-free dry mass (AFDM) of the periphyton and expressed as  $\mu\text{g CO}_2 \text{ mg}^{-1} \text{ AFDM h}^{-1}$ .

Community level physiological profiles (CLPP) of the heterotrophic components of periphyton communities were obtained through substrate-induced respiration (SIR) using the MicroResp system (Tlili et al. 2011). A set of 17 substrates (*i.e.*, citric acid, D-galactose, D-galacturonic acid, D-glucose, D,L- $\alpha$ -glycerol phosphate, D-lactose, D-mannitol, glucose-1-phosphate, N-acetyl-D-glucosamine, putrescine, pyruvic acid methyl ester, D-xylose, MOPS, glycine, sucrose, and sorbitol) were selected to represent different degradation pathways and environmentally relevant processes to obtain a profile of the degradation capacities of different periphyton

communities (Insam 1997). Similarly to respiration measurements, substrate in a concentration of total carbon of 25 mM was offered to periphyton suspensions and the diffused CO<sub>2</sub> produced from substrate degradation was quantified by a change of absorbance at 572 nm in the MicroResp detection gel after a 18-hour incubation. Three analytical replicates were prepared and measured. The average change in absorbance was normalized to the AFDM of the periphyton and expressed as percentage of the basal respiration, *i.e.*, respiration in the absence of added substrate.

Potential activities of the extracellular enzymes  $\beta$ -glucosidase (GLU), alkaline phosphatase (AP) and leucine aminopeptidase (LAP), which are involved in C, P and N cycling, were assayed by means of fluorescent substrate analogues (*i.e.* 4-methylumbelliferyl- $\beta$ -D glucopyranoside, L-leucine-7-amido-4-methylcoumarin hydrochloride and 4-methylumbelliferyl phosphate disodium salt, respectively) (Romaní et al. 2004). One-mL aliquots of the periphyton suspensions were incubated at saturating concentrations of the substrate analogues (1 mM) at 25 °C in the dark. After 40 min, the enzymatic reactions were stopped by adding 1 mL of 1 M glycine buffer (pH 10.55) and centrifuging the periphyton suspensions for 10 min at 24000  $\times$  g (Microcentrifuge 2417R, Eppendorf, Hamburg, Germany). Aliquots of the supernatant (200  $\mu$ L) were transferred to a black 96-well microplate (Greiner-Bio-One GmbH, Frickenhausen, Germany) to measure fluorescence of the enzymatic products at excitation/emission wavelengths of 366/442 nm, in the case of GLU and AP, or 340/436 nm for LAP.

Primary production of autotrophs was measured by <sup>14</sup>C incorporation into carbohydrates (Dorigo & Leboulanger 2001). A 2-mL aliquot of each periphyton suspension was transferred to 20 mL scintillation vials (Perkin Elmer, Waltham, MA), and 25  $\mu$ L of NaH<sup>14</sup>CO<sub>3</sub> (2.09 GBq mmol<sup>-1</sup>, Hartmann Analytic GmbH, Braunschweig, Germany) was added to reach a radioactivity of 0.25  $\mu$ Ci mL<sup>-1</sup>. Vials were incubated with the labelled inorganic carbon source in the light during 1 hour to allow periphyton to perform photosynthesis. The reaction was stopped by adding formaldehyde (3.7% final concentration), followed by 200  $\mu$ L glacial acetic acid to remove the <sup>14</sup>C carbon that was not incorporated. Periphyton suspensions were dried overnight at 60 °C before adding 1 mL of DMSO and incubating for one more hour at 60° to dissolve the labelled organic matter. A volume of 15 mL of scintillation cocktail (Ultima Gold LLT, Perkin Elmer) was added to each sample, and <sup>14</sup>C was quantified on a Tri-Carb 2200CA liquid scintillation counter (Packard, Rockville, MD). Primary production was expressed as the <sup>14</sup>C incorporation in  $\mu$ g <sup>14</sup>C g<sup>-1</sup> AFDM day<sup>-1</sup>.

Secondary production of heterotrophs was measured by the incorporation of <sup>14</sup>C-labelled leucine into proteins (Buesing & Gessner 2003). An aliquot of 2.9 mL of periphyton suspension was transferred into a glass scintillation vial. Before the incubation, controls were prepared where the incorporation of leucine was prevented by the addition of trichloroacetic acid (TCA, 5%). Samples were incubated in the dark at 15 °C in the presence of 50  $\mu$ M leucine containing 4.5  $\mu$ M <sup>14</sup>C-leucine (12.36 GBq mmol<sup>-1</sup>, Hartmann Analytic GmbH, Braunschweig, Germany) to reach a radioactivity of 0.23  $\mu$ Ci mL<sup>-1</sup>. After 30 minutes of incubation, leucine incorporation was stopped in all the samples with the addition of TCA to a final concentration of 5 %. Periphyton suspensions were filtered onto 0.2  $\mu$ m polycarbonate filters (Whatman, Maidstone, UK), and

rinsed sequentially with 2 mL TCA (5%), 1 mL leucine (40 mM), 1 mL ethanol (80%), and 1 mL nanopure water to remove the  $^{14}\text{C}$ -leucine that was not incorporated. Polycarbonate filters containing periphyton were transferred to 2-ml screw-cap microcentrifuge tubes (Carl Roth, Karlsruhe, Germany) containing 1.5 mL of a mixture of sodium dodecyl sulfate (0.1 %), EDTA (25 mM) and NaOH (0.5 M). Samples were heated 1 hour at 90°C to dissolve the proteins and, once they reached ambient temperature, centrifuged for 10 min at 14000  $\times$  g. A volume of 250  $\mu\text{L}$  from the supernatant was transferred to scintillation vials and mixed with 5 ml Hionic Fluor scintillation cocktail (Perkin Elmer). Radioactivity was determined using a Tri-Carb 2200CA liquid scintillation counter (Packard, Rockville, MD). Secondary production was expressed as the  $^{14}\text{C}$  incorporation in  $\mu\text{g } ^{14}\text{C g}^{-1} \text{AFDM day}^{-1}$ .

Ash-free dry mass of periphyton (AFDM) was quantified in 1-mL aliquots of the suspensions collected on pre-weighed glass fiber filters (GF/F, 25 mm diameter, 0.7  $\mu\text{m}$  average pore size; Whatman Ltd., Maidstone, UK). AFDM was calculated as the difference between the weight of filters dried for 24 hours at 105 °C, and after combusting the organic matter for 1 hour at 480 °C in a muffle furnace (LE 1/11, Nabertherm GmbH, Lilienthal, Germany). Periphyton biomass was expressed as AFDM per area of colonized glass, g AFDM  $\text{m}^{-2}$ .

### **Periphyton community analysis**

Molecular fingerprints of the periphyton community were obtained through denaturing gradient gel electrophoresis (DGGE) (Muyzer et al. 1993). DNA was extracted from the pellets of 2-mL periphyton suspension aliquots after centrifuging for 30 minutes at 24000  $\times$  g, using a commercial kit (PowerBiofilm DNA Isolation Kit, MO BIO Laboratories, Carlsbad, CA). Conserved 18S and 16S rDNA fragments were amplified using the universal primer pairs Euk1Af/Euk516r-GC and 341f-GC/907rM for eukaryotes and prokaryotes, respectively, which are commonly used in the literature (Amann et al. 1990, Muyzer & Smalla 1998, Schauer et al. 2003, Sogin & Gunderson 1987). PCR products were loaded in acrylamide gels containing a concentration gradient of a denaturing agent (7 M urea and 40 % formamide, Axon Lab, Baden, Switzerland). Denaturing gradients were 40-65 % in gels for the separation of 18S rDNA fragments and 40-80 % for 16S fragments. Electrophoresis was run for 18 hours at 100 mV (DCodeSystem, BioRad, Hercules, CA). DNA in the acrylamide gels was stained using SYBR Gold (VWR, Radnor, PA) and imaged (Molecular Imager Gel Doc XR, BioRad). Images were processed with the software ImageJ (Abramoff et al. 2004), bands were identified, and the absence/presence in the different samples was recorded.

Photosynthetic pigments were measured as a proxy for the composition of the autotrophic community in periphyton, based on the three main phototroph groups typically present in periphyton: cyanobacteria, diatoms and green algae (Dorigo et al. 2007). Pigments were extracted from 5 mL of periphyton suspension by centrifuging for 30 minutes at 15000  $\times$  g to remove excess water, adding 4 mL of methanol : 0.5 M ammonium acetate (98 : 2, v:v), and sonicating for 1 min at 100 W and 50 % activity (Labsonic M, Sartorius Stedim, Tagelswangen, Switzerland). Extracts were purified by centrifuging for 10 minutes at 3220  $\times$  g, and filtering

through a 0.2 µm PFTE filter (CHROMAFIL, Macherey-Nagel AG, Oensingen, Switzerland). Pigment extracts were analyzed using high-performance liquid chromatography (HPLC) (Garrido & Zapata 1993). Pigments were separated through a Nucleodur C<sub>18</sub>-ec column with 5 µm particle size and dimensions of 250 mm of length and 4 mm i.d. (Macherey-Nagel AG, Oensingen, Switzerland) following a binary gradient elution. The gradient elution program started isocratically with 100% of eluent A (methanol : acetonitrile : 1 M ammonium acetate, 5 : 3 : 2) during 2 min, followed by a gradient to reach 100% of eluent B (acetonitrile : ethyl acetate, 1 : 1) after 26 min, and 100% B was held for 5 min more. After each run, the mobile phase gradually returned to 100% A during 10 min, and it was held isocratically for 2 minutes. Pigments were monitored by absorption at 440 ± 20 nm, and identified according to their retention times and through pigment standards for chlorophyll a, lutein, fucoxanthin, and zeaxanthin (DHI Lab Products, Hoersholm, Denmark). Chlorophyll a was quantified as mg chlorophyll a g<sup>-1</sup> AFDM and served as a proxy for algal biomass (Kasprzak et al. 2008), while chlorophyll b and lutein, fucoxanthin, and zeaxanthin were used as markers for green algae, diatoms and cyanobacteria, respectively (Dorigo et al. 2007). Four additional pigments were quantified for structural comparison purposes, but were not identified (*i.e.*, unknown 1, which is a chlorophyll c-like pigment, and unknowns 2 to 4, which are xanthophyll-like pigments). The peak area of each pigment was quantified and expressed as the percentage of the total peak area.

### Data analysis

Toxicity parameters and statistical significance were assessed using SigmaPlot for Windows version 12.0 (Systat Software Inc., San Jose, CA). Effects of AgNP and AgNO<sub>3</sub> on functional parameters after long-term exposure were expressed as absolute values, and statistical significance was tested using one-way ANOVA followed by Dunnett's test for post-hoc multiple comparisons between treatments.

In the short-term bioassays, the effects of AgNP, AgNO<sub>3</sub> and CuSO<sub>4</sub> were measured as percentage activity relative to controls. The corresponding concentration-response curves were fitted to a logistic model to derive the concentrations causing 50 % inhibition relative to the controls (EC<sub>50</sub>):

$$Activity (\%) = 100\% / [1 + ([Me] / EC_{50})^{-H}]$$

where *[Me]* is the concentration of metal (*i.e.*, AgNP, AgNO<sub>3</sub>, or CuSO<sub>4</sub>) in the treatment and *H* is the Hill slope of the curve. A statistically significant difference between the EC<sub>50</sub> values of exposed and non-exposed periphyton communities for the same chemical was assumed when the 95% confidence intervals did not overlap.

In the case of a non-monotonic concentration-response relationship, the Cedergreen-Ritz-Streibig model describing hormesis was used (Cedergreen et al. 2005):

$$Activity (\%) = (100\% + f e^{-1/[Me]}) / (1 + e^{a[\ln([Me]) - \ln(b)]})$$

where *a* and *b* are parameters related to the steepness of the curve and the EC<sub>50</sub> value, respectively. The estimation of the EC<sub>50</sub> value was resolved using the package "drc" (Ritz & Streibig 2005) in R (R Core Team 2014).

DGGE and pigment analysis data were submitted to detrended correspondence analysis (DCA). Maximum gradient length was smaller than three standard deviations for all measured parameters, indicating that linear methods were appropriate. Principal component analysis (PCA) was then performed using the software CANOCO version 4.5 (Ter Braak & Smilauer 1998).

Additionally, quotients of similarity ( $QS$ ) between pairs of treatments based on DGGE data were calculated using the Sørensen index (Sørensen 1948):

$$QS = 2C / (A + B)$$

where  $A$  and  $B$  are the number of DGGE bands present in samples  $A$  and  $B$ , and  $C$  is the number of common DGGE bands to both samples.

### 3.3 Results

#### Silver nanoparticle characterization

AgNP size in 1 and 10  $\mu\text{M}$  suspensions remained stable in the fresh PERIQUIL, with an average diameter of  $49 \pm 1$  to  $73 \pm 5$  nm, up to 72 hours (Figure 3.1). Similarly, the 10  $\mu\text{M}$  AgNP suspension in conditioned PERIQUIL maintained an average diameter below 100 nm, ranging from  $68 \pm 3$  to  $81 \pm 3$  nm. In the 1  $\mu\text{M}$  AgNP dilution in conditioned PERIQUIL, particles immediately formed larger agglomerates with an average size of  $131 \pm 23$  nm, which increased in size to  $264 \pm 38$  nm after 72 hours. NTA measurements showed agglomeration in 1 and 10  $\mu\text{M}$  AgNP suspensions in conditioned PERIQUIL (Figure B.3 in Appendix B).  $\zeta$ -potential of AgNP suspensions ranged between  $-5 \pm 1$  and  $-18 \pm 1$  mV, being more neutral in conditioned medium and in the lower AgNP concentration (Figure 3.1). UV-Vis spectra of 10  $\mu\text{M}$  AgNP suspensions showed characteristic plasmon resonance peaks for AgNP in the range of 414 and 419 nm (Figure B.3). AgNP suspensions in conditioned PERIQUIL showed an increased absorbance at larger wavelengths, indicating agglomeration. Overall, AgNP were less stable in suspensions of lower AgNP concentrations and in the presence of secreted biomolecules in the conditioned PERIQUIL, which led to the formation of agglomerates.

Dissolved Ag(I) in AgNP suspensions, as determined by ultrafiltration, was 1 % of the total silver at the start of the exposure and increased to  $11 \pm 1$  and  $9 \pm 1$  % after 72 hours in fresh and conditioned PERIQUIL, respectively. The calculated speciation of dissolved Ag(I) was comparable across the range of concentrations tested and it revealed that two silver species were dominant: 52 to 54 % of dissolved Ag(I) was present as free  $\text{Ag}^+$  ion, and 43 to 45 % as  $\text{AgCl}(\text{aq})$  (Table B.3). No significant precipitation of solid species of silver was predicted. Water chemistry was comparable across the three treatments during the experiment 2 (Table B.2). Concentrations of  $\text{Ca}^{2+}$  were higher in conditioned than in fresh medium at 7 days, due to equilibration between periphyton and PERIQUIL. Periphyton accumulated relatively high amounts of  $\text{Ca}^{2+}$  from Chriesbach water, which was used for the colonization.

#### Silver distribution in periphyton

The largest fraction of silver in microcosms of the AgNP treatment at the end of the 21-day

exposure in experiment 1 was measured in the non-DMPS-exchangeable silver fraction in periphyton ( $84 \pm 6$  to  $98 \pm 1$  % of total silver) (Table 3.1). Less than 5 % was present in the soluble EPS or sorbed to periphyton, and  $1.0 \pm 0.4$  to  $14 \pm 7$  % was measured in the exposure medium. The silver distribution in the  $0.1 \mu\text{M}$   $\text{AgNO}_3$  treatment was comparable to the AgNP treatments, with  $93 \pm 1$  % of total silver quantified in the non-DMPS-exchangeable fraction, 1 % in the soluble EPS or sorbed to periphyton, and 5 % in medium. Silver distribution was also comparable between experiments 1 and 2.

The non-DMPS-exchangeable fraction of silver in control periphyton was  $0.17 \pm 0.06 \text{ nmol Ag mg}^{-1}$  AFDM. Silver accumulation in periphyton (non-DMPS-exchangeable fraction) upon exposure to 0.1, 1 and  $10 \mu\text{M}$  AgNP was  $5.99 \pm 0.63$ ,  $47.86 \pm 4.87$  and  $3717 \pm 658 \text{ nmol Ag mg}^{-1}$  AFDM, respectively. In the case of  $0.1 \mu\text{M}$   $\text{AgNO}_3$ ,  $5.47 \pm 0.89 \text{ nmol Ag mg}^{-1}$  AFDM were measured. Accumulation of silver at the same total silver concentration ( $0.1 \mu\text{M}$ ) was comparable, whether dosed as AgNP or  $\text{AgNO}_3$ . The concentrations measured in periphyton in the  $0.1 \mu\text{M}$   $\text{AgNO}_3$  and  $10 \mu\text{M}$  AgNP treatments in experiment 2 were  $83.25 \pm 22.25$  and  $4997 \pm 93 \text{ nmol Ag mg}^{-1}$  AFDM, respectively. Therefore, silver accumulation in the  $10 \mu\text{M}$  AgNP treatment was also comparable between both experiments, while the accumulation in the  $0.1 \mu\text{M}$   $\text{AgNO}_3$  treatment was one order of magnitude lower in the experiment 2.

### Effects of AgNP and $\text{AgNO}_3$ on biological functions of periphyton

Control periphyton in experiment 1 showed an increased photosynthetic yield, and AP and LAP activities after 21 days, compared to the start of the experiment, while respiration and GLU remained constant (Table B.4). At the start of the experiment, average periphyton biomass was  $2.60 \pm 0.08 \text{ g AFDM m}^{-2}$ , which increased to  $3.05 \pm 0.46 \text{ g AFDM m}^{-2}$  at the end of the exposure.

After 7 days, no inhibitory effects of AgNP exposure were observable, except for a 10 % decrease of the SIR of glycerol phosphate by  $1 \mu\text{M}$  AgNP, and a 15 % of glucose-1-phosphate in the CLPP of periphyton exposed to 1 and  $10 \mu\text{M}$  AgNP (Figures B.4 and B.5). However, a stimulation of respiration of between 4 and 25 % by all AgNP treatments was observed, which was not concentration-dependent (Figure B4). Similarly,  $0.1 \mu\text{M}$  AgNP increased the SIR of D-mannitol, and  $10 \mu\text{M}$  of D-glucose, D-lactose, D-galactose, N-acetyl-D-glucosamine, D-xylose and sucrose up to 20 %.

After 21 days, periphyton exposed to  $0.1 \mu\text{M}$  AgNP did not show differences in biological functions compared to control communities, except for a  $25 \pm 10$  % decrease of LAP activity (Figure 3.2). Exposure to  $1 \mu\text{M}$  AgNP only caused effects to respiration, with a  $36 \pm 1$  % inhibition. However,  $10 \mu\text{M}$  AgNP caused effects on most parameters. A 90 % increase in the biomass of periphyton exposed to  $10 \mu\text{M}$  AgNP compared to control periphyton was observed after 21 days, reaching  $5.80 \pm 1.50 \text{ g AFDM m}^{-2}$ . This biomass increase was accompanied by a slight increase of the photosynthetic yield ( $8.5 \pm 3.2$  %) and a marked increase,  $246 \pm 78$  %, of the secondary production. Inhibitory effects were observed in the case of respiration, which was reduced by  $61 \pm 1$  %, and primary production, which decreased by  $63 \pm 6$  %. After 21 days, SIR was generally lower than at 7 days and no significant effects caused by AgNP were observed (Figure 3.3).

Periphyton exposed to 0.1  $\mu\text{M}$   $\text{AgNO}_3$  showed signs of inhibition of respiration after 7 days, with a  $18 \pm 2$  % decrease. After 21 days, inhibition of respiration increased to  $31 \pm 1$  %. No other toxic effects were observed, except for a  $40 \pm 7$  % inhibition of LAP activity. 0.1  $\mu\text{M}$   $\text{AgNO}_3$  also caused a 16 % increase in SIR was measured in the presence of glycerol phosphate.

The relative change in responses of biological functions in experiment 2 differed from experiment 1, but followed similar trends despite being two independently colonized periphyton communities (Figure B.6).

### **Effects on the periphyton community structure**

The analysis of the pigment composition in periphyton across treatments showed no differences in chlorophyll a content relative to AFDM of periphyton after 21 days of exposure to 10  $\mu\text{M}$  AgNP or 0.1  $\mu\text{M}$   $\text{AgNO}_3$  (Figure B.7).

For the structural analysis of the phototrophic components of periphyton by PCA, a total of seven pigments were considered. Zeaxanthin, the marker pigment for cyanobacteria, could not be quantified in any of the samples, indicating a very low abundance of these organisms in periphyton, while lutein, used as one of two markers for green algae, was not detected in any of the samples from experiment 2 (Table B.5). Measurements from experiment 2 were used for the study of tolerance study and are shown in Figure 3.4. The two first principal components (PC) accounted for 98 % of the total variance in the measurements. No clear separation of treatments by PC1 was found. However, PC2, separated the AgNP treatment from the control and  $\text{AgNO}_3$  treatments (Figure 3.4). PC2 was negatively correlated with chlorophyll b content in the samples. Control communities from experiments 1 and 2 were comparable in their pigment content (Figure B.8). In the PCA analysis of data from experiment 1, the first two PC accounted for 82 % of the variance. No separation of communities by treatment was observed along PC1, but there was a separation of AgNP treated communities from controls in PC2. PC2 was negatively correlated to lutein content.

The molecular community fingerprints obtained by DGGE (Figure 3.5) indicated that prokaryotic and eukaryotic communities differed among the treatments after 21 days of exposure in experiment 2. A total of 27 bands were identified in the eukaryotic gel (18S rDNA), while 38 were identified in the prokaryotic DGGE gel (16S rDNA). When DGGE fingerprints of eukaryotic communities were analyzed by PCA, the two first PCs accounted for 66 % of the total variance. PC1 showed a separation of the control and the 0.1  $\mu\text{M}$   $\text{AgNO}_3$  treated communities from the 10  $\mu\text{M}$  AgNP-treated, while control and  $\text{AgNO}_3$ -exposed periphyton were separated in PC2. Quotients of similarity between treatments were 0.86 for control and AgNP, 0.82 for control and  $\text{AgNO}_3$ , and 0.75 between AgNP and  $\text{AgNO}_3$ . In the analysis of DGGE community fingerprints of prokaryotes, the two first PCs accounted for 61 % of the total variance. Similarly, PC1 separated control and  $\text{AgNO}_3$  from AgNP, while PC2 separated all three treatments from each other. Quotients of similarity between treatments were 0.93 for control and AgNP, 0.88 for control and  $\text{AgNO}_3$  and 0.87 between AgNP and  $\text{AgNO}_3$ .

DGGE fingerprints of eukaryotes and prokaryotes in control communities from experiment 1

and 2 differed from each other, with a quotients of similarity of 0.62 and 0.84, respectively (Figure B.9). Similarly to experiment 2, there was a difference in eukaryotic and prokaryotic communities among the three treatments. In the case of eukaryotes, PC1 and PC2 accounted for 63 % of the variance. PC1 separated control treatment from both AgNP and AgNO<sub>3</sub> treatments, while all three treatments were separated along PC2. Quotients of similarity between treatments were 0.62 for control and AgNP, 0.71 for control and AgNO<sub>3</sub>, and 0.83 between AgNP and AgNO<sub>3</sub>. In the case of prokaryotes, the first two PC accounted for 82 %. PC1 separated AgNP treatment from the control, while PC2 separated all three treatments. Quotients of similarity between treatments were 0.33 for control and AgNP, 0.81 for control and AgNO<sub>3</sub> and 0.41 between AgNP and AgNO<sub>3</sub>.

### **Assessment of pollution induced community tolerance to AgNP, AgNO<sub>3</sub> and CuSO<sub>4</sub>**

The short-term sensitivity of functional endpoints, expressed as EC<sub>50</sub>, in control periphyton communities at the end of the 21-day experiment 2, are shown in Table 3.2. AgNO<sub>3</sub> showed a higher toxicity than AgNP and CuSO<sub>4</sub> to all functional parameters investigated, while AgNP and CuSO<sub>4</sub> showed similar EC<sub>50</sub> values. Long-term exposure of periphyton to 10 µM AgNP caused an increased tolerance to subsequent exposure to higher concentrations of AgNP and AgNO<sub>3</sub> compared to control periphyton, based on secondary production measurements. EC<sub>50</sub> values of these communities were 3 and 3.6 times higher than those of communities from the AgNO<sub>3</sub> treatment and control. Communities from the AgNP treatment were more tolerant to further AgNP exposure based on primary production measurements, with a 2.4 times increase of the EC<sub>50</sub> value. These communities also displayed a non-monotonic response of respiration towards AgNP, AgNO<sub>3</sub> and CuSO<sub>4</sub> (Figure B.10). EC<sub>50</sub> values could not be calculated in the case of AgNP and AgNO<sub>3</sub>, since all the concentrations caused a stimulation of respiration over 100 %. In the case of CuSO<sub>4</sub>, an EC<sub>50</sub> of 106 µM was estimated, indicating a 2.1 times increase compared to the EC<sub>50</sub> of 50 µM in the control community. Long-term exposure to AgNO<sub>3</sub> did not have an impact on the tolerance of periphyton to AgNO<sub>3</sub>, AgNP or CuSO<sub>4</sub>, except for a slight increase in sensitivity of the secondary production to AgNP, with an EC<sub>50</sub> value 1.4 times lower than the control community.

### **3.4 Discussion**

In the present study, we investigated the potential of periphyton to accumulate silver upon long-term exposure to AgNP and AgNO<sub>3</sub>, as well as the subsequent impacts on relevant biological functions and community structure of periphyton. Quantification of silver distribution in microcosms after the 21-day exposure revealed that AgNP was efficiently accumulated in periphyton. A high accumulation of metals in periphyton has been described in the literature (Bradac et al. 2009b, Meylan et al. 2003, Ramelow et al. 1987, Serra et al. 2009), but limited evidence exists in the case of nanomaterials (Ferry et al. 2009). This finding is not expected to be caused by sedimentation on the surface of periphyton, but rather by a diffusion of AgNP in the periphyton, since exposure were carried out under shaking and periphyton was



thoroughly washed before metal measurements. The ability of AgNP to diffuse in biofilms depends on its agglomeration state (Peulen & Wilkinson 2011). Agglomeration was more important in the lower AgNP concentrations and in conditioned PERIQUIL, and could have been enhanced by the higher  $\text{Ca}^{2+}$  concentrations at the beginning of the experiment originated from periphyton, which was colonized in Chriesbach water, impairing the diffusion of AgNP in the periphyton (Piccapietra et al. 2012b). However, in the present study, AgNP and  $\text{AgNO}_3$  were accumulated in periphyton in comparable amounts when dosed at the same total silver concentration, indicating no limitation of diffusion.

Differences in the bioavailability of silver to periphyton organisms are expected to occur, despite the total silver content in periphyton being similar at equimolar AgNP and  $\text{AgNO}_3$  concentrations. In the case of  $\text{AgNO}_3$ , calculations on the speciation of dissolved silver in PERIQUIL revealed that two species dominated the soluble silver species, the free  $\text{Ag}^+$  ion and  $\text{AgCl(aq)}$ . Free  $\text{Ag}^+$  ions are taken up rapidly and are highly toxic to microorganisms (Piccapietra et al. 2012a), while  $\text{AgCl(aq)}$  has a lower toxicity due to its limited bioavailability (Bradford et al. 2009, Chambers et al. 2014, Lee et al. 2004). Bioavailability of  $\text{Ag}^+$  can also be reduced by complexation to exudated molecules in exposure medium or to the EPS (Lombardi et al. 2005, Zhang et al. 2012), and by reduction of dissolved  $\text{Ag}^+$  ions to nanosized  $\text{Ag}^0$  (Adegboyega et al. 2013, Kroll et al. 2014). However, in the present study, the soluble fraction of the periphyton EPS showed a limited complexing capacity for dissolved  $\text{Ag}^+$  ions, which is comparable to findings from a study on lead accumulation in periphyton carried out in our laboratory (Stewart et al. 2015). In the case of AgNP, although most of the silver in periphyton was associated with the biomass, there is limited evidence in the literature for the internalization of AgNP in algae and bacteria (Piccapietra et al. 2012a, Ribeiro et al. 2015). However, AgNP in the close vicinity of organisms are susceptible of being oxidized by metabolic products like as  $\text{H}_2\text{O}_2$  (He et al. 2012). The oxidation of AgNP can lead to high local concentrations of  $\text{Ag}^+$  ions, which are rapidly taken up by microorganisms (Piccapietra et al. 2012a).

Long-term exposure experiments of periphyton showed that the activity of LAP, respiration and CLPP were the only functional parameters affected by both AgNP and  $\text{AgNO}_3$ . In the case of LAP, the enzymatic activity was inhibited by 0.1 and 10  $\mu\text{M}$  AgNP and 0.1  $\mu\text{M}$   $\text{AgNO}_3$  after 21 days, though not in a concentration-dependent manner. A previous study revealed an AgNP-specific inhibition of the extracellular enzyme LAP in addition to toxicity by dissolved  $\text{Ag}^+$  ions (Gil-Allué et al. 2015). In the case of respiration and CLPP, a non-monotonic effect was observed in the presence of AgNP after 7 days, which is a response that has been previously reported for low concentrations of metals (Devi Prasad & Devi Prasad 1982). Inhibitory effects on respiration were concentration- and time-dependent. After 7 days, respiration was only inhibited by 0.1  $\mu\text{M}$   $\text{AgNO}_3$ , while after 21 days also by 1 and 10  $\mu\text{M}$  AgNP. The late manifestation of AgNP inhibitory effects was expected considering the continuous renewal of the exposure medium and an accumulation of silver in periphyton during the 21 days. Despite the decrease of respiration, exposure to 10  $\mu\text{M}$  AgNP caused an increase of secondary

production after 21 days, which was accompanied by an increase in biomass. Enhanced biomass accrual in bacterial communities upon AgNP exposure has been observed in previous studies (Colman et al. 2012, Das et al. 2012). At the same time, primary production decreased and no significant effects on photosynthesis were observed. These results show that mutual interactions within the community were disturbed by AgNP. The mechanisms of this disturbance are not understood. Earlier studies showed that under conditions of nutrient enrichment, there was a decoupling of algal-bacterial interactions in periphyton (Scott et al. 2008).

Community structures of the algal and bacterial components in periphyton exposed to AgNP and AgNO<sub>3</sub> diverged from the control after 21 days, further indicating effects on species interactions and interspecific differences in sensitivity to AgNP. Furthermore, periphyton communities exposed to 10 µM AgNP and 0.1 µM AgNO<sub>3</sub> also differed from each other, which could be due to distinct effects of AgNP and AgNO<sub>3</sub> on the periphyton community or a difference in the concentration of bioavailable silver. No significant differences were observed in the CLPP of periphyton communities after 21 days, highlighting the functional redundancy present in these communities despite the structural changes. Chlorophyll a content per unit of biomass in periphyton was comparable across all treatments, suggesting that the algal-bacterial ratios were also similar even when communities differed. A change in the major groups of autotrophs could be identified in the 10 µM AgNP treatment based on pigment content in the periphyton communities. In both experiments, a higher ratio of pigments related to green algae (*i.e.*, chlorophyll b and lutein) were quantified, indicating a relative increase of green algae in the periphyton community exposed to 10 µM AgNP. However, there is not enough evidence in the literature to conclude that general differences in sensitivity to AgNP exist among autotrophic groups.

The relationship between structure and tolerance of periphyton communities was analyzed to infer on causes of detected structural changes. In this study, long-term exposure to AgNP indeed caused an increased tolerance to AgNP, confirming the expectation based on the structural changes induced in AgNP treatments. The level of tolerance increase, which in this study was increased by a factor of 3, depends on various factors, such as biomass and input of new inoculum. In the present study, the periphyton community was well established and no organisms could enter the system. Nevertheless, the relative abundance of bacterial and algal species within each treatment might change. For instance, dormant bacteria in microbial communities can turn to a metabolic active state when conditions are favorable (Smith & Del Giorgio 2003). Such changes might favor the dominance of opportunistic species that are not particularly tolerant to AgNP. EC<sub>50</sub> values for metals have been reported to be more than two orders of magnitude higher in resistant bacteria compared to sensitive strains (Díaz-Raviña & Bååth 1996).

Co-tolerance, which is defined as the increased tolerance towards chemicals to which organisms were not previously exposed, was also examined between AgNP and Ag<sup>+</sup>. In the present study, co-tolerance between these two chemicals was not observed. Although most toxic effects of AgNP to periphyton are expected to be caused by dissolved Ag<sup>+</sup> ions (Gil-Allué et al. 2015),

long-term exposure to  $\text{AgNO}_3$  did not induce increased tolerance of the community towards AgNP, and in the case of secondary production, periphyton showed a slightly lower tolerance to AgNP compared to control periphyton. While tolerance decrease was minimal, it is plausible that slight decreases in diversity can cause a higher sensitivity towards a second stressor (Clements & Rohr 2009). Co-tolerance of periphyton to  $\text{CuSO}_4$  after long-term exposure to AgNP- or  $\text{AgNO}_3$  was examined considering the similarity of  $\text{Ag}^+$  and  $\text{Cu}^{2+}$  with regard to their uptake and molecular interactions in algae (Fortin & Campbell 2000, Pillai et al. 2014, Solioz & Odermatt 1995). However, no increased co-tolerance to  $\text{CuSO}_4$  in the  $\text{AgNO}_3$  treatment was observed in the present study, which was expected due to the lack of tolerance development to  $\text{Ag}^+$ . Differently, in a previous study, periphyton exposed to high concentrations of  $\text{CuSO}_4$  showed an increased co-tolerance to  $\text{Ag}^+$  (Soldo & Behra 2000). In the case of the AgNP treatment, periphyton communities showed a non-monotonic concentration-response relationship to  $\text{CuSO}_4$ , likely attributable to a hormetic response, which has been observed in other studies as an “overcompensation” in response to low toxic effects of metals (Devi Prasad & Devi Prasad 1982). Calculated  $\text{EC}_{50}$  values were indicative of an increased tolerance towards  $\text{Cu}^{2+}$ . The fact that periphyton exposed to AgNP but not that exposed to  $\text{AgNO}_3$  developed co-tolerance to  $\text{Cu}^{2+}$  might result from differences in total silver exposure concentration and in accumulation.

### **Environmental implications**

Although the concentrations applied in this study are higher than the estimated concentrations in surface waters for AgNP (Sun et al. 2014) and dissolved Ag(I) (Lanceleur et al. 2011, Tappin et al. 2010), limited effects were measured in periphyton functions after long-term exposure to AgNP and  $\text{AgNO}_3$ . PICT proved to be a sensitive tool to integrate functional and structural effects on the periphyton community. Periphyton efficiently accumulated AgNP, which corroborates the role of periphyton as an important entry of nanomaterials and metals in the trophic chain (Ferry et al. 2009, Kulacki et al. 2012). However, there is scarce knowledge on the effects of dietborne exposure to nanomaterials to aquatic organisms, which might be a more important uptake route than the water column due to reduced stability of nanomaterials in the aquatic environment.

### 3.5 Figures and tables

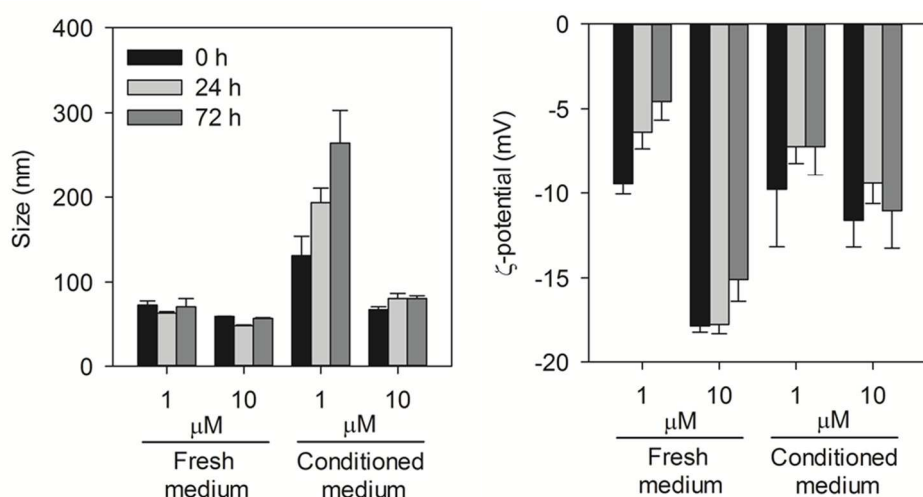


**Figure 3.1.** Comparison of  $\zeta$ -potential and particle diameters measured by DLS in 1 and 10  $\mu\text{M}$  AgNP suspensions of fresh and conditioned exposure medium (PERIQUIL) for 0 (black bars), 24 (light gray bars) and 72 hours (dark gray bars). Error bars correspond to standard deviations of three analytical replicates.

**Table 3.1.** Distribution of total silver in different fractions of periphyton and in exposure medium (PERIQUIL) after 21 days of exposure in both experiments. Standard deviations were calculated from three biological replicates.

Experiment	Treatment	Total Ag distribution (%)			
		Medium	EPS-associated	DMPS-exchangeable	Non-DMPS-exchangeable
1	0.1 $\mu\text{M}$ AgNP	14.3 $\pm$ 6.6	0.9 $\pm$ 0.2	0.4 $\pm$ 0.6	84.4 $\pm$ 6.2
	1 $\mu\text{M}$ AgNP	7.7 $\pm$ 3.4	3.0 $\pm$ 0.2	4.4 $\pm$ 2.2	85.0 $\pm$ 5.8
	10 $\mu\text{M}$ AgNP	1.0 $\pm$ 0.4	0.6 $\pm$ 0.1	0.5 $\pm$ 0.1	97.9 $\pm$ 0.5
	0.1 $\mu\text{M}$ AgNO <sub>3</sub>	5.4 $\pm$ 1.4	0.8 $\pm$ 0.1	1.0 $\pm$ 0.5	93.4 $\pm$ 1.2
2	10 $\mu\text{M}$ AgNP	2.4 $\pm$ 0.4	0.1 $\pm$ 0.1	0.6 $\pm$ 0.1	96.9 $\pm$ 1.0
	0.1 $\mu\text{M}$ AgNO <sub>3</sub>	4.2 $\pm$ 0.9	0.3 $\pm$ 0.1	0.2 $\pm$ 0.1	95.2 $\pm$ 1.0

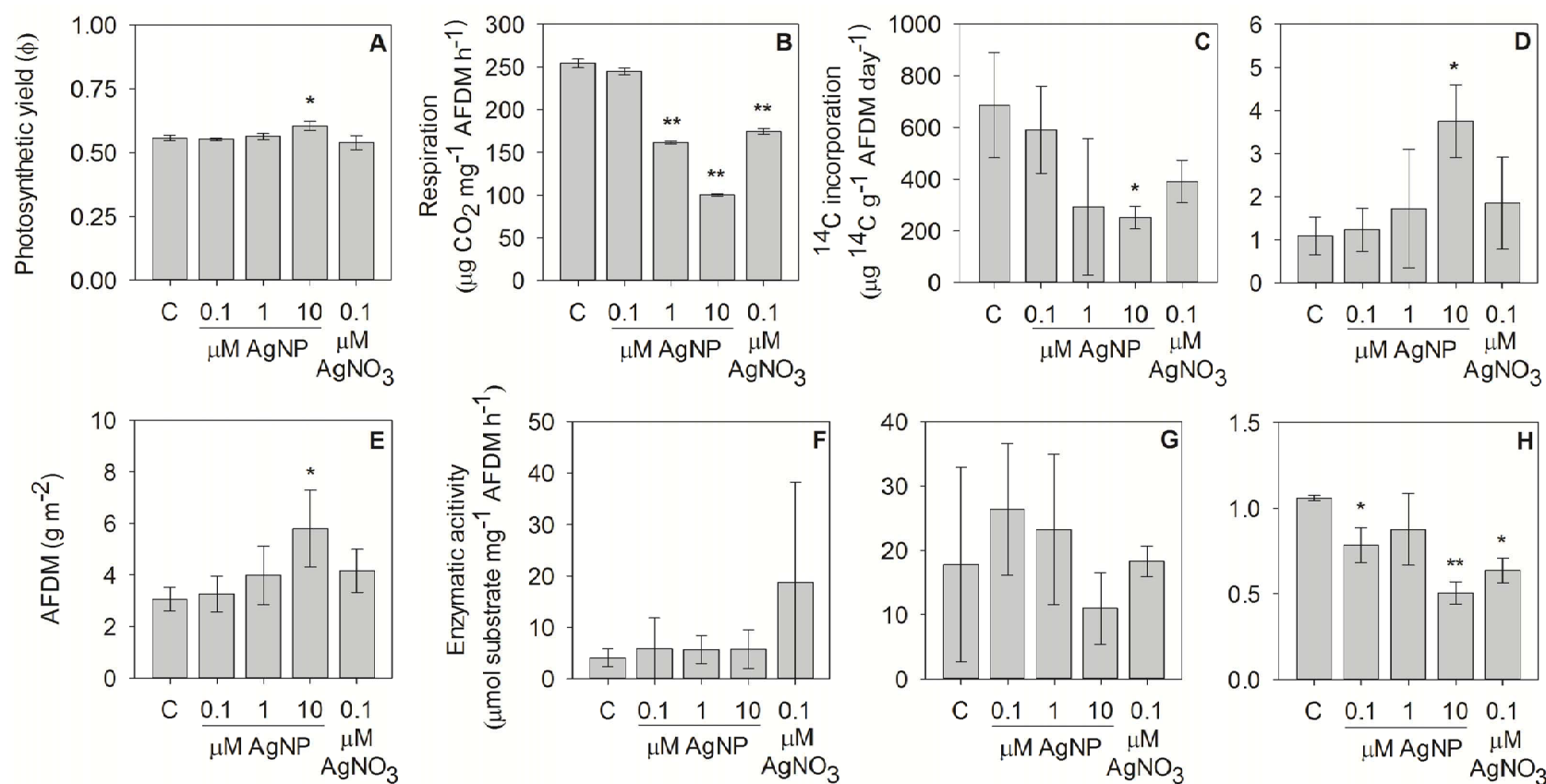


**Figure 3.2.** Effects of AgNP and AgNO<sub>3</sub> to periphyton after 21 days of exposure on photosynthetic yield (A), respiration (B), primary production (C), secondary production (D), ash-free dry mass (AFDM) (E), and the activity of extracellular enzymes β-glucosidase (F), alkaline phosphatase (G) and leucine aminopeptidase (H). Standard deviations correspond to three analytical replicates. Statistically significant differences between treatments and controls were assessed by one-way ANOVA and Dunnett's test (\*  $p < 0.05$ , \*\*  $p < 0.001$ ). Only data for experiment 1 is presented here, a comparison with experiment 2 is shown in Figure B.4 in Appendix B.

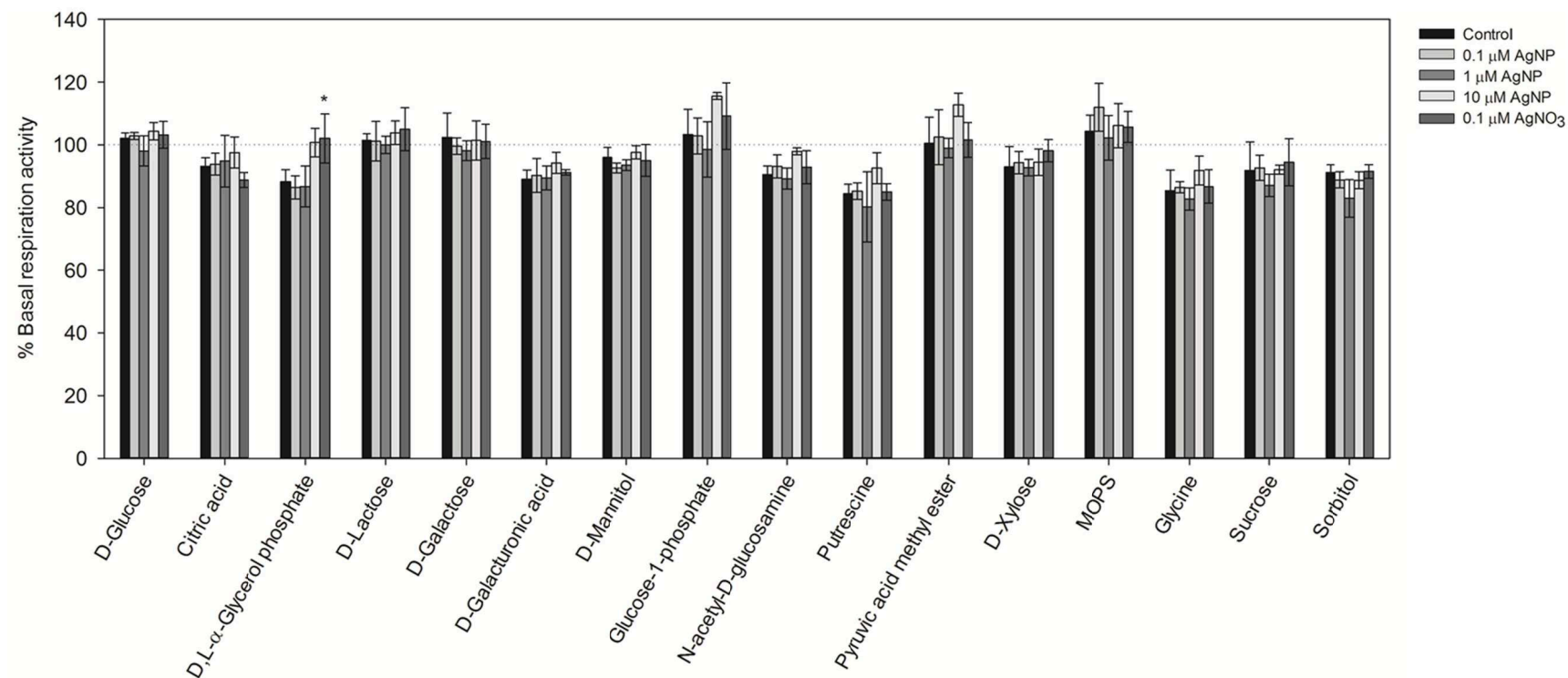


**Figure 3.3.** Community-level physiological profile as determined by substrate-induced respiration (SIR), after 21 days of exposure to 0.1, 1 and 10  $\mu\text{M}$  AgNP, or 0.1  $\mu\text{M}$  AgNO<sub>3</sub>. Statistical significance was tested by one-way ANOVA and Dunnett's test, \*  $p < 0.05$ .

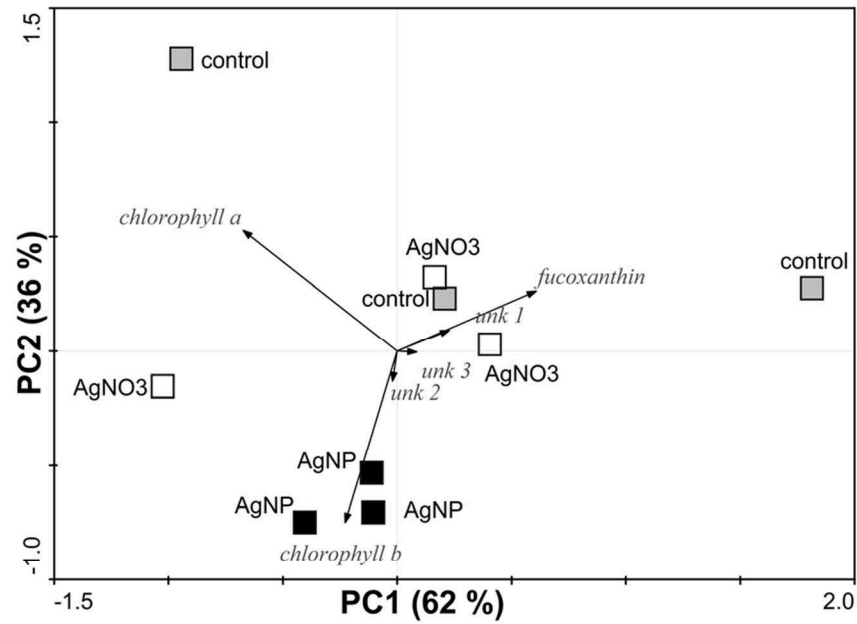


**Figure 3.4.** Principal component analysis of the content of marker pigments in periphyton of experiment 2, after 21 days of exposure to 10  $\mu\text{M}$  AgNP and 0.1  $\mu\text{M}$  AgNO<sub>3</sub>. Pigments were quantified in periphyton extracts using HPLC. Three replicates from each treatment were analyzed.

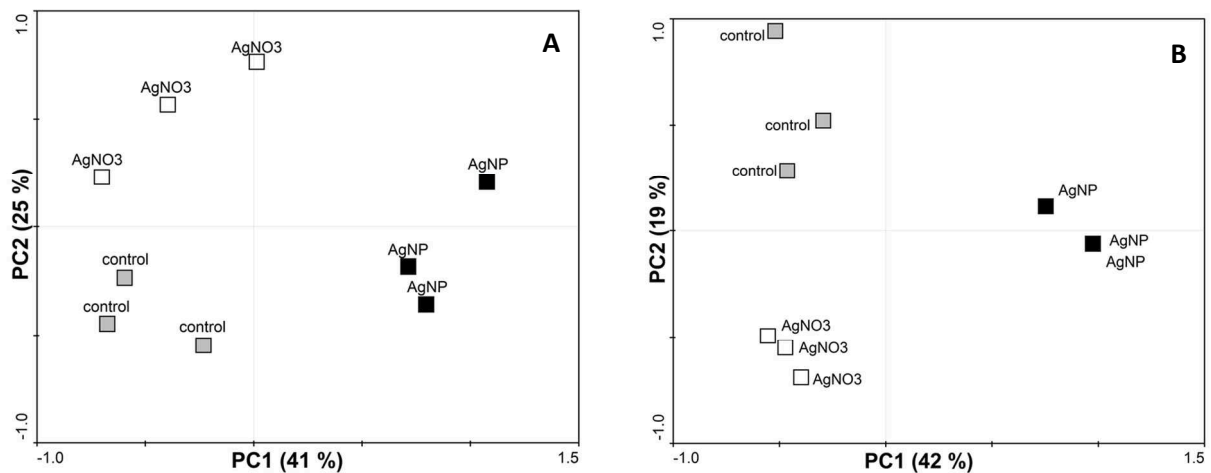


**Figure 3.5.** Principal component analysis of the community structure of periphyton, as determined by denaturing gradient gel electrophoresis (DGGE) with conserved 18S (A) and 16S (B) rDNA fragments, after 21 days of exposure to 10  $\mu\text{M}$  AgNP and 0.1  $\mu\text{M}$  AgNO<sub>3</sub> in experiment 2. From each treatment, three replicate community fingerprints were obtained.

**Table 3.2.** EC<sub>50</sub> values from photosynthesis, respiration, and primary and secondary production from 2-hour bioassays data in experiment 2 for the assessment of pollution-induced community tolerance (PICT). 95% confidence intervals are indicated in parentheses. Asterisks indicate a statistical difference from the control community. Statistical significance was tested by one-way ANOVA and Dunnett's test, \*  $p < 0.05$ .

End point	Treatment	EC <sub>50</sub> (μM)		
		AgNP	AgNO <sub>3</sub>	CuSO <sub>4</sub>
Photosynthetic yield	Control	221 (208-234)	11 (9-14)	404 (119-688)
	10 μM AgNP	305 (156-455)	17 (8-25)	> 200
	0.1 μM AgNO <sub>3</sub>	228 (220-237)	10 (8-12)	340 (123-556)
Respiration	Control	175 (23-327)	8 (0-16)	50 (34-65)
	10 μM AgNP	> 200	> 25	106 (93-121) *
	0.1 μM AgNO <sub>3</sub>	161 (63-259)	16 (2-30)	64 (55-73)
Primary production	Control	24 (21-28)	8 (2-14)	39 (29-50)
	10 μM AgNP	58 (42-74) *	9 (0-20)	29 (19-39)
	0.1 μM AgNO <sub>3</sub>	33 (22-45)	7 (2-12)	29 (17-40)
Secondary production	Control	17 (17-18)	1 (1-1)	31 (27-34)
	10 μM AgNP	62 (44-79) *	3 (2-5) *	30 (27-38)
	0.1 μM AgNO <sub>3</sub>	12 (9-15) *	1 (1-1)	38 (18-58)



## Chapter 4. Trophic transfer of silver nanoparticles from stream periphyton to the aquatic snail *Physa acuta*

Carmen Gil-Allué, Kristin Schirmer, Ahmed Tlili, Mark O. Gessner, and Renata Behra.

*In preparation.*

Silver nanoparticles present in consumer products and industrial applications are susceptible of being released into the environment during the life cycle of goods. Fate studies have identified the benthic compartment as a target for the accumulation of nanomaterials in the aquatic ecosystem, therefore, a better understanding of the trophic transfer potential of nanomaterials and its consequences are needed. In this study, the trophic transfer of silver from periphyton, a benthic microbial community, to a grazer upon dietary exposure was investigated. Periphyton was loaded with AgNP and AgNO<sub>3</sub>, reaching concentrations of  $20.26 \pm 0.82$  and  $1.72 \pm 0.06$  nmol Ag mg<sup>-1</sup> DW, respectively. Aquatic snails (*Physa acuta*) were allowed to graze on contaminated periphyton during five days to assess the potential of silver assimilation and consequent toxic effects. No significant mortality occurred in the AgNP and AgNO<sub>3</sub> treatments. Snails accumulated silver from food with assimilation efficiencies between 51 and 85 %, and no differences were observed between AgNP and AgNO<sub>3</sub> treatments. Snail soft tissue burden was  $5.31 \pm 2.50$  and  $1.01 \pm 0.08$  nmol Ag mg<sup>-1</sup> DW after feeding on AgNP- and AgNO<sub>3</sub>-loaded periphyton, respectively. Feeding rate of snails was reduced by  $50 \pm 21$  % in the AgNO<sub>3</sub> treatment, and defecation rates were reduced by more than 40 % in both AgNP and AgNO<sub>3</sub> treatments, indicating a disturbance of digestion. The reproductive output of snails, measured as the number of egg clutches and numbers of eggs per clutch, was unaffected by the accumulation of silver in tissues. After 28 days of embryonic development, hatching success was reduced to  $15 \pm 5$  % and  $9 \pm 5$  % of the total egg count for AgNP and AgNO<sub>3</sub>, respectively. Snail embryos that had not hatched presented an impaired development and malformations. Overall, the present study confirmed an efficient transfer of silver in an aquatic trophic chain, which can have consequences for trophic relationships and survival of invertebrates in aquatic ecosystems.

### 4.1 Introduction

Silver nanoparticles (AgNP) are added to different consumer products as an antimicrobial agent (Sondi & Salopek-Sondi 2004), and can be released into the environment during the production, use and disposal of such goods (Benn & Westerhoff 2008, Farkas et al. 2011, Kaegi et al. 2010). AgNP can reach the aquatic environment through direct discharge or from waste water effluents. Concentrations of AgNP in surface waters have been estimated to be in the

nanogram per liter range (Sun et al. 2014).

Once in the aquatic environment, nanomaterials will interact with the local water chemistry and undergo modifications such as aggregation and agglomeration, dissolution or changes in speciation (Behra et al. 2013, Levard et al. 2012). Fate studies have identified the sediment compartment as a likely sink of nanomaterials entering freshwaters due to particle aggregation and sedimentation, and sorption. Sedimenting nanomaterials can be transferred to benthic organisms, and high accumulation has been observed in biofilms and filter feeders (Behra et al. 2013, Cleveland et al. 2012, Ferry et al. 2009, Lowry et al. 2012). Although no studies have examined the trophic transfer from biofilms to higher trophic levels so far, there is evidence of trophic transfer of quantum dots in bacteria, protozoa and crustaceans (Bouldin et al. 2008, Holbrook et al. 2008, Werlin et al. 2011). Dietborne exposure of nanomaterials might be more important than waterborne exposure. Exposure to AgNP and other nanomaterials through contaminated food lead to efficient assimilation and slow depuration in aquatic snails, reaching high body burdens (Croteau et al. 2014, Croteau et al. 2011a, Croteau et al. 2011b).

In this study, the trophic transfer of silver from a benthic biofilm, *i.e.*, periphyton, preexposed to AgNP or AgNO<sub>3</sub> to the aquatic snail *Physa acuta* was assessed. Periphyton is an important primary producer in aquatic ecosystems, and many invertebrates feed on it in early life stages (*e.g.*, insect larvae) or during their whole lives (*e.g.*, gastropods) (Minshall 1978, Wetzel 1963). Periphyton has been shown to efficiently accumulate metals and nanomaterials (Bradac et al. 2009a, Serra et al. 2009). Therefore, there is a high potential for dietary exposure of these organisms, and toxicity might result due to high local concentrations of metals. *Physa acuta* (Draparnaud 1805) is a pulmonate hermaphrodite gastropod with a distribution in freshwaters of North America and Europe, and constitutes an important link between primary producers and higher trophic levels like fish. The aim of the present study was to investigate the potential of trophic transfer from periphyton to snails and identify toxic effects derived from the dietary exposure to survival, feeding and reproduction, which are processes relevant for the trophic relationships in aquatic ecosystems.

## 4.2 Materials and methods

### Silver nanoparticles

Citrate-coated AgNP were purchased from NanoSys GmbH (Wolfhalden, Switzerland) as an aqueous suspension with a nominal silver concentration of 9.27 mM, expressed as the molar concentration of total silver. All AgNP suspensions and AgNO<sub>3</sub> solutions were prepared in defined, reconstituted fresh water medium (PERIQUIL) (Stewart et al. 2015) to ensure stability of AgNP and control silver speciation during exposure experiments. The composition of PERIQUIL is showed in Table B.1 in Appendix B. All silver solutions were stored in the dark to prevent photoreduction. All PERIQUIL components, and AgNO<sub>3</sub>, were purchased from Sigma-Aldrich (Buchs SG, Switzerland).

Characterization of 10 µM AgNP suspensions in PERIQUIL under exposure conditions is shown in chapter 3 (Figure 3.1) and Appendix B (Figure B.3). Briefly, AgNP suspensions

remained stable in PERIQUIL up to 72 hours, with average particle diameters between  $49 \pm 1$  to  $73 \pm 5$  nm and  $\zeta$ -potential ranging between  $-5 \pm 1$  and  $-18 \pm 1$  mV. Dissolved Ag(I) fraction in AgNP suspensions remained as 1 % of total silver after 2 hours (data not shown).

### **Snail culture**

*Physa acuta* adult individuals were sampled from Lake Greifen, Switzerland. A batch culture was started from egg clutches of the same age. Snails were kept in shallow 5-L polypropylene boxes filled with 2 L groundwater at 15 °C, constant aeration, and a 12-hour light/dark photoperiod under BioSun fluorescent tubes (MLT Moderne Licht-Technik AG, Wettingen, Switzerland). Young snails were fed spirulina powder and young adult snails a mixture of fish food (TetraMin, Tetra, Blacksburg, VA) and boiled spinach. Snails with an average shell length of  $6.8 \pm 0.9$  mm were sampled 8 weeks after reproduction was first observed in the batch culture, and were placed in PERIQUIL during 24 hours to allow depuration and acclimatization prior to the experiment.

### **Periphyton colonization and silver loading**

Periphyton was colonized on glass slides (76 x 26 mm) in indoor flow-through channels fed with stream water as described in Gil-Allué et al. (2015). The colonized slides were sampled after five weeks, placed in PERIQUIL and transported to the laboratory. Six colonized slides were placed in polystyrene microcosms (180 x 134 x 60 mm; Semadeni AG, Ostermundigen, Switzerland) filled with 300 mL of PERIQUIL. Periphyton was loaded by exposing colonized slides to 10  $\mu$ M AgNP (periphyton<sub>AgNP</sub>) or 0.1  $\mu$ M AgNO<sub>3</sub> (periphyton<sub>AgNO<sub>3</sub></sub>) during 2 hours. Concentrations were selected to obtain comparable dissolved Ag(I) concentrations (*i.e.*, 1 % in the AgNP suspension), and a low toxicity based on a previous study (Gil-Allué et al. 2015). The Ag-loaded slides were then transferred to new microcosms with 300 mL of fresh PERIQUIL where the feeding experiments took place. Eight microcosms with six slides each were prepared per periphyton-loading treatment.

### **Feeding experiments with *Physa acuta***

Five snails per microcosm were placed in four out of the eight microcosms per treatment, and the other four were kept as controls without grazers. Feeding experiments were carried out during five days at 15 °C and 12-hour light/dark photoperiod under BioSun fluorescent tubes (MLT Moderne Licht-Technik AG, Wettingen, Switzerland). Microcosms were inspected daily for new egg clutches, and dead snails, which were removed. After five days, the experiment was stopped by removing the snails from the microcosms. Snails from the same microcosm were transferred into separate glass beakers with 50 mL of fresh PERIQUIL, and were depurated for 24 hours.

### **Trophic transfer of silver**

Total silver was quantified in periphyton suspensions after silver-loading of periphyton and at

the end of the feeding experiment, as well as in snail soft tissue to assess the accumulation of silver after five days of exposure. Periphyton was scraped off the slides with a polystyrene spatula. The pooled samples of the six slides from a given microcosm were homogeneously suspended in 50 mL of fresh PERIQUIL. A 10-mL aliquot was centrifuged for 10 min at  $3220 \times g$  to separate the soluble exopolysaccharides (EPS) from periphyton (Stewart et al. 2015). Silver was quantified in the periphyton pellet, and in the supernatant. The soft body tissue was separated from the shell of snails previously anesthetized by a brief exposure to 3.5%  $MgCl_2$ , and was immediately stored at  $-80^\circ C$ . Frozen periphyton and snail tissue samples were lyophilized in a Lyovac GT2 (Leybold Heraeus) for 72 hours and weighed before acidic digestion. Total silver in medium at the end of the exposure was also quantified in a 1-mL aliquot from each microcosm.

Samples were acid digested to dissolve AgNP and bring  $Ag^+$  ions in solution in an ultraCLAVE 4 microwave digestion system (MLS GmbH, Leutkirch, Germany). One mL of liquid sample or a known amount of lyophilized sample was transferred into a Teflon tube and acidified with 4 mL of 65 % Suprapur  $HNO_3$  (Merck, Darmstadt, Germany). The digestion program ran for 24 minutes with maximum temperature of  $200^\circ C$  and pressure of 100 bar. The digests were diluted 50 times with nanopure water before total silver was quantified by measuring the isotope  $^{109}Ag$  on an Element 2 High Resolution Sector Field ICP-MS (Thermo Scientific Inc.). A certified reference for water with a known silver concentration (National Water Research Institute, Burlington, Canada) was analyzed to assure the accuracy of the measurements.

Assimilation efficiency (AE) of silver in snails feeding on periphyton $_{AgNP}$  and periphyton $_{AgNO_3}$  was estimated by two different approaches. The first method ( $AE_1$ ) is based on a mass balance of the total silver quantified in snail soft tissue and feces (Croteau et al. 2011b):

$$AE_1 (\%) = Ag_{snails} / (Ag_{snails} + Ag_{feces}) \times 100 \%$$

where  $Ag_{snails}$  corresponds to the total silver (nmol) quantified in all snails of a given microcosm, and  $Ag_{feces}$  to the total silver (nmol) quantified in fecal pellets collected from the same microcosm. The second method ( $AE_2$ ) is based on the difference between the total silver concentration measured in periphyton and the silver concentration remaining in feces:

$$AE_2 (\%) = 100 \% - ([Ag]_{feces} / [Ag]_{periphyton}) \times 100 \%$$

where  $[Ag]_{feces}$  corresponds to the total silver concentration ( $nmol\ mg^{-1}\ DM_{feces}$ ) quantified in fecal pellets collected from a given microcosm, and  $[Ag]_{periphyton}$  to the total silver concentration ( $nmol\ mg^{-1}\ DM_{periphyton}$ ) quantified in periphyton collected from the same microcosm. Assimilated silver is defined in the present study as the silver associated with snail soft tissue after 24 hours of depuration in fresh PERIQUIL without food.

### Biological parameters

Periphyton biomass in the microcosms was measured as the dry mass (DM) by filtering three 1-mL aliquots of the suspensions through pre-weighed glass fiber filters (GF/F, 25 mm diameter,  $0.7\ \mu m$  average pore size; Whatman Ltd., Maidstone, UK), drying the filters for 24

hours at 105 °C, weighing them to the nearest 0.01 mg. Ash-free dry mass (AFDM) was determined by combusting the organic matter on filters after DM determination for 1 hour at 480 °C in a muffle furnace (LE 1/11, Nabertherm GmbH, Lilienthal, Germany), and re-weighing the filters.

Feeding rate of snail over the five-day experiment was determined as the consumed periphyton dry mass per individual and day. Consumed periphyton was determined as the difference in biomass between microcosms without snails and with snails within a treatment. Defecation rate was calculated as the total fecal dry mass produced during the feeding experiment, and including the mass excreted during the 24-hour depuration, per individual and day. Fecal pellets were collected by filtering the contents of the microcosms at the end of the experiment, after having removed the colonized slides and the snails, on pre-weighed cellulose filters (pore size 0.45 µm; Sartorius AG, Gottingen, Germany). Filters were dried at 60°C for 48 hours, and re-weighed to the nearest 0.01 mg. The contribution of detached material from periphyton to  $DM_{feces}$  was corrected by subtracting the quantified DM from microcosms without snails after the same procedure. Survival of snails on each day of the experiment was taken into account in the calculation of feeding and defecation rates.

Reproduction of snails was monitored daily for the duration of the experiment. The days to the observation of the first egg clutch and the number of clutches per microcosm were monitored. At the end of the experiment, the number of eggs per clutch was counted by microscopy. After the end of the experiment, egg clutches were kept in aerated microcosms and fresh PERIQUIL, and the hatching success was assessed by light microscopy after 28 days (Musee et al. 2010).

Statistical significance was assessed using SigmaPlot for Windows version 12.0 (Systat Software Inc., San Jose, CA). Prior to statistical analysis, equal variance was confirmed and normality of the data was tested by Shapiro-Wilk test ( $\alpha = 0.05$ ). One-way ANOVA followed by Dunnett's test for post-hoc multiple comparisons were used to identify effects of AgNP- and AgNO<sub>3</sub>-pre-exposure on the measured parameters.

## 4.3 Results

### Trophic transfer of silver to *Physa acuta*

Control periphyton contained a background concentration of silver of  $0.07 \pm 0.04$  nmol Ag mg<sup>-1</sup> DM<sub>periphyton</sub>. Upon 2-hour exposure to 10 µM AgNP and 0.1 µM AgNO<sub>3</sub>, periphyton accumulated silver significantly. At the start of the experiment, concentrations of total silver measured in AgNP- and AgNO<sub>3</sub>-loaded periphyton were  $20.26 \pm 0.82$  and  $1.72 \pm 0.06$  nmol Ag mg<sup>-1</sup> DM<sub>periphyton</sub>, respectively (not shown). Total silver content remained constant in the AgNP treatment until the end of the five-day feeding experiment, and was  $19.93 \pm 1.08$  nmol Ag mg<sup>-1</sup> DM<sub>periphyton</sub> (Table 4.1). A decrease in the silver content of periphyton was observed in the AgNO<sub>3</sub> treatment, to  $1.01 \pm 0.08$  nmol Ag mg<sup>-1</sup> DM<sub>periphyton</sub>. Comparable concentrations of total silver were measured in the absence of snails.

Snails accumulated  $5.31 \pm 2.5$  nmol Ag mg<sup>-1</sup> DM<sub>snail</sub> upon feeding on periphyton<sub>AgNP</sub> for five days, while less silver,  $0.44 \pm 0.25$  nmol Ag mg<sup>-1</sup> DM<sub>snail</sub>, was measured in snails feeding on

periphyton<sub>AgNO<sub>3</sub></sub>. Snails feeding on control periphyton had a background silver concentration of  $0.08 \pm 0.03 \text{ nmol Ag mg}^{-1} \text{ DM}_{\text{snail}}$ . Total silver content in feces of snails feeding on periphyton<sub>AgNP</sub> was  $2.86 \pm 0.40 \text{ nmol Ag mg}^{-1} \text{ DM}_{\text{feces}}$ , while  $0.17 \pm 0.03 \text{ nmol Ag mg}^{-1} \text{ DM}_{\text{feces}}$  was measured in snails feeding on periphyton<sub>AgNO<sub>3</sub></sub>. Assimilation efficiency (AE) of silver in snails feeding on periphyton<sub>AgNP</sub> calculated by the first method (AE<sub>1</sub>), which was based on a mass balance between snails and feces, was  $51.40 \pm 4.09 \%$ . The second method (AE<sub>2</sub>) was based on a mass balance between periphyton and feces, yielded an assimilation efficiency of  $84.57 \pm 1.34 \%$ . Assimilation efficiencies of silver in snails feeding on periphyton<sub>AgNP</sub> calculated by the two methods did not significantly differ from those of snails feeding on periphyton<sub>AgNO<sub>3</sub></sub>, which were  $55.70 \pm 6.18$  (AE<sub>1</sub>) and  $79.37 \pm 4.36 \%$  (AE<sub>2</sub>) (Table C.1 in Appendix C).

Quantification of total silver in medium of after five days revealed concentrations of  $0.03 \pm 0.01 \mu\text{M}$ , indicating a slight release of silver from the AgNP-loaded periphyton. In the case of AgNO<sub>3</sub>-loaded periphyton, silver concentrations in medium were below the detection limit of  $0.01 \mu\text{M}$  (Table C.2). Total silver measured in the supernatant after centrifugation of the periphyton suspension, which contains the soluble periphyton EPS fraction and loosely sorbed silver, was  $0.05 \pm 0.01 \mu\text{M}$  in the AgNP treatment, and was below the detection limit of  $0.01 \mu\text{M}$  in the AgNO<sub>3</sub> treatment. The presence of snails in the microcosm did not have significant effects on the total silver concentrations measured in exposure medium, or in the EPS and loosely sorbed fraction.

### **Effects of diet exposure to silver on survival, feeding behavior and reproduction of *Physa acuta***

At the beginning of the experiment,  $48.42 \pm 4.32 \text{ mg AFDM}$  of periphyton was offered to the snails, as determined from a representative sample of colonized periphyton. No significant differences in the periphyton biomass were present among treatments at the beginning of the experiment after AgNP- and AgNO<sub>3</sub>-loading. After five days, no significant increase or decrease in biomass was measured in all microcosms with snails (Figure C.1). Differently, periphyton biomass increased between  $28 \pm 11$  and  $19 \pm 5 \%$  in all microcosms without snails.

At the end of the five-day experiment, snail mortality in the control treatment was  $20 \pm 16 \%$ . No significant lethal effects of exposure to AgNP and AgNO<sub>3</sub> were observed. Feeding rate of snails feeding on control periphyton averaged  $0.92 \pm 0.20 \text{ mg DM}_{\text{periphyton}} \text{ individual}^{-1} \text{ day}^{-1}$  over the duration of the experiment (Figure 4.1). Feeding of snails in the AgNP treatment was not significantly affected by silver contamination of periphyton. Differently, feeding rates of snails in the AgNO<sub>3</sub> treatment decreased by  $50 \pm 21 \%$ . Defecation rate of snails feeding on control periphyton was  $1.02 \pm 0.33 \text{ mg DM}_{\text{feces}} \text{ individual}^{-1} \text{ day}^{-1}$ . Defecation rates were  $43 \pm 14$  and  $42 \pm 6 \%$  lower in snails from the AgNP and AgNO<sub>3</sub> treatments, respectively.

Reproduction of snails feeding on control periphyton started on the second day of the experiment (Table 4.2). After five days, a total of 14 egg clutches were counted in the four microcosm replicates, with an average of  $4 \pm 2$  clutches per microcosm. Egg clutches contained  $12 \pm 6$  eggs per clutch, yielding a total of 114 eggs. Reproductive output of snails feeding on

periphyton<sub>AgNO<sub>3</sub></sub> did not significantly differ from that of the control. In the case of snails feeding on periphyton<sub>AgNP</sub>, comparable reproductive output to the control was measured in two microcosms, while in the other two snails did not reproduce at all.

Hatching success was quantified 28 days after the end of the experiment (Table 4.2). In the control microcosms,  $72 \pm 5$  % of the embryos had hatched. Hatching success was reduced to  $9 \pm 5$  and  $15 \pm 5$  % in the AgNP and AgNO<sub>3</sub> treatments, respectively. Visual examination showed egg clutches in control microcosms to be mostly empty or containing developed juveniles, some of which had observable heartbeat (Figure 4.2). Differently, no normally developed juveniles were observed in the egg clutches from the AgNP treatment. Embryos appeared to have stopped developing in early stages or presented severe malformations, most noticeable in the shell. Heartbeat was observable in some embryos. In the AgNO<sub>3</sub> treatment, the vast majority of embryos appeared to have stopped developing in early stages. Heartbeat was not observable in any of the embryos.

#### 4.4 Discussion

In the present study, the dietary transfer of silver from periphyton previously exposed to AgNP or AgNO<sub>3</sub> to the aquatic snail *Physa acuta* was investigated. Our results indicate that periphyton efficiently accumulated silver during the two hours of exposure to AgNP and AgNO<sub>3</sub>. The higher levels of silver in periphyton<sub>AgNP</sub> compared to periphyton<sub>AgNO<sub>3</sub></sub> are indicative of the accumulation of particles in periphyton and confirm its significance as sink for nanomaterials. Considering that periphyton slides were rinsed before silver quantification, particles appear to have diffused within the periphyton matrix rather than merely being deposited on the surface. Furthermore, since the flux of silver into biofilms is diffusion-limited (Peulen & Wilkinson 2011) smaller particles rather than agglomerates might have diffused into the periphyton matrix.

Snails efficiently accumulated silver upon feeding on both periphyton<sub>AgNP</sub> and periphyton<sub>AgNO<sub>3</sub></sub>. Assimilation efficiencies of silver in snails were high, ranging from 51 to 85 %, as calculated by the two different approaches. Calculated efficiencies using the first approach, AE<sub>1</sub>, were slightly lower than those from the second approach, AE<sub>2</sub>. The first approach was previously applied by Croteau et al. (2011b), and it is based on a mass balance of silver quantified in snails and feces. Since only snails that were alive at the end of the experiment were analyzed for silver, whereas all the feces in the microcosm were considered, this method is likely to underestimate the assimilation of silver. In the present study, we also found similar assimilation efficiencies between AgNP and AgNO<sub>3</sub> treatments. Our results are comparable to those calculated for the aquatic snail *Lymnaea stagnalis* feeding on Ag-loaded diatoms (Croteau et al. 2011b), although in that study AgNP were slightly less efficiently assimilated than dissolved Ag(I), with AE values of  $58 \pm 8$  % and  $73 \pm 5$  %, respectively.

The efficient silver assimilation from AgNP-contaminated food in snails measured in the present study and in that of Croteau et al. (2011b) can originate from absorption of AgNP through the gut epithelium, absorption of dissolved Ag(I) from AgNP due to the acidic gut

environment, or from adsorbed AgNP on the gut surface. Uptake of AgNP can occur in gut epithelial cells of invertebrates, as observed in the polychaete *Nereis diversicolor* (García-Alonso et al. 2011). Cellular uptake of AgNP in snails was recently shown to follow multiple pathways, including clathrin- and caveolae-mediated endocytosis (Khan et al. 2015). Once they are taken up, AgNP might be transported to other organs within the body of the snail. The digestive gland of *Physa acuta* and other molluscs is known to accumulate high concentrations of metals in contaminated sites (Zaldibar et al. 2006), and could therefore be a major target of AgNP.

Feeding rate of snails feeding on periphyton<sub>AgNP</sub> was comparable to the control. This finding is contrary to other studies on invertebrates where they avoided AgNP-contaminated food and exposure medium (Bernot & Brandenburg 2013, Croteau et al. 2011b, Justice & Bernot 2014). A significantly lower feeding rate was quantified in snails feeding on periphyton<sub>AgNO<sub>3</sub></sub> compared to controls. Metal-induced reduction of feeding was previously determined to depend on a decrease in palatability (Kulacki et al. 2012, Zubrod et al. 2015) or on different nutritional values of metal-contaminated food to invertebrates (McTeer et al. 2014). However, the comparable growth of periphyton among the treatments during the experiment points to an unlikely difference of its nutritional characteristics (Figure C.1).

Considering the lower defecation rates in both treatments, it might be indicative of a disturbance of digestion. The reduction of the defecation rate upon feeding on periphyton<sub>AgNO<sub>3</sub></sub> might be a consequence of the lower feeding rate. Presence of AgNP in the gut of organisms has also been linked to inefficient digestion, which could be due to a disturbance of the gut microbial flora or cytotoxicity of gut epithelial cells (Croteau et al. 2011b, Merrifield et al. 2013). Considering the relatively high variability of feeding and defecation rates compared to the actual assimilation by individual snails, apparent differences between mean feeding and defecation rates are small. Moreover, this variability might have masked effects of AgNP on the feeding rate of snails.

Reproduction of snails was observed after two days, independently of the treatment. No effects on the number of clutches and eggs were observed in snails feeding on periphyton<sub>AgNO<sub>3</sub></sub>. No comparable data exists in the literature on the effects of AgNO<sub>3</sub> on the reproductive output of aquatic snails, but a reduction of the reproductive output of *Daphnia magna* upon exposure to AgNO<sub>3</sub> in the presence of algae as a food source was reported (Ribeiro et al. 2014). Different results were measured in snails feeding on periphyton<sub>AgNP</sub>. While snails from two microcosms showed no effects on the reproductive output, snails from the two others did not reproduce during the experiment. One possible explanation is that a small change in available silver caused inhibitory effects, due to the steep concentration-response curves often reported for dissolved Ag(I) and AgNP (Gil-Allué et al. 2015, Navarro et al. 2008b). Strong effects on reproduction of *Physa acuta* were detected also upon exposure of snails to AgNP and alumina nanoparticles (Bernot & Brandenburg 2013, Musee et al. 2010). However, it remains to be examined, whether the effects are caused directly by the nanoparticles.

Egg hatching and embryonic development were strongly impaired by AgNP and AgNO<sub>3</sub>.



Upon examination of the eggs after 28 days from the end of the experiment, evidence of embryonic developmental toxicity was found. Metal ions have been previously observed to disturb the normal development of mollusc embryos (Das & Khangarot 2011, Gomot 1998, Khangarot & Das 2010), and evidence also exists for AgNP and alumina nanoparticles (Musee et al. 2010, Ringwood et al. 2010). Different mechanisms could have contributed to the effects measured in the present study. One possibility is the maternal transfer of metal ions and nanomaterials from adults feeding on contaminated food, as it has been previously measured in invertebrates (Kim et al. 2013) and fish (Cazan & Klerks 2014, Lowry et al. 2012). However, we cannot exclude that effects were caused by traces of silver released from periphyton and to which clutches were exposed during the first three days of development, before being moved into clean medium. Silver concentration in medium at the end of the feeding experiment was 30 nM in the AgNP treatment, and presence of silver below the detection limit of 10 nM could not be excluded in the AgNO<sub>3</sub> treatment. These traces of AgNP or dissolved Ag(I) could diffuse through the chorion once eggs have been released. AgNP have been observed to enter fish eggs through chorion pore canals (Lee et al. 2007). However, snail eggs are protected by gelatinous material of the egg clutch in addition to the chorion, and the role of these structural barriers in the uptake of metal ions and nanoparticles should be investigated (Behra et al. 2013, Cheung & Lam 1998).

### **Environmental implications**

In the present study, effects of AgNP on the feeding behavior, digestion and embryonic development were identified. Changes in the feeding behavior and digestion could have impacts on the energy transfer along the trophic chain, since aquatic snails are an important link between primary producers and higher organisms like fish. Furthermore, reproduction is crucial for survival of species, and the stability of snail populations might be put at risk due to decreased hatching rates. Further investigations on the effects of nanomaterials on later generations of invertebrates are necessary in order to discern the long-term effects on the ecosystem.

## 4.5 Figures and tables

**Table 4.1.** Total silver concentrations in periphyton, snails and feces as determined by ICP-MS. Average values and standard deviations calculated from four microcosm replicates per treatment.

Periphyton treatment	Periphyton (nmol mg <sup>-1</sup> DM <sub>periphyton</sub> )	Snails (nmol mg <sup>-1</sup> DM <sub>snails</sub> )	Feces (nmol mg <sup>-1</sup> DM <sub>feces</sub> )
Control - snails	0.05 ± 0.01	-	-
AgNP - snails	21.84 ± 1.61	-	-
AgNO <sub>3</sub> - snails	1.04 ± 0.23	-	-
Control + snails	0.07 ± 0.04	0.08 ± 0.03	0.02 ± 0.02
AgNP + snails	19.93 ± 1.08	5.31 ± 2.50	2.86 ± 0.40
AgNO <sub>3</sub> + snails	1.01 ± 0.08	0.44 ± 0.25	0.17 ± 0.03

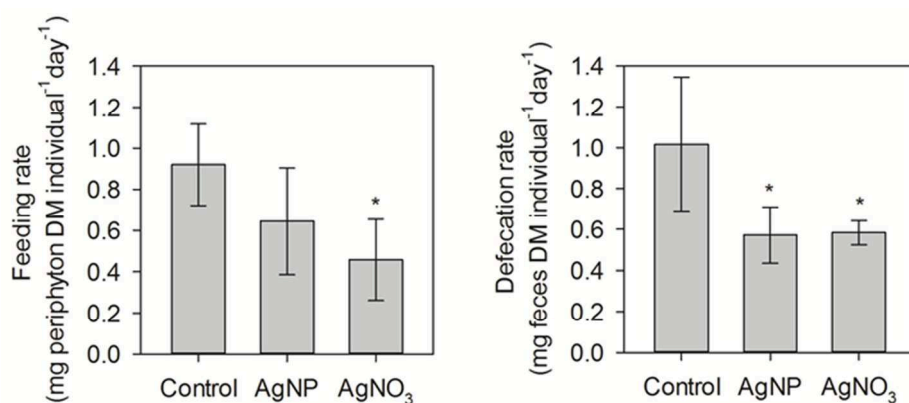


**Figure 4.1.** Feeding and defecation rates of snails upon feeding on AgNP- and AgNO<sub>3</sub>-preexposed periphyton. Survival of snails per day was taken into account in the determination of the rates. Statistical significance was tested by one-way ANOVA followed by Dunnett's test. \*  $p < 0.05$ .

**Table 4.2.** Reproduction output and hatching success of snails upon feeding on AgNP- and AgNO<sub>3</sub>-preexposed periphyton. Average values and standard deviations are calculated from four replicate microcosms in each treatment containing five snails each, total values within a treatment are given in parentheses. Statistical significance was tested by one-way ANOVA followed by Dunnett's test. \*\*  $p < 0.001$ .

Periphyton treatment	N	Days to reproduction	# Egg clutches	# Eggs	# Eggs per clutch	Hatching success (%)
Control	4	2	4 ± 2 (14)	36 ± 11 (144)	12 ± 6	72 ± 5
AgNP	2	2	7 ± 1 (13)	50 ± 6 (100)	8	9 ± 5 **
	2	> 5	0	0	-	-
AgNO <sub>3</sub>	4	2	4 ± 2 (16)	36 ± 27 (142)	8 ± 2	15 ± 5 **

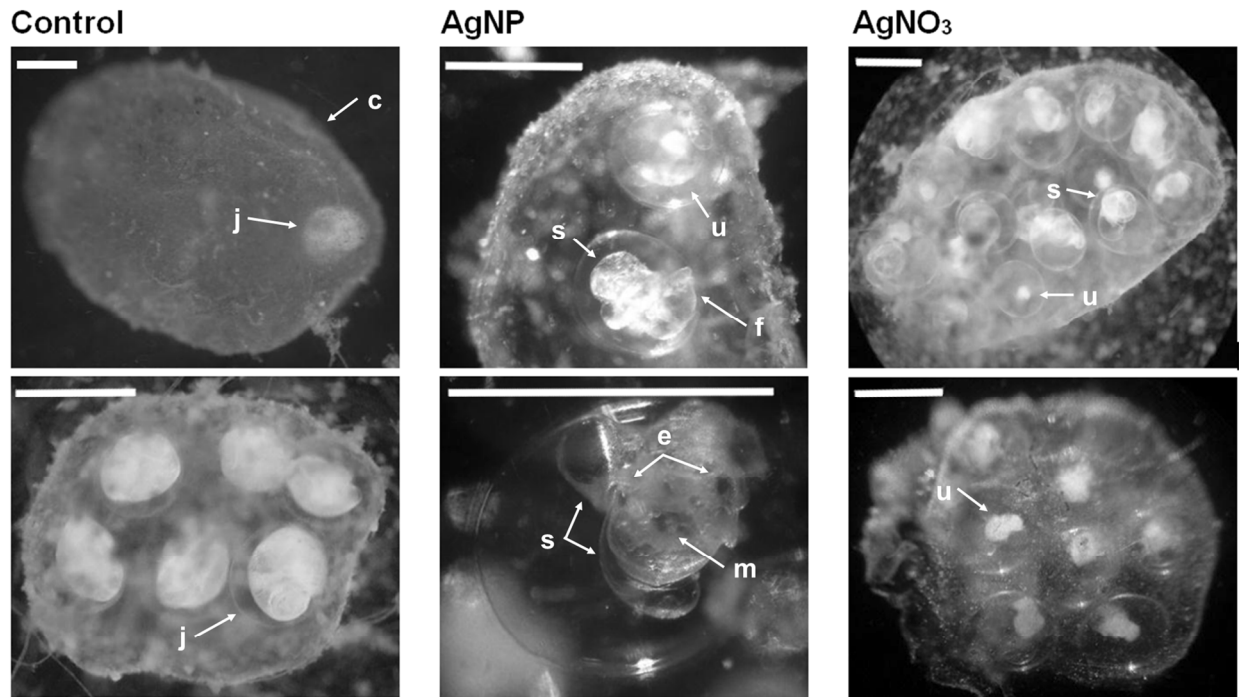


**Figure 4.2.** Development of snail embryos after 28 days of incubation in fresh PERIQUIL after the end of the experiment. Pictures show two different egg clutches that are representative of the observations in the control, AgNP, and AgNO<sub>3</sub> treatments. White bar corresponds to 0.8 mm. c = clutch, e = eye, f = foot, j = juvenile, m = mouth, s = shell, u = undeveloped embryo.



## Chapter 5. Outlook

Toxicity of AgNP has been investigated in relevant single species of aquatic organisms, however, at the time of the completion of this thesis, only a few studies on their impact on ecological processes driven by aquatic communities were published. The present thesis has demonstrated that AgNP have the potential to disturb the function and community structure of periphyton, and to efficiently accumulate in periphyton and in grazers upon trophic transfer, causing toxic effects also on higher trophic levels. Therefore, the findings of the present thesis contribute to fill knowledge gaps relevant to the risk assessment of AgNP in the aquatic environment. In the following sections, further research questions that arise from the findings of this thesis are discussed.

### 5.1 Interaction of silver nanoparticles with extracellular enzymes of periphyton

In chapter 2, it was shown that AgNP inhibited biological functions in periphyton related to autotrophic and heterotrophic fractions of the community. In all cases, AgNP exhibited lower or similar toxicity to dissolved Ag(I). By using a silver ligand, the role of Ag<sup>+</sup> in the toxicity of AgNP was examined. It was evident that for most parameters studied, including the extracellular enzymes  $\beta$ -glucosidase and alkaline phosphatase, dissolved Ag<sup>+</sup> ions were the sole source of toxicity. However, the extracellular enzyme leucine aminopeptidase was specifically inhibited by AgNP.

Extracellular enzymes carry out an important role in nutrient acquisition from substrates that are not readily bioavailable, and therefore contribute to nutrient cycling in the ecosystem (Chróst 1991). Some extracellular enzymes are located freely in the EPS, like  $\beta$ -glucosidase, while others are associated with the surface of organisms. Because of their extracellular localization, they are likely to directly interact with nanomaterials. Therefore, it is of relevance to further study the inhibitory effects of AgNP on extracellular enzymes of periphyton, as well as of other aquatic microbial communities like leaf litter decomposers, which have different dominant microorganisms, in the case of the latter, bacteria and fungi (Gessner et al. 1999). For this study, additional extracellular enzymes relevant to different ecological processes carried out by aquatic microbial communities, could also be considered. For example,  $\beta$ -xylosidase is a commonly studied extracellular enzyme involved in the degradation of hemicellulose present in the algal and plant cell walls (Espeland et al. 2001).

To eliminate the confounding factors of AgNP effects on the concomitant secretion of enzyme from periphyton organisms, and the interaction of AgNP with other components of periphyton, commercially available isolated extracellular enzymes in a buffered system could be used. The enzyme kinetics could be followed by measuring the conversion of substrate over time using fluorescent substrate analogs, allowing to gain more information on the interaction of AgNP. The isolated enzymes could be incubated with AgNP and AgNO<sub>3</sub>, as a source of

dissolved Ag(I), during short-term exposures. The use of a silver ion ligand, such as cysteine or DMPS, would allow to discern between direct and indirect toxicity of AgNP. Moreover, it would be of interest to systematically assess the role of the AgNP surface properties in the inhibition of extracellular enzymes, since interactions with enzymes have been reported to be governed by surface properties of AgNP (Wigginton et al. 2010). A suggested approach would be to include other surface modifications of AgNP in addition to citrate coating (*e.g.*, polyvinylpyrrolidone), and to assess the inhibitory potential of coatings alone and of inert nanomaterials, such as polystyrene nanoparticles.

## **5.2 Pollution-induced community tolerance in periphyton upon exposure to silver nanoparticles**

In chapter 3, it was shown that AgNP caused a change in the composition of the autotrophic and heterotrophic fractions of the periphyton community. By studying the tolerance of the different periphyton communities after long-term exposures, a causal relationship could be drawn between exposure to AgNP and a change in the community structure. Pollution-induced community tolerance studies have mainly been applied in the field, where tolerance development to pollutants in periphyton was compared between polluted and pristine sites (Blanck 2002). In previous studies, colonization of periphyton was done *in situ*, while in the present thesis, experiments were carried out in closed microcosms with already established periphyton communities. The microcosm approach was suitable for the study of impacts of AgNP on function and structure of periphyton while producing minimal nanowaste, but also had limitations that could attenuate the observed effects on tolerance development. Most importantly, no new organisms could enter the system, which restricted the magnitude of the change in community structure and tolerance development. Furthermore, experiments were carried out with established periphyton communities, but early colonization of periphyton might be particularly sensitive to AgNP toxicity due to possible protective properties of the EPS and the physical structure of periphyton (Thuptimdang et al. 2015).

As a way to overcome the limitations of the setup used in the present thesis, further experiments with a flow-through setup, which would allow new organisms to enter the community, are therefore suggested. Flow-through channels used for the colonization of periphyton on glass slides could be used as exposure chambers by connecting the inlet and outlet to a recirculating system with a large reservoir to ensure constant exposure conditions. In such a setup, sensitivity and development of tolerance of periphyton at different stages of colonization could be assessed. An example is the use of the flow-through system to perform short pre-colonization of periphyton on submerged substrates before starting long-term exposures to the pollutant, which would allow the assessment of tolerance in a developing community and achieve a higher degree of tolerance than in the approach presented in the present thesis. Furthermore, it is of interest to examine whether tolerance of periphyton to silver also confers co-tolerance or increased sensitivity to other chemicals. In the present thesis, co-tolerance to copper, which was expected considering similar detoxification mechanisms

and a previous report of co-tolerance in periphyton, was assessed (Soldo & Behra 2000). Other chemicals to be tested include those expected to have different biochemical modes of detoxification, such as herbicides. The criteria to select chemicals would be based on their high toxicity to microorganisms and their likelihood to occur in the aquatic environment.

### **5.3 Early life stage and multigeneration toxicity studies with silver nanoparticles and *Physa acuta***

In chapter 4, an efficient accumulation of AgNP and strong association with periphyton organisms resulted in a trophic transfer to the grazing snail *Physa acuta*. Dietborne uptake was similarly efficient in AgNP or AgNO<sub>3</sub> treatments. A marked hatching inhibition occurred in both treatments and, upon examination, malformations were observed in the majority of embryos. It remains unclear whether toxicity was caused by 1) maternal transfer of silver from adults feeding on contaminated periphyton, or 2) by diffusion of dissolved or particulate silver present in the exposure medium through the gelatinous egg clutch and chorion. In the first case, the silver assimilated through dietary exposure by adult snails could have been transported to the reproductive organs, entering in contact with the developing egg clutches. Alternatively, indirect effects on the embryonic development could be caused by toxicity of silver to the mother. In the second case, exposure through the medium could have occurred during the 5-day duration of the feeding experiment. At the end of the experiment, and before medium exchange, a total silver concentration in exposure medium of up to 30 nM was measured in the AgNP treatment, which was presumably released by the silver-loaded periphyton, and up to 10 nM (*i.e.*, the limit of detection) might have been present in the AgNO<sub>3</sub> treatment.

Several studies could be carried out to discern the route of exposure of embryos. A snail embryo assay (Bandow & Weltje 2012) would allow to determine the sensitivity of embryos in intact clutches to waterborne AgNP exposures. Egg clutches produced from non-exposed adults would be collected and exposed to a range of concentrations of AgNP and AgNO<sub>3</sub>. In this case, the use of a silver ion ligand could be used as well to discern between direct and indirect effects of AgNP on the embryos. The development and hatching would be followed for up to 28 days by observations with an optical microscope. To further investigate the maternal effects on the snail embryos, adult snails could be briefly exposed to food contaminated with AgNP or AgNO<sub>3</sub> and translocated to fresh medium before the start of reproduction. The development of embryos from exposed and unexposed snails would be monitored for up to 28 days. Additionally, to assess the maternal transfer of silver, quantification of total silver should be carried out in egg clutches of exposed adult snails after they have been depurated and transferred to clean exposure medium. Egg clutches that have been produced in the fresh medium would be collected and pooled by replicate, lyophilized, acid-digested and total silver quantified by ICP-MS. By following these approaches, the route

of exposure of snail embryos or the magnitude of its contribution to the effects observed in the present thesis would be discerned.

In a second step, AgNP concentrations that caused low hatching inhibition and visible developmental toxicity in the embryo assay could be used in a multigenerational study to assess the life-long effects of embryonic exposure and the potential of transfer to subsequent generations, as it has been observed in other studies (Bundschuh et al. 2012, Kim et al. 2013, Völker et al. 2013). Survival, reproductive output and sensitivity to AgNP of exposed snails during the embryonic stage would be assessed during the life cycle of two generations in order to assess the potential of AgNP to cause effects that will be carried on to next generations.



## Appendix A. Supporting information of Chapter 2

**Table A.1.** Composition of exposure medium. Asterisks indicate modifications to the original composition used by Le Faucheur et al. (2005).  $\text{Ca}(\text{NO}_3)_2$  was substituted for  $\text{CaCl}_2$  to limit  $\text{AgCl}_n$  formation.  $\text{NaNO}_3$  and  $\text{Na}_2\text{SiO}_3$  were added to increase ionic strength and facilitate diatom growth, respectively.

Component	Concentration (mM)
<i>Salts</i>	
$\text{Ca}(\text{NO}_3)_2^*$	0.10
$\text{MgSO}_4$	0.15
$\text{NaHCO}_3$	1.20
$\text{NaNO}_3^*$	0.80
$\text{Na}_2\text{SiO}_3^*$	0.05
<i>Nutrients</i>	
$\text{K}_2\text{HPO}_4$	0.005
$\text{NH}_4\text{NO}_3$	1.00
<i>Trace elements</i>	
$\text{CoCl}_2$	$5.00 \times 10^{-5}$
$\text{H}_3\text{BO}_3$	0.05
$\text{Na}_2\text{MoO}_4$	$8.00 \times 10^{-5}$
$\text{CuSO}_4$	$1.63 \times 10^{-4}$
$\text{MnCl}_2$	$1.22 \times 10^{-3}$
$\text{ZnSO}_4$	$1.58 \times 10^{-4}$
$\text{FeCl}_3$	$9.00 \times 10^{-4}$
<i>Metal ligand</i>	
$\text{Na}_2$ EDTA	0.02
<i>Buffer</i>	
MOPS, pH 7.5	10.00
<b>Ionic strength</b>	<b>13.90</b>

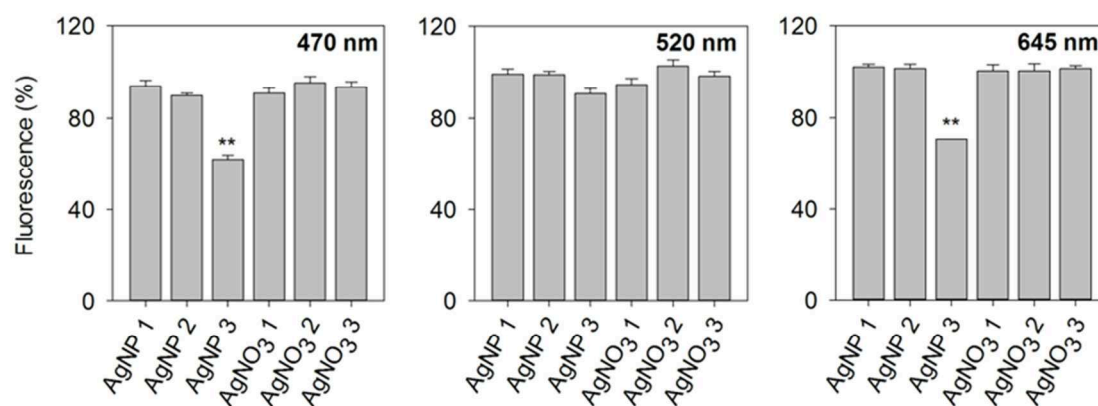


**Figure A.1.** Ratios of fluorescence at 470, 520 and 645 nm to fluorescence at 665 nm of control periphyton suspensions for each of the six independently colonized communities used in toxicity tests. Error bars correspond to standard deviations of three analytical replicates. Statistical significance was tested using Tukey's test (\*\* $p < 0.001$ ) following an ANOVA on arcsine square root transformed data.

**Table A.2.** Total activities of  $\beta$ -glucosidase (GLU), alkaline phosphatase (AP) and leucine aminopeptidase (LAP) of control periphyton suspensions for each of three independent experiments. Standard deviations refer to three analytical replicates.

Experiment	Enzymatic activity		
	( $\mu\text{mol substrate g}^{-1} \text{AFDM h}^{-1}$ )		
	GLU	AP	LAP
AgNP 1	3 $\pm$ 1	13 $\pm$ 1	55 $\pm$ 1
AgNP 2	11 $\pm$ 1	10 $\pm$ 1	10 $\pm$ 1
AgNP 3	35 $\pm$ 1	18 $\pm$ 2	18 $\pm$ 2
AgNO <sub>3</sub> 1	52 $\pm$ 3	124 $\pm$ 9	15 $\pm$ 1
AgNO <sub>3</sub> 2	162 $\pm$ 41	238 $\pm$ 58	9 $\pm$ 1
AgNO <sub>3</sub> 3	431 $\pm$ 32	138 $\pm$ 13	11 $\pm$ 1

**Table A.3.** Particle diameter characterization by nanoparticle tracking analysis (NTA) and dynamic light scattering (DLS). Standard deviations refer to three analytical replicates.

Sample		NTA		DLS	
Concentration ( $\mu\text{M}$ )	Medium	Exposure time (h)	Avg. diameter (nm)	Avg. diameter (nm)	PdI
100	Stock suspension*	0	48	$35 \pm 1$	$0.28 \pm 0.01$
12.5	Fresh	2	42	$35 \pm 1$	$0.32 \pm 0.05$
12.5	Fresh	20	70	$51 \pm 5$	$0.32 \pm 0.10$
12.5	Conditioned	2	60	$50 \pm 1$	$0.44 \pm 0.01$
12.5	Conditioned	20	75	$56 \pm 3$	$0.43 \pm 0.03$
100	Fresh	2	45	$30 \pm 1$	$0.37 \pm 0.05$
100	Fresh	20	56	$32 \pm 0$	$0.45 \pm 0.01$
100	Conditioned	2	95	$95 \pm 1$	$0.22 \pm 0.01$
100	Conditioned	20	134	$116 \pm 1$	$0.22 \pm 0.01$

\* Dilution in nanopure water

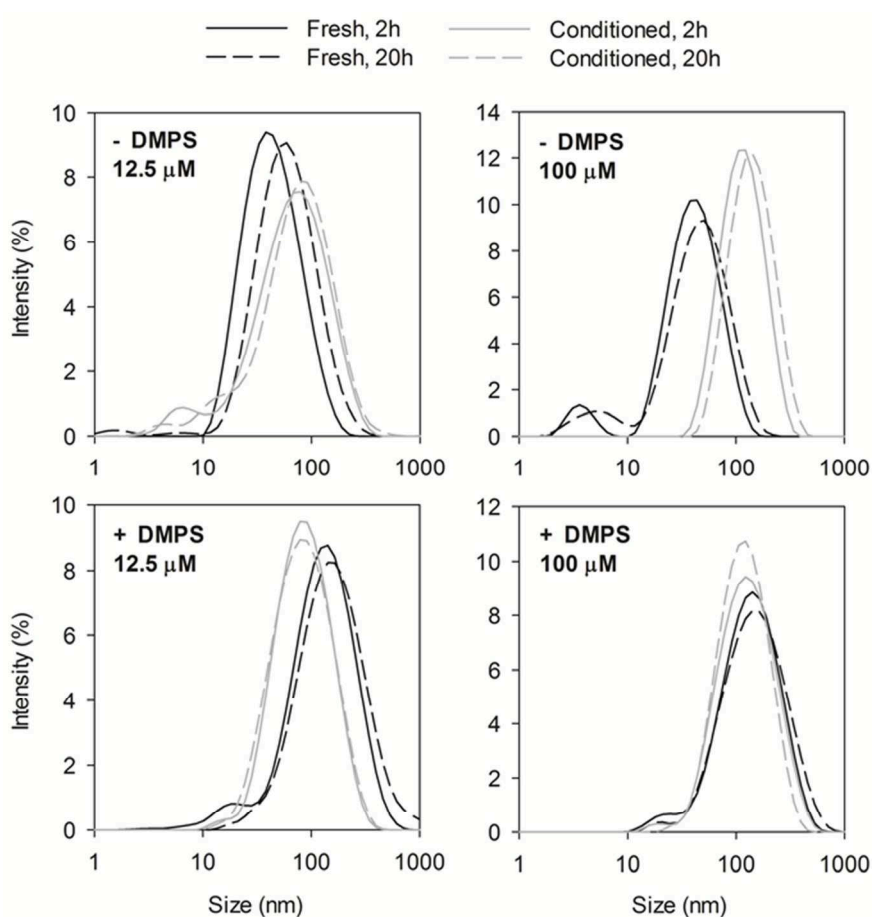


**Figure A.2.** Particle diameter distributions as measured by DLS of 12.5 and 100  $\mu\text{M}$  AgNP suspensions in fresh and conditioned medium after 2 and 20 hours of exposure, and in the presence or absence of the  $\text{Ag}^+$  ion ligand DMPS. Lines correspond to the average intensity per size class of three measurements.

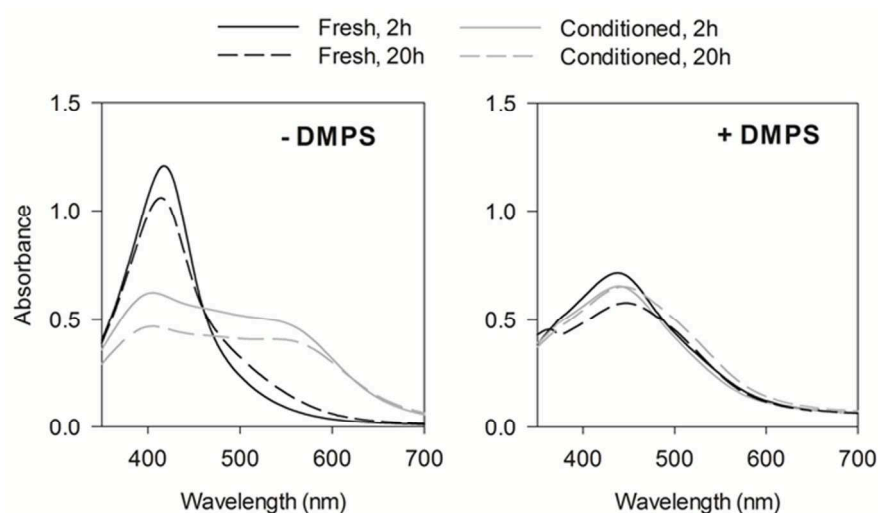


**Figure A.3.** UV-Vis spectra of AgNP suspensions in fresh and conditioned medium after 2 and 20 hours of exposure and in the presence or absence of the Ag<sup>+</sup> ion ligand DMPS. All suspensions had a nominal AgNP concentration of 100  $\mu$ M.

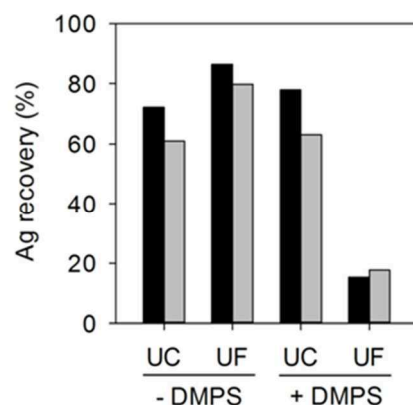


**Figure A.4.** Silver recovery with the ultracentrifugation (UC) and ultrafiltration (UF) method in fresh (black) and conditioned (grey) medium in the absence and presence of DMPS. Medium was spiked with 1  $\mu$ M AgNO<sub>3</sub> in all cases.

**Table A.4.** Speciation of silver at the range of  $\text{AgNO}_3$  concentrations tested in exposure medium, as calculated by Visual MINTEQ version 3.0 Beta.

Species	$\text{AgNO}_3$ ( $\mu\text{M}$ )	
	1.25	25
$\text{Ag}^+$	96.33 %	97.28 %
$\text{AgCl (aq)}$	1.02 %	0.07 %
$\text{AgSO}_4^-$	0.20 %	0.20 %
$\text{AgNH}_3^+$	2.12 %	2.13 %
$\text{Ag(NH}_3)_2^+$	0.23 %	0.23 %
$\text{AgNO}_3 \text{ (aq)}$	0.10 %	0.10 %

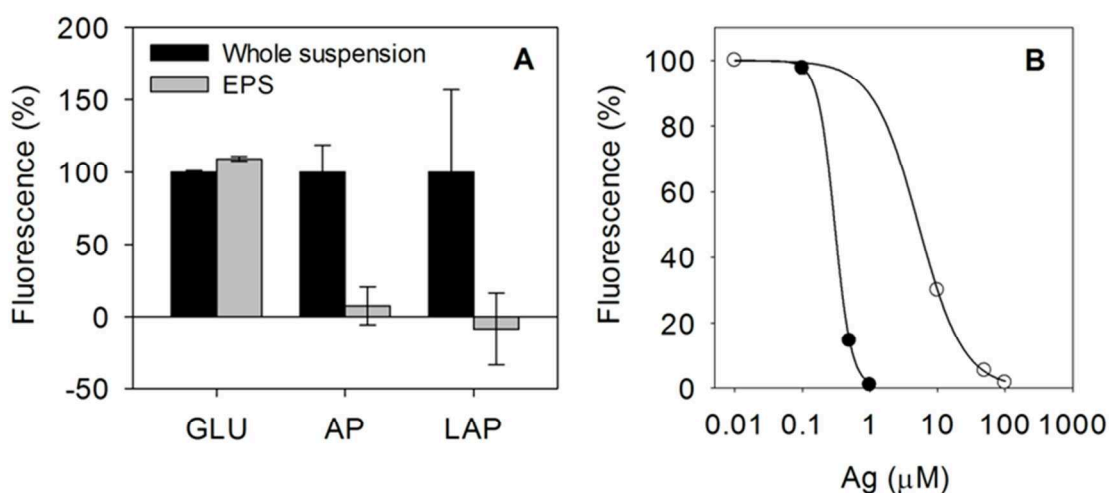


**Figure A.5.** Activities of  $\beta$ -glucosidase (GLU), alkaline phosphatase (AP) and leucine aminopeptidase (LAP) in whole periphyton suspensions and filtrates containing the periphyton EPS matrix (A) and effects of AgNP (○) and  $\text{AgNO}_3$  (●) on GLU activity present in the periphyton EPS matrix (B). Error bars correspond to standard deviations of three analytical replicates in both panels; they are too small to be clearly visible in panel B.

**Table A.5.** EC<sub>50</sub> values of AgNP and AgNO<sub>3</sub> for photosynthesis, respiration, and activity of  $\beta$ -glucosidase (GLU) based on total silver in AgNP suspensions, AgNP, or as a function of dissolved Ag<sup>+</sup>, AgNP (Ag<sup>+</sup>). Dissolved Ag<sup>+</sup> corresponds to the measured dissolved Ag<sup>+</sup> fraction in AgNP suspensions after exposure times of 20 hours for respiration and 2 hours for photosynthesis and GLU. Standard errors refer to three experimental replicates.

Response variable	Dissolved Ag <sup>+</sup> (%)	EC <sub>50</sub> ( $\mu$ M)		
		AgNP	AgNP (Ag <sup>+</sup> )	AgNO <sub>3</sub>
Photosynthesis	1.5	83 $\pm$ 3	1.3 $\pm$ 0.1	3.5 $\pm$ 0.2
Respiration	3.0	22 $\pm$ 3	0.6 $\pm$ 0.1	4.1 $\pm$ 0.3
GLU	1.5	17 $\pm$ 6	0.3 $\pm$ 0.1	2.4 $\pm$ 0.5





## Appendix B. Supporting information of Chapter 3

**Table B.1.** Composition of the exposure medium PERIQUIL used in all experiments (Stewart et al. 2015).

Component	Concentration (mM)
<i>Salts</i>	
CaCl <sub>2</sub>	0.20
Ca(NO <sub>3</sub> ) <sub>2</sub>	0.10
MgSO <sub>4</sub>	0.15
NaHCO <sub>3</sub>	1.20
KNO <sub>3</sub>	0.10
Na <sub>2</sub> SiO <sub>3</sub>	0.05
<i>Nutrients</i>	
K <sub>2</sub> HPO <sub>4</sub>	5.00 x 10 <sup>-3</sup>
NH <sub>4</sub> NO <sub>3</sub>	0.10
<i>Trace elements</i>	
CoCl <sub>2</sub>	5.00 x 10 <sup>-5</sup>
H <sub>3</sub> BO <sub>3</sub>	0.05
Na <sub>2</sub> MoO <sub>4</sub>	8.00 x 10 <sup>-5</sup>
CuSO <sub>4</sub>	1.63 x 10 <sup>-4</sup>
MnCl <sub>2</sub>	1.22 x 10 <sup>-3</sup>
ZnSO <sub>4</sub>	1.58 x 10 <sup>-4</sup>
FeCl <sub>3</sub>	9.00 x 10 <sup>-4</sup>
<i>Metal ligand</i>	
Na <sub>2</sub> EDTA	0.02
<i>Buffer</i>	
MOPS, pH 7.5	10.00
NaOH	7.00

**Table B.2.** Water chemistry of exposure medium samples from all microcosms, sampled weekly after medium exchanges during the 21-day exposure in experiment 2. \* Lower measured concentrations due to the predicted precipitation of hydroxyapatite ( $\text{Ca}_5(\text{PO}_4)_3$ ) and quartz ( $\text{SiO}_2$ ) with the software Visual MINTEQ v3.0 Beta (<http://vminteq.lwr.kth.se/>).

Time (days)	Treatment	pH	Ca (mg L <sup>-1</sup> )	Cl (mg L <sup>-1</sup> )	K (mg L <sup>-1</sup> )	Mg (mg L <sup>-1</sup> )	Na (mg L <sup>-1</sup> )	Total N (mg N L <sup>-1</sup> )	NO <sub>3</sub> <sup>-</sup> (mg N L <sup>-1</sup> )	PO <sub>4</sub> <sup>-3</sup> (μg L <sup>-1</sup> )	H <sub>4</sub> SiO <sub>4</sub> (mg L <sup>-1</sup> )	SO <sub>4</sub> <sup>-2</sup> (mg L <sup>-1</sup> )
	Control (nominal)	7.5	12	14.4	4.3	3.6	192	147	5.6	475 *	11.2 *	14.4
0	Control	7.7	13.2	15.2	4.7	4.4	195	143	5.8	160	5.3	16.9
7	Control	8.0 ± 0.1	29.7 ± 3.4	15.1 ± 0.2	4.8 ± 0.3	4.4 ± 0.1	197 ± 3	140 ± 1	4.7 ± 0.7	3.0 ± 0.7	ND	16.3 ± 0.1
	AgNP	8.0 ± 0.1	33.4 ± 3.4	15.1 ± 0.1	4.7 ± 0.2	4.6 ± 0.1	197 ± 2	140 ± 1	5.1 ± 0.4	3.1 ± 1.4	ND	15.4 ± 0.2
	AgNO <sub>3</sub>	8.0 ± 0.1	35.0 ± 5.3	15.1 ± 0.2	4.6 ± 0.1	4.6 ± 0.1	196 ± 3	140 ± 1	4.6 ± 0.9	3.3 ± 2.4	ND	15.9 ± 0.5
14	Control	7.8 ± 0.1	13.4 ± 0.3	15.2 ± 0.1	4.3 ± 0.1	4.5 ± 0.1	187 ± 1	157 ± 21	3.8 ± 1.0	3.5 ± 0.7	ND	15.0 ± 0.7
	AgNP	7.8 ± 0.1	14.6 ± 1.4	15.1 ± 0.1	4.2 ± 0.1	4.5 ± 0.1	187 ± 1	141 ± 1	3.8 ± 0.8	3.3 ± 0.8	ND	13.9 ± 0.6
	AgNO <sub>3</sub>	7.8 ± 0.1	13.7 ± 0.7	15.2 ± 0.1	4.4 ± 0.1	4.6 ± 0.1	188 ± 1	139 ± 4	3.9 ± 1.5	2.3 ± 1.4	ND	15.3 ± 0.9
21	Control	7.7 ± 0.1	12.6 ± 0.2	14.8 ± 0.1	5.0 ± 0.6	4.4 ± 0.1	185 ± 2	140 ± 2	3.5 ± 0.8	2.7 ± 2.1	ND	15.8 ± 1.1
	AgNP	7.8 ± 0.1	12.6 ± 0.2	14.7 ± 0.2	4.6 ± 0.1	4.5 ± 0.1	185 ± 1	141 ± 1	2.9 ± 0.8	2.1 ± 0.2	ND	12.7 ± 0.6
	AgNO <sub>3</sub>	7.8 ± 0.1	12.5 ± 0.2	14.6 ± 0.1	4.4 ± 0.1	4.5 ± 0.1	185 ± 1	138 ± 1	2.4 ± 1.6	3.9 ± 1.9	ND	14.2 ± 0.7

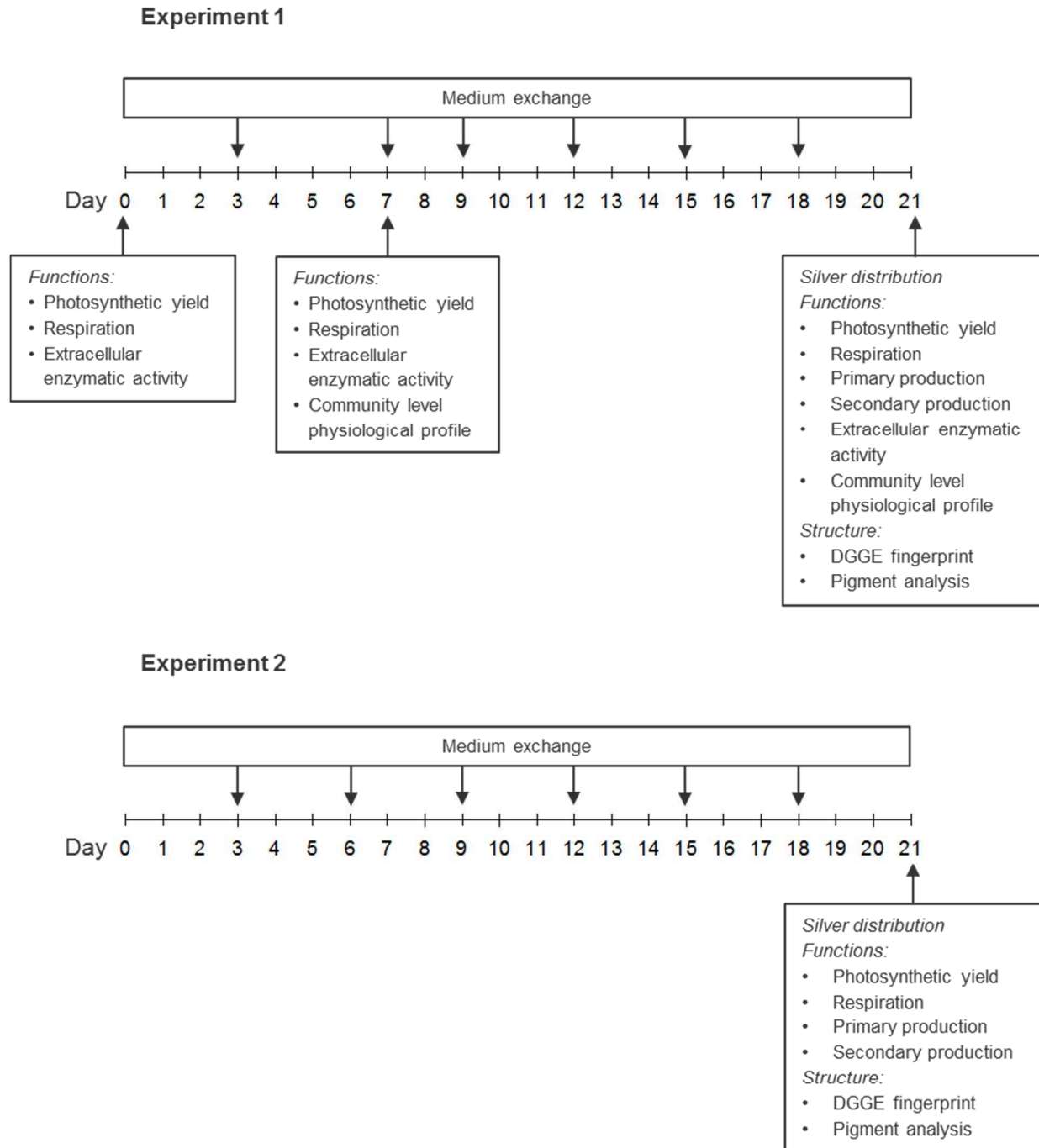


**Figure B.1.** Diagram of the timeline of measurements and medium exchanges in experiments 1 and 2.

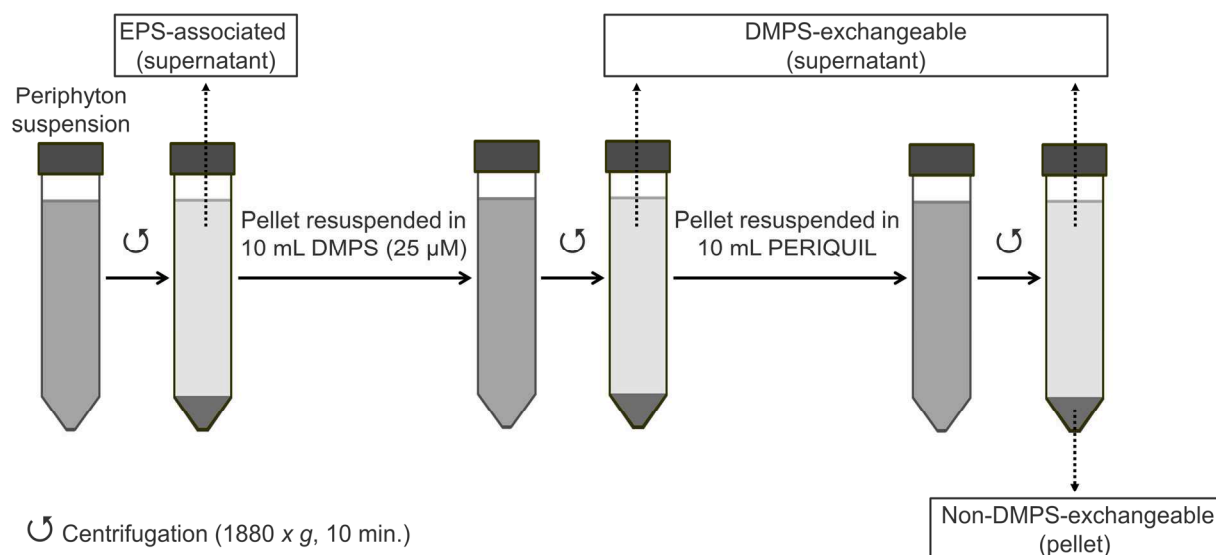


**Figure B.2.** Diagram of the periphyton fractionation procedure for the quantification of silver distribution. Silver was measured in the EPS-associated (loosely sorbed), DMPS-exchangeable (strongly sorbed to periphyton), and non-DMPS-exchangeable (strongly associated or internalized in periphyton biomass) fractions.

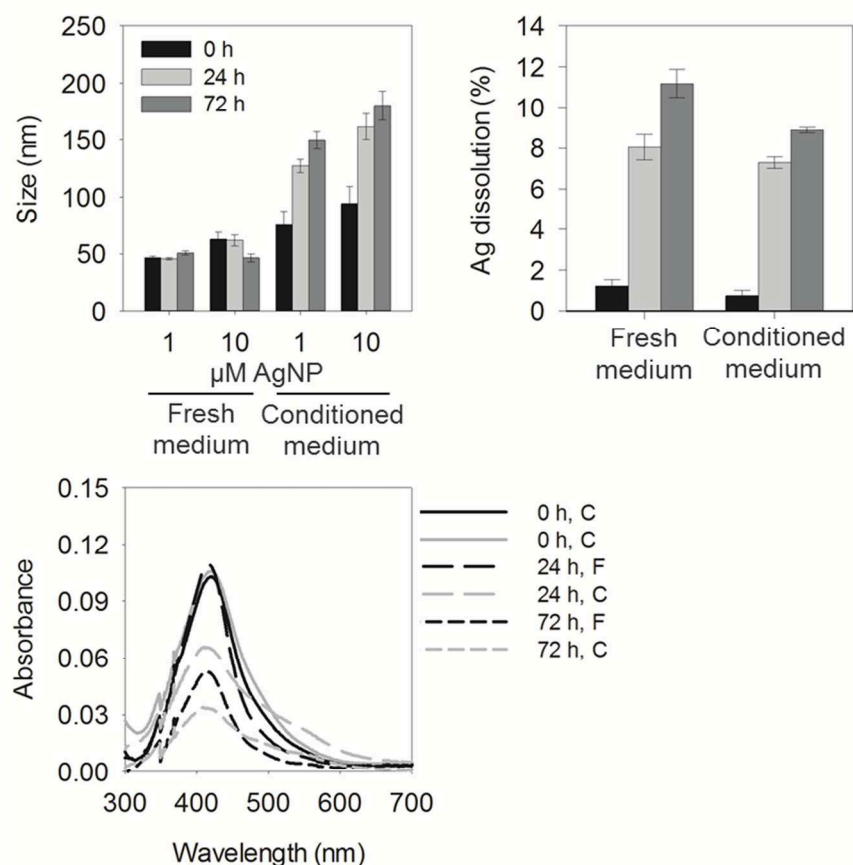


**Figure B.3.** Complementary characterization of silver nanoparticles (AgNP). Size distributions of 1 and 10  $\mu\text{M}$  AgNP suspensions in fresh and conditioned exposure medium at 0 (black bars), 24 (light gray bars), and 72 hours (dark gray bars) were measured as the hydrodynamic diameter by nanoparticle tracking analysis (NTA). Dissolution 10  $\mu\text{M}$  AgNP suspensions were measured in fresh and conditioned exposure medium by ultrafiltration. The optical properties of 10  $\mu\text{M}$  AgNP suspensions were determined from their UV-VIS absorbance spectra in fresh (F) and conditioned (C) exposure medium at 0, 24 and 72 hours.

**Table B.3.** Speciation of silver in the range of  $\text{AgNO}_3$  concentrations tested in exposure medium (which are comparable to the dissolved  $\text{Ag}^+$  ions in AgNP suspensions), as calculated by Visual MINTEQ v3.0 Beta.

Species	$\text{Ag}^+$ ( $\mu\text{M}$ )		
	0.1	10	25
$\text{Ag}^+$	52.35 %	52.96 %	53.92 %
$\text{AgCl (aq)}$	44.55 %	43.99 %	43.10 %
$\text{AgCl}_2^-$	1.66 %	1.60 %	1.51 %
$\text{AgNH}_3^+$	1.15 %	1.16 %	1.18 %
$\text{Ag(NH}_3)_2^+$	0.12 %	0.12 %	0.11 %
$\text{AgNO}_3 \text{ (aq)}$	0.06 %	0.06 %	0.06 %
$\text{AgSO}_4^-$	0.10 %	0.10 %	0.13 %

**Table B.4.** Measurements of biomass accrual and biological function responses in control periphyton over the duration of long-term exposures in experiment 1.

End point	Unit	Days		
		0	7	21
AFDM	$\text{g m}^{-2}$	$2.60 \pm 0.08$	$2.49 \pm 0.24$	$3.05 \pm 0.46$
Photosynthetic yield	-	$0.39 \pm 0.01$	$0.40 \pm 0.02$	$0.56 \pm 0.01$
Respiration	$\mu\text{g CO}_2 \text{ mg}^{-1} \text{AFDM h}^{-1}$	$299 \pm 2$	$205 \pm 2$	$254 \pm 5$
GLU	$\mu\text{mol substrate mg}^{-1} \text{AFDM h}^{-1}$	$6.41 \pm 1.20$	$34.79 \pm 31.91$	$4.11 \pm 1.70$
AP	$\mu\text{mol substrate mg}^{-1} \text{AFDM h}^{-1}$	$1.76 \pm 0.08$	$17.41 \pm 15.96$	$17.78 \pm 15.11$
LAP	$\mu\text{mol substrate mg}^{-1} \text{AFDM h}^{-1}$	$0.36 \pm 0.11$	$0.74 \pm 0.18$	$1.06 \pm 0.02$

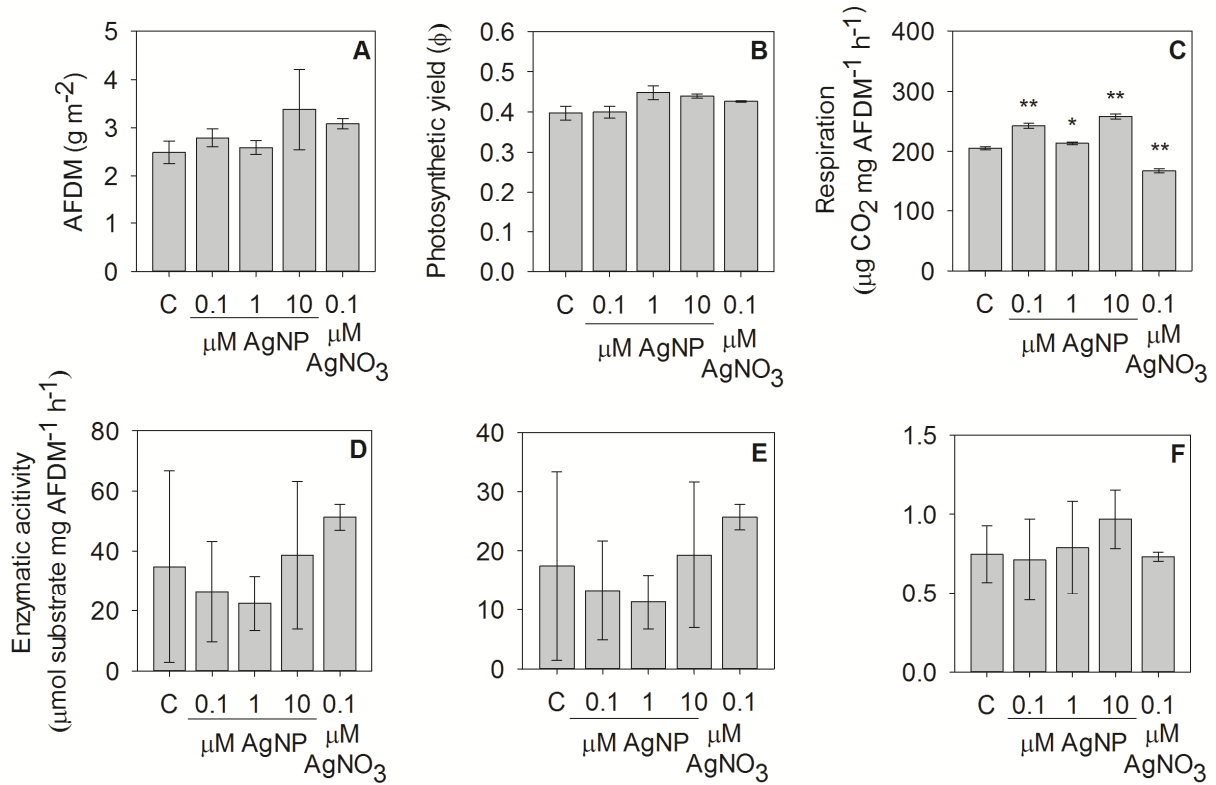


**Figure B.4.** Effects of 0.1, 1 and 10 μM AgNP and 0.1 μM AgNO<sub>3</sub> after 7 days of exposure in experiment 1 on the ash-free dry mass (A), photosynthetic yield (B), respiration (C), and extracellular enzymatic activity of β-glucosidase (D), alkaline phosphatase (E) and leucine aminopeptidase (F). Statistical significance was tested by one-way ANOVA followed by Dunnett's test, \*  $p < 0.05$ , \*\*  $p < 0.001$ .

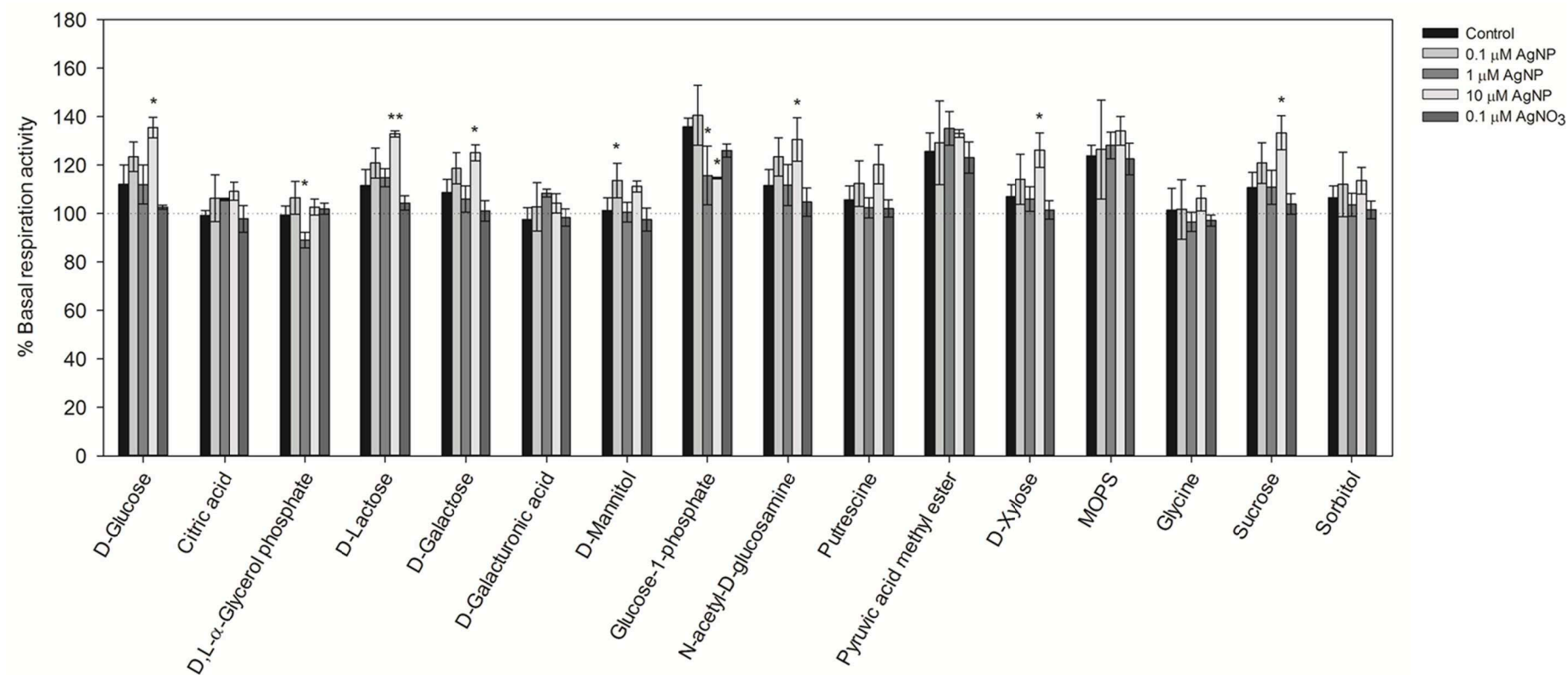


**Figure B.5.** Community-level physiological profile as determined by substrate-induced respiration (SIR), after 7 days of exposure to 0.1, 1 and 10 μM AgNP, or 0.1 μM AgNO<sub>3</sub>. Statistical significance was tested by one-way ANOVA followed by Dunnett's test, \*  $p < 0.05$ , \*\*  $p < 0.001$ .



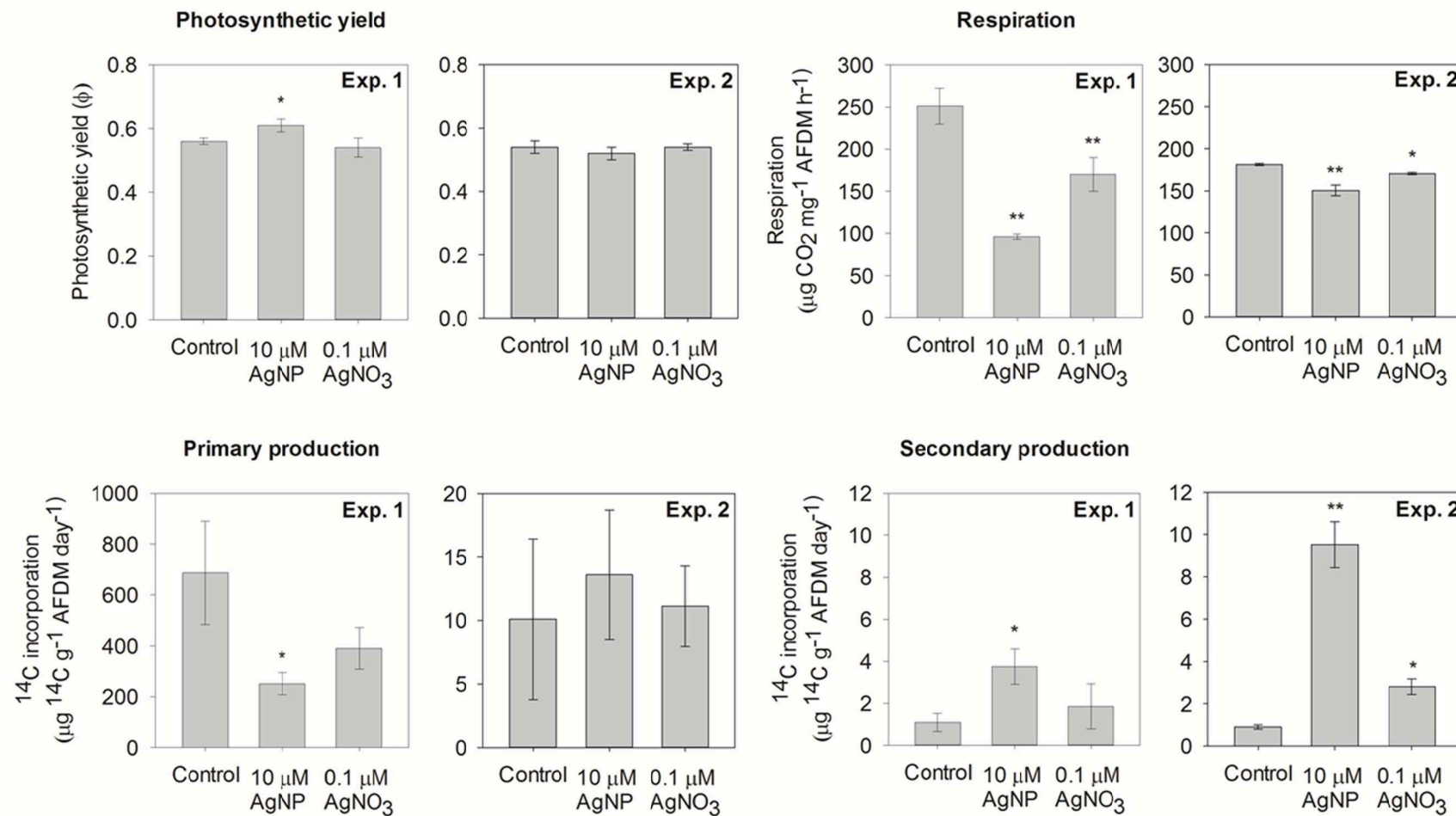


**Figure B.6.** Comparison of the response of biological functions to 21-day exposures to 10  $\mu$ M AgNP and 0.1  $\mu$ M AgNO<sub>3</sub> between experiments 1 (**Exp. 1**) and 2 (**Exp. 2**), for photosynthetic yield, respiration, primary production and secondary production. Statistical significance was tested by one-way ANOVA followed by Dunnett's test, \*  $p < 0.05$ , \*\*  $p < 0.001$ .

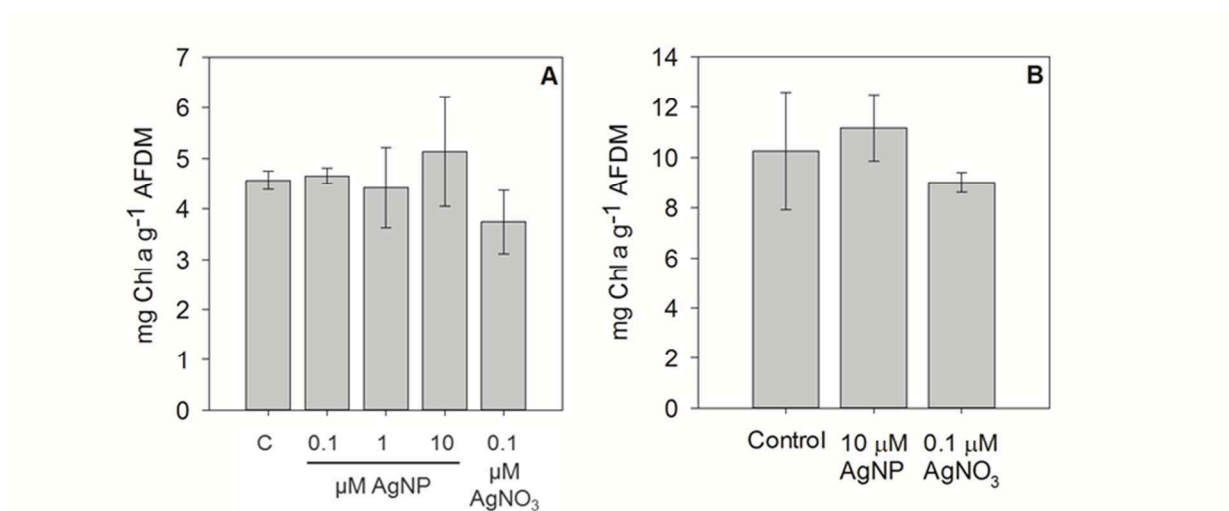


**Figure B7.** Chlorophyll a content in periphyton across the treatments in experiments 1 (A) and 2 (B), as determined by HPLC from pigment extracts of three biological replicates. Statistical significance was tested by one-way ANOVA.

**Table B.5.** Relative content of quantified pigments in periphyton across the treatments in experiments 1 and 2, as determined by HPLC from pigment extracts of three biological replicates.

Experiment	Treatment	Relative content (%)								
		Chlorophyll a	Chlorophyll b	Fucoxanthin	Lutein	Unk 1	Unk 2	Unk 3	Unk 4	Zeaxanthin
1	Control	40 ± 6	14	18 ± 2	4 ± 2	10 ± 1	4 ± 1	4 ± 1	5	ND
	10 µM AgNP	40 ± 3	21 ± 6	10	10 ± 2	3 ± 1	4 ± 1	10 ± 1	3	ND
	0.1 µM AgNO <sub>3</sub>	33 ± 2	14 ± 1	17	9 ± 2	9	7	6 ± 1	5	ND
2	Control	46 ± 6	18 ± 2	16 ± 2	ND	7 ± 1	8 ± 1	4 ± 1	ND	ND
	10 µM AgNP	41 ± 1	25 ± 1	14 ± 1	ND	6	10	5 ± 1	ND	ND
	0.1 µM AgNO <sub>3</sub>	41 ± 1	20	18 ± 1	ND	7 ± 1	8	5	ND	ND

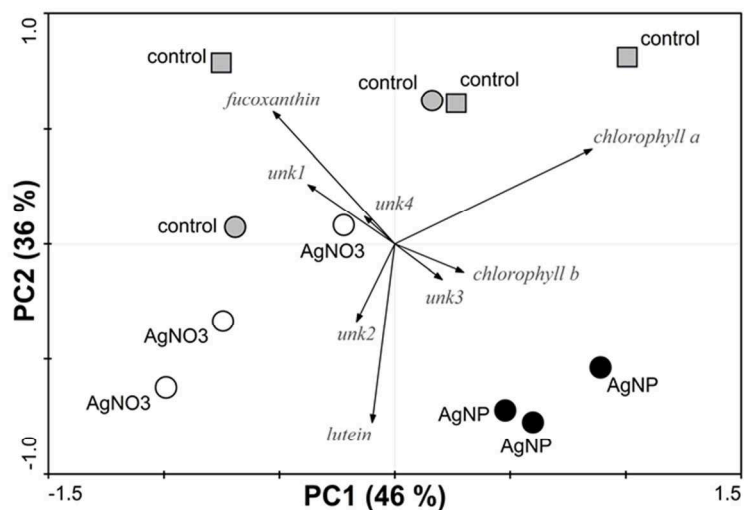


**Figure B.8.** Principal component analysis of the content of marker pigments in periphyton of experiment 2 (circles), after 21 days of exposure to 10  $\mu\text{M}$  AgNP and 0.1  $\mu\text{M}$  AgNO<sub>3</sub>. Pigments were quantified in periphyton extracts using HPLC. Three replicates from each treatment were analyzed. Control measurements from experiment 2 (squares) are shown for comparison purposes.

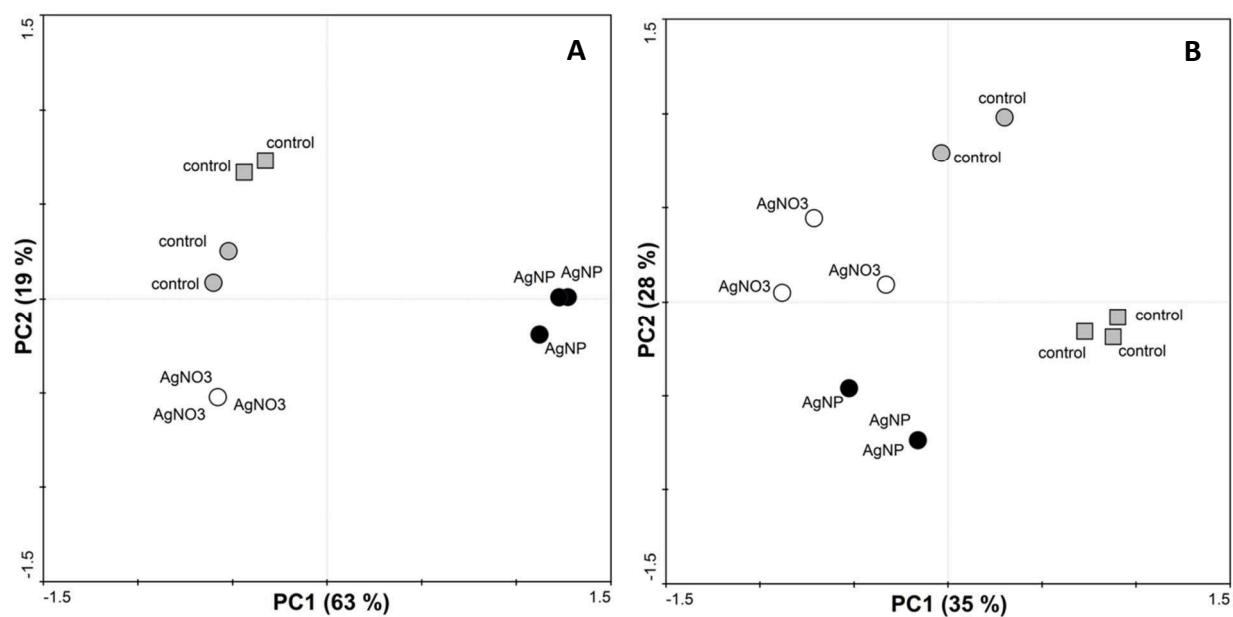


**Figure B.9.** Principal component analysis of the community structure of periphyton, as determined by denaturing gradient gel electrophoresis (DGGE) with conserved 18S (A) and 16S (B) rDNA fragments, after 21 days of exposure to 10  $\mu\text{M}$  AgNP and 0.1  $\mu\text{M}$  AgNO<sub>3</sub> in experiment 1 (circles). Control measurements from experiment 2 (squares) are shown for comparison purposes. From each treatment, three replicate community fingerprints were obtained.

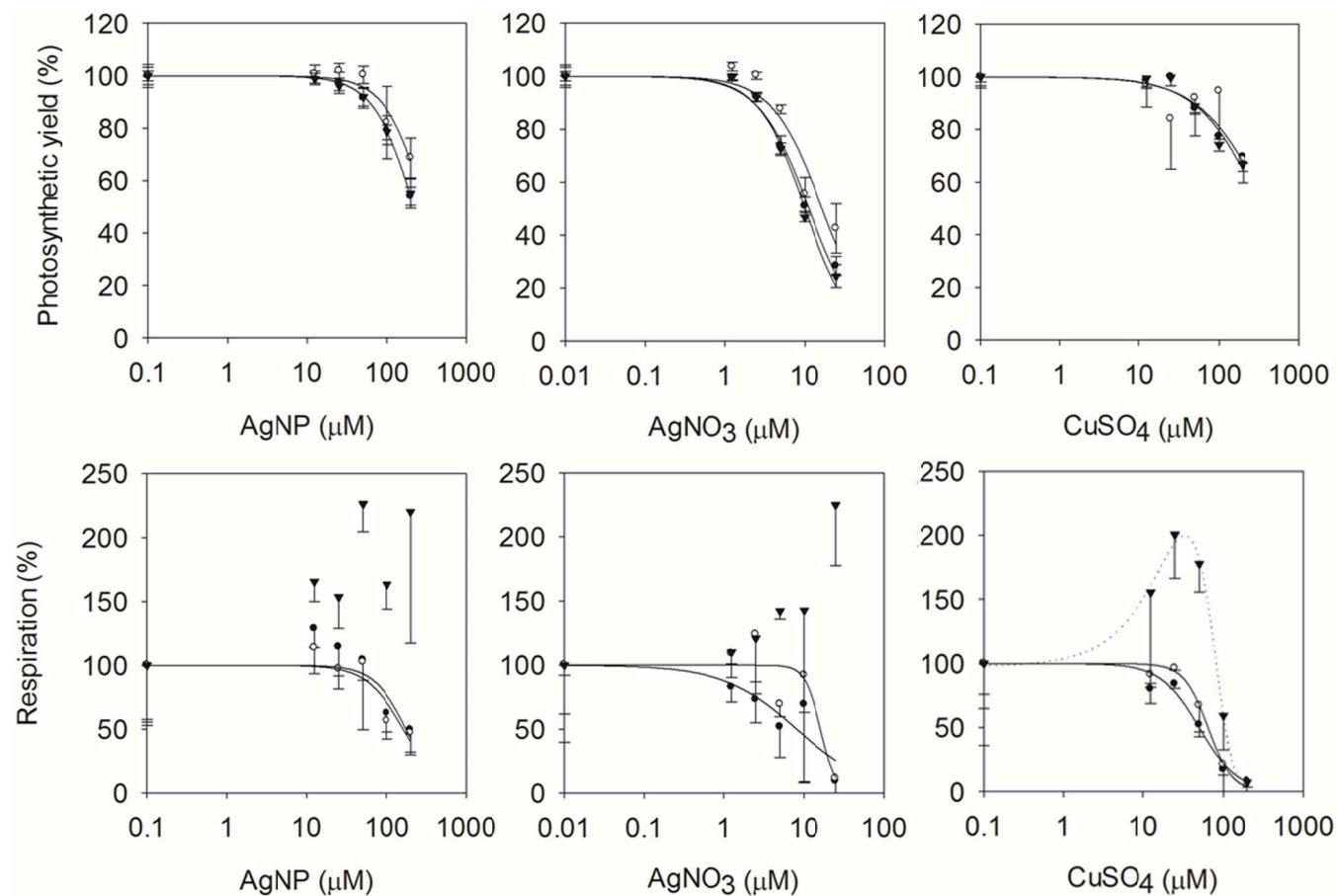


**Figure B.10.** Concentration-response curves obtained from short-term bioassays to assess the pollution-induced community tolerance of periphyton pre-exposed during 21 days to 10  $\mu\text{M}$  AgNP (▼) and 0.1  $\mu\text{M}$  AgNO<sub>3</sub> (○), compared to non-preexposed control periphyton (●). Error bars correspond to three replicates. Solid lines represent the fit of the logistic model used to estimate EC<sub>50</sub> values for the comparison of sensitivities among the communities, which are shown in Table 2. The dotted line indicates the data for which the non-monotonic model was applied.

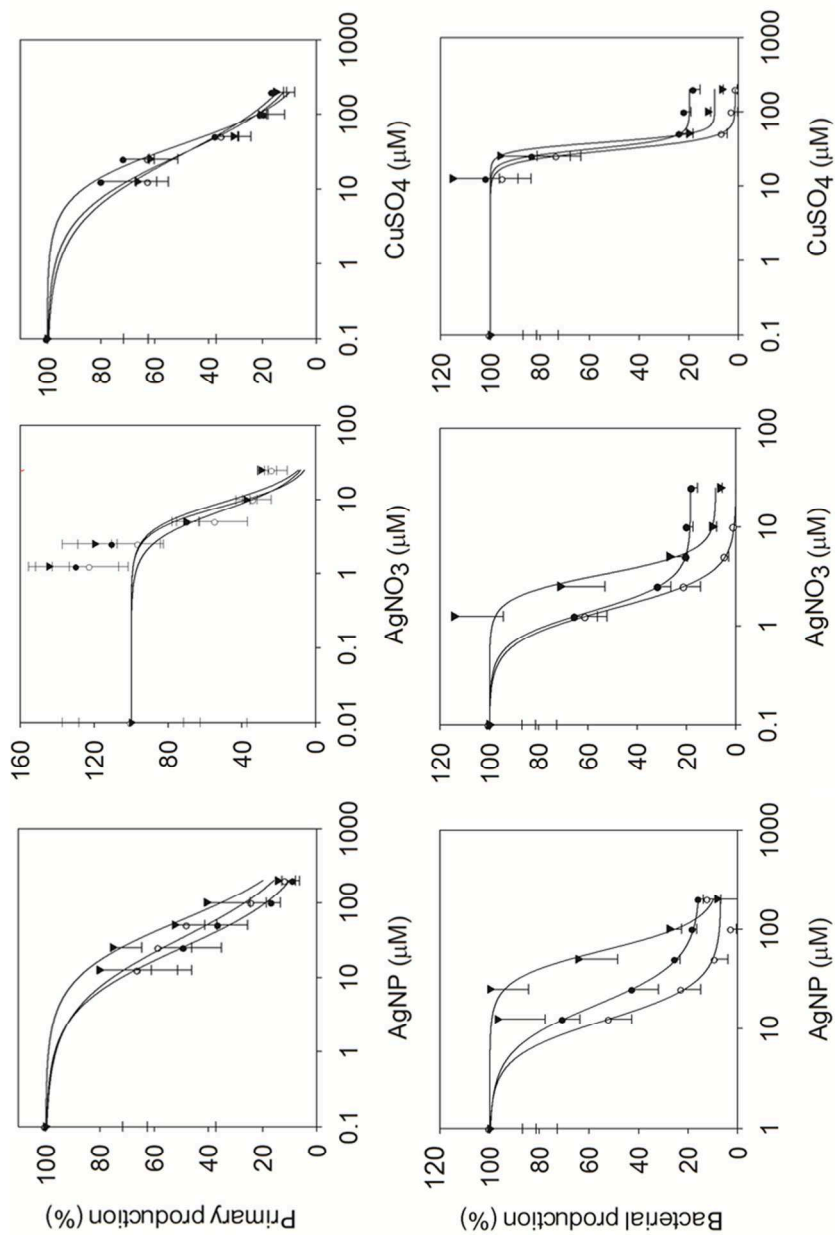
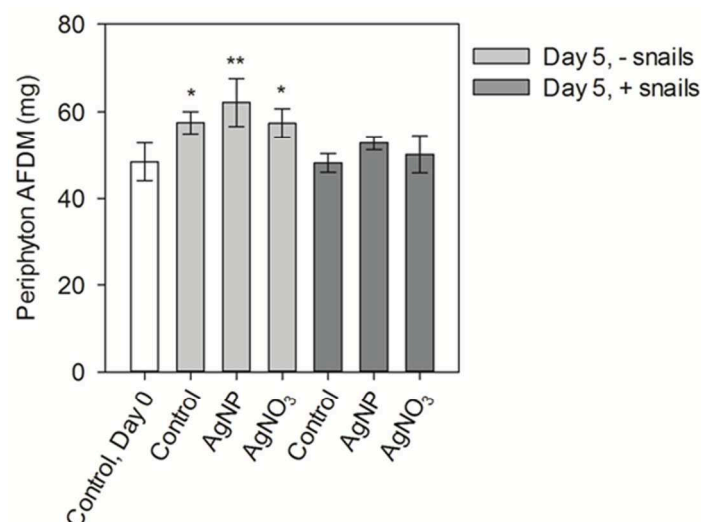


Figure B.10. (Continued).

## Appendix C. Supporting information of Chapter 4



**Figure C.1.** Biomass of periphyton as the total ash-free dry mass in the microcosm at day 0 (white bar) and day 5, in absence (light gray) and presence (dark gray) of snails. Error bars represent the standard deviation of four microcosms per treatment. Statistical significance was tested by one-way ANOVA followed by Dunnett's test. \*  $p < 0.05$ , \*\*  $p < 0.001$ .

**Table C.1.** Estimation of the range of silver assimilation efficiency (AE) in snails over the five-day feeding experiment by two methods.

**A)**  $AE_1 (\%) = Ag_{snails} / (Ag_{snails} + Ag_{feces}) \times 100 \%$  (Croteau et al. 2011b)

Treatment	$Ag_{snails}$ (nmol)	$Ag_{feces}$ (nmol)	$AE_1 (\%)$
AgNP 1	72.15	54.08	57
AgNP 2	40.88	44.92	48
AgNP 3	43.18	41.34	51
AgNP 4	51.06	51.64	50
AgNO <sub>3</sub> 1	5.31	3.15	63
AgNO <sub>3</sub> 2	3.36	3.67	48
AgNO <sub>3</sub> 3	4.17	3.13	57
AgNO <sub>3</sub> 4	4.47	3.64	55
AgNP			$51 \pm 4$
AgNO <sub>3</sub>			$56 \pm 6$

**Table C.1.** (Continued).

**B)**  $AE_2 (\%) = 100 \% - [(Ag]_{feces} / [Ag]_{periphyton}) \times 100 \%$

Treatment	[Ag] <sub>periphyton</sub> (nmol mg <sup>-1</sup> DM <sub>periphyton</sub> )	[Ag] <sub>feces</sub> (nmol mg <sup>-1</sup> DM <sub>feces</sub> )	AE <sub>2</sub> (%)
AgNP 1	18.62	2.52	86
AgNP 2	20.42	3.30	84
AgNP 3	21.11	3.27	85
AgNP 4	19.56	3.23	83
AgNO <sub>3</sub> 1	1.06	0.17	84
AgNO <sub>3</sub> 2	0.91	0.24	74
AgNO <sub>3</sub> 3	1.08	0.19	82
AgNO <sub>3</sub> 4	0.99	0.22	78
AgNP			85 ± 1
AgNO <sub>3</sub>			79 ± 4

**Table C.2.** Total silver concentrations in exposure medium, and exopolysaccharide matrix (EPS) of periphyton, which contains complexed Ag<sup>+</sup> ions and loosely sorbed silver, as determined by ICP-MS. Average values and standard deviations calculated from four microcosm replicates per treatment.

Periphyton treatment	Exposure medium (μmol)	EPS (μmol)
Control - snails	< 0.01	< 0.01
AgNP - snails	0.05 ± 0.01	0.06 ± 0.01
AgNO <sub>3</sub> - snails	< 0.01	< 0.01
Control + snails	< 0.01	< 0.01
AgNP + snails	0.03 ± 0.01	0.05 ± 0.01
AgNO <sub>3</sub> + snails	< 0.01	< 0.01



## References

- Abramoff MD, Magalhaes PJ, Ram SJ. 2004. Image processing with ImageJ. *Biophotonics International* 11(7): 36-42.
- Adegboyega NF, Sharma VK, Siskova K, Zboril R, Sohn M, Schultz BJ, Banerjee S. 2013. Interactions of aqueous Ag<sup>+</sup> with fulvic acids: Mechanisms of silver nanoparticle formation and investigation of stability. *Environmental Science & Technology* 47(2): 757-764.
- Ali D, Yadav PG, Kumar S, Ali H, Alarifi S, Harrath AH. 2014. Sensitivity of freshwater pulmonate snail *Lymnaea luteola* L., to silver nanoparticles. *Chemosphere* 104(0): 134-140.
- Amann RI, Binder BJ, Olson RJ, Chisholm SW, Devereux R, Stahl DA. 1990. Combination of 16S rRNA-targeted oligonucleotide probes with flow cytometry for analyzing mixed microbial populations. *Applied and Environmental Microbiology* 56(6): 1919-1925.
- Auffan M, Rose J, Bottero J-Y, Lowry GV, Jolivet J-P, Wiesner MR. 2009. Towards a definition of inorganic nanoparticles from an environmental, health and safety perspective. *Nature Nanotechnology* 4(10): 634-641.
- Bae E, Park HJ, Lee J, Kim Y, Yoon J, Park K, Choi K, Yi J. 2010. Bacterial cytotoxicity of the silver nanoparticle related to physicochemical metrics and agglomeration properties. *Environmental Toxicology and Chemistry* 29(10): 2154-2160.
- Bandow C, Weltje L. 2012. Development of an embryo toxicity test with the pond snail *Lymnaea stagnalis* using the model substance tributyltin and common solvents. *Science of the Total Environment* 435-436(0): 90-95.
- Barranguet C, Van Den Ende FP, Rutgers M, Breure AM, Greijdanus M, Sinke JJ, Admiraal W. 2003. Copper-induced modifications of the trophic relations in riverine algal-bacterial biofilms. *Environmental Toxicology and Chemistry* 22(6): 1340-1349.
- Battin TJ, Kammer FVD, Weilhartner A, Ottofuelling S, Hofmann T. 2009. Nanostructured TiO<sub>2</sub>: Transport behavior and effects on aquatic microbial communities under environmental conditions. *Environmental Science & Technology*: 8098-8104.
- Battin TJ, Kaplan LA, Denis Newbold J, Hansen CME. 2003. Contributions of microbial biofilms to ecosystem processes in stream mesocosms. *Nature* 426(6965): 439-442.
- Baun A, Hartmann NB, Grieger K, Kusk KO. 2008. Ecotoxicity of engineered nanoparticles to aquatic invertebrates: A brief review and recommendations for future toxicity testing. *Ecotoxicology* 17: 387-395.
- Behra R, Sigg L, Clift MJD, Herzog F, Minghetti M, Johnston B, Petri-Fink A, Rothen-Rutishauser B. 2013. Bioavailability of silver nanoparticles and ions: From a chemical and biochemical perspective. *Journal of The Royal Society Interface* 10(87).
- Bell RA, Kramer JR. 1999. Structural chemistry and geochemistry of silver-sulfur compounds: Critical review. *Environmental Toxicology and Chemistry* 18(1): 9-22.
- Benn TM, Westerhoff P. 2008. Nanoparticle silver released into water from commercially available sock fabrics. *Environmental Science & Technology* 42(11): 4133-4139.

- Berges JA, Charlebois DO, Mauzerall DC, Falkowski PG. 1996. Differential effects of nitrogen limitation on photosynthetic efficiency of photosystems I and II in microalgae. *Plant Physiology* 110(2): 689-696.
- Bernhardt ES, Colman BP, Hochella MF, Cardinale BJ, Nisbet RM, Richardson CJ, Yin L. 2010. An ecological perspective on nanomaterial impacts in the environment. *Journal of Environmental Quality* 39: 1954-1965.
- Bernot RJ, Brandenburg M. 2013. Freshwater snail vital rates affected by non-lethal concentrations of silver nanoparticles. *Hydrobiologia* 714(1): 25-34.
- Bielmyer-Fraser GK, Jarvis TA, Lenihan HS, Miller RJ. 2014. Cellular partitioning of nanoparticulate versus dissolved metals in marine phytoplankton. *Environmental Science & Technology* 48(22): 13443-13450.
- Blanck H. 2002. A critical review of procedures and approaches used for assessing pollution-induced community tolerance (PICT) in biotic communities. *Human and Ecological Risk Assessment* 8(5): 1003-1034.
- Blanck H, Wängberg S-A, Molander S. 1988. Pollution induced community tolerance (PICT) - a new ecotoxicological tool. In: Cairns J, Pratt JP, editors. *Functional testing of aquatic biota for estimating hazard of chemicals*. Philadelphia: American Society for Testing and Materials. p 219-230.
- Blenkinsopp S, Lock MA. 1994. The impact of storm-flow on river biofilm architecture. *Journal of Phycology* 30: 807-818.
- Bouldin JL, Ingle TM, Sengupta A, Alexander R, Hannigan RE, Buchanan RA. 2008. Aqueous toxicity and food chain transfer of Quantum Dots™ in freshwater algae and *Ceriodaphnia dubia*. *Environmental Toxicology and Chemistry* 27(9): 1958-1963.
- Bradac P, Behra R, Sigg L. 2009a. Accumulation of cadmium in periphyton under various freshwater speciation conditions. *Environmental Science and Technology* 43(19): 7291-7296.
- Bradac P, Navarro E, Odzak N, Behra R, Sigg L. 2009b. Kinetics of cadmium accumulation in periphyton under freshwater conditions. *Environmental Toxicology and Chemistry* 28(10): 2108-2116.
- Bradford A, Handy RD, Readman JW, Atfield A, Muhling M. 2009. Impact of silver nanoparticle contamination on the genetic diversity of natural bacterial assemblages in estuarine sediments. *Environmental Science & Technology* 43(12): 4530-4536.
- Buesing N, Gessner MO. 2003. Incorporation of radiolabeled leucine into protein to estimate bacterial production in plant litter, sediment, epiphytic biofilms, and water samples. *Microbial Ecology* 45(3): 291-301.
- Bundschuh M, Seitz F, Rosenfeldt RR, Schulz R. 2012. Titanium dioxide nanoparticles increase sensitivity in the next generation of the water flea *Daphnia magna*. *Plos One* 7(11): e48956.
- Canesi L, Ciacci C, Fabbri R, Marcomini A, Pojana G, Gallo G. 2012. Bivalve molluscs as a unique target group for nanoparticle toxicity. *Marine Environmental Research* 76(0): 16-21.
- Cazan A, Klerks P. 2014. Evidence of maternal copper and cadmium transfer in two live-bearing fish species. *Ecotoxicology* 23(9): 1774-1783.

- Cedergreen N, Ritz C, Streibig JC. 2005. Improved empirical models describing hormesis. *Environmental Toxicology and Chemistry* 24(12): 3166-3172.
- Chambers BA, Afrooz ARMN, Bae S, Aich N, Katz L, Saleh NB, Kirisits MJ. 2014. Effects of chloride and ionic strength on physical morphology, dissolution, and bacterial toxicity of silver nanoparticles. *Environmental Science & Technology* 48(1): 761-769.
- Cheung CCC, Lam PKS. 1998. Effect of cadmium on the embryos and juveniles of a tropical freshwater snail, *Physa acuta* (Draparnaud, 1805). *Water Science and Technology* 38(7): 263-270.
- Chinnapongse SL, MacCuspie RI, Hackley VA. 2011. Persistence of singly dispersed silver nanoparticles in natural freshwaters, synthetic seawater, and simulated estuarine waters. *Science of the Total Environment* 409(12): 2443-2450.
- Choi O, Hu Z. 2008. Size dependent and reactive oxygen species related nanosilver toxicity to nitrifying bacteria. *Environmental Science and Technology* 42(12): 4583-4588.
- Choi O, Yu CP, Esteban Fernández G, Hu Z. 2010. Interactions of nanosilver with *Escherichia coli* cells in planktonic and biofilm cultures. *Water Research* 44(20): 6095-6103.
- Chróst RJ. 1991. Microbial enzymes in aquatic environments. Chróst RJ, editor. New York: Springer-Verlag. 317 p.
- Clements WH, Hickey CW, Kidd KA. 2012. How do aquatic communities respond to contaminants? It depends on the ecological context. *Environmental Toxicology and Chemistry* 31(9): 1932-1940.
- Clements WH, Rohr JR. 2009. Community responses to contaminants: Using basic ecological principles to predict ecotoxicological effects. *Environmental Toxicology and Chemistry* 28(9): 1789-1800.
- Cleveland D, Long SE, Pennington PL, Cooper E, Fulton MH, Scott GI, Brewer T, Davis J, Petersen EJ, Wood L. 2012. Pilot estuarine mesocosm study on the environmental fate of silver nanomaterials leached from consumer products. *Science of the Total Environment* 421-422: 267-272.
- Colman B, Wang S-Y, Auffan M, Wiesner M, Bernhardt E. 2012. Antimicrobial effects of commercial silver nanoparticles are attenuated in natural streamwater and sediment. *Ecotoxicology* 21(7): 1867-1877.
- Colman BP, Espinasse B, Richardson CJ, Matson CW, Lowry GV, Hunt DE, Wiesner MR, Bernhardt ES. 2014. Emerging contaminant or an old toxin in disguise? Silver nanoparticle impacts on ecosystems. *Environmental Science & Technology* 48(9): 5229-5236.
- Cong Y, Banta GT, Selck H, Berhanu D, Valsami-Jones E, Forbes VE. 2014. Toxicity and bioaccumulation of sediment-associated silver nanoparticles in the estuarine polychaete, *Nereis (Hediste) diversicolor*. *Aquatic Toxicology* 156: 106-115.
- Croteau M-N, Misra SK, Luoma SN, Valsami-Jones E. 2014. Bioaccumulation and toxicity of CuO nanoparticles by a freshwater invertebrate after waterborne and dietborne exposures. *Environmental Science & Technology* 48(18): 10929-10937.

- Croteau MN, Dybowska AD, Luoma SN, Valsami-Jones E. 2011a. A novel approach reveals that zinc oxide nanoparticles are bioavailable and toxic after dietary exposures. *Nanotoxicology* 5(1): 79-90.
- Croteau MN, Misra SK, Luoma SN, Valsami-Jones E. 2011b. Silver bioaccumulation dynamics in a freshwater invertebrate after aqueous and dietary exposures to nanosized and ionic Ag. *Environmental Science & Technology* 45(15): 6600-6607.
- Cumberland SA, Lead JR. 2009. Particle size distributions of silver nanoparticles at environmentally relevant conditions. *Journal of Chromatography A* 1216(52): 9099-9105.
- Das P, Metcalfe CD, Xenopoulos MA. 2014. Interactive effects of silver nanoparticles and phosphorus on phytoplankton growth in natural waters. *Environ Sci Technol* 48(8): 4573-4580.
- Das P, Williams CJ, Fulthorpe RR, Hoque ME, Metcalfe CD, Xenopoulos MA. 2012. Changes in bacterial community structure after exposure to silver nanoparticles in natural waters. *Environ Sci Technol* 46(16): 9120-9128.
- Das S, Khangarot BS. 2011. Bioaccumulation of copper and toxic effects on feeding, growth, fecundity and development of pond snail *Lymnaea luteola* L. *Journal of Hazardous Materials* 185(1): 295-305.
- Dasari TP, Hwang H-M. 2010. The effect of humic acids on the cytotoxicity of silver nanoparticles to a natural aquatic bacterial assemblage. *Science of the Total Environment* 408(23): 5817-5823.
- Devi Prasad PV, Devi Prasad PS. 1982. Effect of cadmium, lead and nickel on three freshwater green algae. *Water, Air & Soil Pollution* 17(3): 263-268.
- Díaz-Raviña M, Bååth E. 1996. Development of metal tolerance in soil bacterial communities exposed to experimentally increased metal levels. *Applied and Environmental Microbiology* 62(8): 2970-2977.
- Dimkpa CO, Calder A, Gajjar P, Merugu S, Huang WJ, Britt DW, McLean JE, Johnson WP, Anderson AJ. 2011. Interaction of silver nanoparticles with an environmentally beneficial bacterium, *Pseudomonas chlororaphis*. *Journal of Hazardous Materials* 188(1-3): 428-435.
- Dobias J, Bernier-Latmani R. 2013. Silver release from silver nanoparticles in natural waters. *Environmental Science & Technology* 47(9): 4140-4146.
- Doiron K, Pelletier E, Lemarchand K. 2012. Impact of polymer-coated silver nanoparticles on marine microbial communities: A microcosm study. *Aquat Toxicol* 124-125(0): 22-27.
- Dorigo U, Leboulanger C. 2001. A pulse-amplitude modulated fluorescence-based method for assessing the effects of photosystem II herbicides on freshwater periphyton. *Journal of Applied Phycology* 13(6): 509-515.
- Dorigo U, Leboulanger C, Bérard A, Bouchez A, Humbert JF, Montuelle B. 2007. Lotic biofilm community structure and pesticide tolerance along a contamination gradient in a vineyard area. *Aquatic Microbial Ecology* 50(1): 91-102.
- Echavarri-Bravo V, Paterson L, Aspray TJ, Porter JS, Winson MK, Thornton B, Hartl MGJ. 2015. Shifts in the metabolic function of a benthic estuarine microbial community following a single pulse exposure to silver nanoparticles. *Environmental Pollution* 201: 91-99.

- El Badawy AM, Luxton TP, Silva RG, Scheckel KG, Suidan MT, Tolaymat TM. 2010. Impact of environmental conditions (pH, ionic strength, and electrolyte type) on the surface charge and aggregation of silver nanoparticles suspensions. *Environmental Science and Technology* 44(4): 1260-1266.
- El Badawy AM, Silva RG, Morris B, Scheckel KG, Suidan MT, Tolaymat TM. 2011. Surface charge-dependent toxicity of silver nanoparticles. *Environmental Science & Technology* 45(1): 283-287.
- Espeland EM, Francoeur SN, Wetzel RG. 2001. Influence of algal photosynthesis on biofilm bacterial production and associated glucosidase and xylosidase activities. *Microbial Ecology* 42(4): 524-530.
- Evans-White MA, Lamberti GA. 2009. Direct and indirect effects of a potential aquatic contaminant on grazer-algae interactions. *Environmental Toxicology and Chemistry* 28(2): 418-426.
- Fabrega J, Luoma SN, Tyler CR, Galloway TS, Lead JR. 2011a. Silver nanoparticles: Behaviour and effects in the aquatic environment. *Environment International* 37(2): 517-531.
- Fabrega J, Renshaw JC, Lead JR. 2009. Interactions of silver nanoparticles with *Pseudomonas putida* biofilms. *Environmental Science and Technology* 43(23): 9004-9009.
- Fabrega J, Zhang R, Renshaw JC, Liu WT, Lead JR. 2011b. Impact of silver nanoparticles on natural marine biofilm bacteria. *Chemosphere* 85(6): 961-966.
- Farkas J, Peter H, Christian P, Gallego Urrea JA, Hassellöv M, Tuoriniemi J, Gustafsson S, Olsson E, Hylland K, Thomas KV. 2011. Characterization of the effluent from a nanosilver producing washing machine. *Environment International* 37(6): 1057-1062.
- Fechner LC, Gourlay-Francé C, Uher E, Tusseau-Vuillemin MH. 2010. Adapting an enzymatic toxicity test to allow comparative evaluation of natural freshwater biofilms' tolerance to metals. *Ecotoxicology* 19(7): 1302-1311.
- Ferry JL, Craig P, Hexel C, Sisco P, Frey R, Pennington PL, Fulton MH, Scott IG, Decho AW, Kashiwada S, Murphy CJ, Shaw TJ. 2009. Transfer of gold nanoparticles from the water column to the estuarine food web. *Nat Nanotechnol* 4(7): 441-444.
- Fortin C, Campbell PGC. 2000. Silver uptake by the green alga *Chlamydomonas reinhardtii* in relation to chemical speciation: Influence of chloride. *Environmental Toxicology and Chemistry* 19(11): 2769-2778.
- Franke S. 2007. Microbiology of the toxic noble metal silver. In: Nies D, Silver S, editors. *Molecular microbiology of heavy metals*: Springer Berlin Heidelberg. p 343-355.
- Gagné F, Auclair J, Turcotte P, Gagnon C. 2013. Sublethal effects of silver nanoparticles and dissolved silver in freshwater mussels. *Journal of Toxicology and Environmental Health - Part A: Current Issues* 76(8): 479-490.
- Gallego-Urrea JA, Tuoriniemi J, Hassellöv M. 2011. Applications of particle-tracking analysis to the determination of size distributions and concentrations of nanoparticles in environmental, biological and food samples. *TrAC - Trends in Analytical Chemistry* 30(3): 473-483.
- García-Alonso J, Khan FR, Misra SK, Turmaine M, Smith BD, Rainbow PS, Luoma SN, Valsami-Jones E. 2011. Cellular internalization of silver nanoparticles in gut epithelia of the

- estuarine polychaete *Nereis diversicolor*. *Environmental Science & Technology* 45(10): 4630-4636.
- Garnier-Laplace J, Baudin JP, Foulquier L. 1992. Experimental study of  $^{110m}\text{Ag}$  transfer from sediment to biota in a simplified freshwater ecosystem. *Hydrobiologia* 235-236(1): 393-406.
- Garrido JL, Zapata M. 1993. High performance liquid chromatography of chlorophylls c3, c1, c2 and a and of carotenoids of chromophyte algae on a polymeric octadecyl silica column. *Chromatographia* 35(9-12): 543-547.
- Gessner MO, Chauvet E, Dobson M. 1999. A perspective on leaf litter breakdown in streams. *Oikos* 85(2): 377-384.
- Gil-Allué C, Schirmer K, Tlili A, Gessner MO, Behra R. 2015. Silver nanoparticle effects on stream periphyton during short-term exposures. *Environmental Science & Technology* 49(2): 1165-1172.
- Gomot A. 1998. Toxic effects of cadmium on reproduction, development, and hatching in the freshwater snail *Lymnaea stagnalis* for water quality monitoring. *Ecotoxicology and Environmental Safety* 41(3): 288-297.
- Gondikas AP, Morris A, Reinsch BC, Marinakos SM, Lowry GV, Hsu-Kim H. 2012. Cysteine-induced modifications of zero-valent silver nanomaterials: Implications for particle surface chemistry, aggregation, dissolution, and silver speciation. *Environ Sci Technol* 46(13): 7037-7045.
- González AG, Mombo S, Leflaive J, Lamy A, Pokrovsky OS, Rols JL. 2014. Silver nanoparticles impact phototrophic biofilm communities to a considerably higher degree than ionic silver. *Environmental Science and Pollution Research* 22(11): 8412-8424.
- Gottschalk F, Sonderer T, Scholz RW, Nowack B. 2009. Modeled environmental concentrations of engineered nanomaterials ( $\text{TiO}_2$ ,  $\text{ZnO}$ ,  $\text{Ag}$ , CNT, fullerenes) for different regions. *Environmental Science & Technology* 43(24): 9216-9222.
- Gottschalk F, Sun T, Nowack B. 2013. Environmental concentrations of engineered nanomaterials: Review of modeling and analytical studies. *Environmental Pollution* 181: 287-300.
- Griffitt RJ, Luo J, Gao J, Bonzongo JC, Barber DS. 2008. Effects of particle composition and species on toxicity of metallic nanomaterials in aquatic organisms. *Environmental Toxicology and Chemistry* 27(9): 1972-1978.
- Guasch H, Paulsson M, Sabater S. 2002. Effect of copper on algal communities from oligotrophic calcareous streams. *Journal of Phycology* 38(2): 241-248.
- Haack TK, Gordon AM. 1982. Nutritional relationships among microorganisms in an epilithic biofilm community. *Microbial Ecology* 8(2): 115-126.
- He D, Dorantes-Aranda JJ, Waite TD. 2012. Silver nanoparticle-algae interactions: Oxidative dissolution, reactive oxygen species generation and synergistic toxic effects. *Environmental Science & Technology* 46(16): 8731-8738.
- Hoheisel SM, Diamond S, Mount D. 2012. Comparison of nanosilver and ionic silver toxicity in *Daphnia magna* and *Pimephales promelas*. *Environmental Toxicology and Chemistry* 31(11): 2557-2563.

- Holbrook RD, Murphy KE, Morrow JB, Cole KD. 2008. Trophic transfer of nanoparticles in a simplified invertebrate food web. *Nature Nanotechnology* 3(6): 352-355.
- Holt KB, Bard AJ. 2005. Interaction of silver(I) ions with the respiratory chain of *Escherichia coli*: An electrochemical and scanning electrochemical microscopy study of the antimicrobial mechanism of micromolar Ag. *Biochemistry* 44(39): 13214-13223.
- Hooper DU, Chapin FS, Ewel JJ, Hector A, Inchausti P, Lavorel S, Lawton JH, Lodge DM, Loreau M, Naeem S, Schmid B, Setälä H, Symstad AJ, Vandermeer J, Wardle DA. 2005. Effects of biodiversity on ecosystem functioning: A consensus of current knowledge. *Ecological Monographs* 75(1): 3-35.
- Insam H. 1997. A new set of substrates proposed for community characterization in environmental samples. In: Insam H, Rangger A, editors. *Microbial communities*: Springer Berlin Heidelberg. p 259-260.
- ISO. 2008. Iso/ts 272687.
- Ivask A, Juganson K, Bondarenko O, Mortimer M, Aruoja V, Kasemets K, Blinova I, Heinlaan M, Slaveykova V, Kahru A. 2013. Mechanisms of toxic action of Ag, ZnO and CuO nanoparticles to selected ecotoxicological test organisms and mammalian cells in vitro: A comparative review. *Nanotoxicology* 8(S1): 57-71.
- Ivask A, Kurvet I, Kasemets K, Blinova I, Aruoja V, Suppi S, Vija H, Käkinen A, Titma T, Heinlaan M, Visnapuu M, Koller D, Kisand V, Kahru A. 2014. Size-dependent toxicity of silver nanoparticles to bacteria, yeast, algae, crustaceans and mammalian cells in vitro. *PLOS ONE* 9(7): e102108.
- Jacobasch C, Völker C, Giebner S, Völker J, Alsenz H, Potouridis T, Heidenreich H, Kayser G, Oehlmann J, Oetken M. 2014. Long-term effects of nanoscaled titanium dioxide on the cladoceran *Daphnia magna* over six generations. *Environmental Pollution* 186(0): 180-186.
- Justice JR, Bernot RJ. 2014. Nanosilver inhibits freshwater gastropod (*Physa acuta*) ability to assess predation risk. *The American Midland Naturalist* 171(2): 340-349.
- Kaegi R, Sinnet B, Zuleeg S, Hagendorfer H, Mueller E, Vonbank R, Boller M, Burkhardt M. 2010. Release of silver nanoparticles from outdoor facades. *Environ Pollut* 158(9): 2900-2905.
- Kaegi R, Voegelin A, Sinnet B, Zuleeg S, Hagendorfer H, Burkhardt M, H aS. 2011. Behavior of metallic silver nanoparticles in a pilot wastewater treatment plant. *Environmental Science & Technology* 45(9): 3902-3908.
- Kasprzak P, Padisák J, Koschel R, Krienitz L, Gervais F. 2008. Chlorophyll a concentration across a trophic gradient of lakes: An estimator of phytoplankton biomass? *Limnologia - Ecology and Management of Inland Waters* 38(3-4): 327-338.
- Khan FR, Misra SK, Bury NR, Smith BD, Rainbow PS, Luoma SN, Valsami-Jones E. 2015. Inhibition of potential uptake pathways for silver nanoparticles in the estuarine snail *Peringia ulvae*. *Nanotoxicology* DOI:10.3109/17435390.2014.948519.
- Khargarot BS, Das S. 2010. Effects of copper on the egg development and hatching of a freshwater pulmonate snail *Lymnaea luteola* L. *Journal of Hazardous Materials* 179(1-3): 665-675.

- Kim SW, Kwak JI, An Y-J. 2013. Multigenerational study of gold nanoparticles in *Caenorhabditis elegans*: Transgenerational effect of maternal exposure. *Environmental Science & Technology* 47(10): 5393-5399.
- Kroll A, Behra R, Kaegi R, Sigg L. 2014. Extracellular polymeric substances (EPS) of freshwater biofilms stabilize and modify CeO<sub>2</sub> and Ag nanoparticles. *PLOS ONE* 9(10): e110709.
- Kulacki KJ, Cardinale BJ, Keller AA, Bier R, Dickson H. 2012. How do stream organisms respond to, and influence, the concentration of titanium dioxide nanoparticles? A mesocosm study with algae and herbivores. *Environmental Toxicology and Chemistry* 31(10): 2414-2422.
- Lanceleur L, Schäfer J, Bossy C, Coynel A, Larrose A, Masson M, Blanc G. 2011. Silver fluxes to the gironde estuary – eleven years (1999–2009) of monitoring at the watershed scale. *Applied Geochemistry* 26(5): 797-808.
- Le Faucheur S, Behra R, Sigg L. 2005. Phytochelatin induction, cadmium accumulation, and algal sensitivity to free cadmium ion in *Scenedesmus vacuolatus*. *Environmental Toxicology and Chemistry* 24(7): 1731-1737.
- Leclerc S, Wilkinson KJ. 2013. Bioaccumulation of nanosilver by *Chlamydomonas reinhardtii*—nanoparticle or the free ion? *Environmental Science & Technology* 48(1): 358-364.
- Lee DY, Fortin C, Campbell PGC. 2004. Influence of chloride on silver uptake by two green algae, *Pseudokirchneriella subcapitata* and *Chlorella pyrenoidosa*. *Environmental Toxicology and Chemistry* 23(4): 1012-1018.
- Lee KJ, Nallathamby PD, Browning LM, Osgood CJ, Xu XHN. 2007. In vivo imaging of transport and biocompatibility of single silver nanoparticles in early development of zebrafish embryos. *ACS Nano* 1(2): 133-143.
- Levard C, Hotze EM, Colman BP, Dale AL, Truong L, Yang XY, Bone AJ, Brown GE, Tanguay RL, Di Giulio RT, Bernhardt ES, Meyer JN, Wiesner MR, Lowry GV. 2013. Sulfidation of silver nanoparticles: Natural antidote to their toxicity. *Environmental Science & Technology* 47(23): 13440-13448.
- Levard C, Hotze EM, Lowry GV, Brown GE. 2012. Environmental transformations of silver nanoparticles: Impact on stability and toxicity. *Environmental Science & Technology* 46(13): 6900-6914.
- Liu JY, Hurt RH. 2010. Ion release kinetics and particle persistence in aqueous nano-silver colloids. *Environmental Science & Technology* 44(6): 2169-2175.
- Lombardi AT, Hidalgo TMR, Vieira AAH. 2005. Copper complexing properties of dissolved organic materials exuded by the freshwater microalgae *scenedesmus acuminatus* (*Chlorophyceae*). *Chemosphere* 60(4): 453-459.
- Lowry GV, Espinasse BP, Badireddy AR, Richardson CJ, Reinsch BC, Bryant LD, Bone AJ, Deonarine A, Chae S, Therezien M, Colman BP, Hsu-Kim H, Bernhardt ES, Matson CW, Wiesner MR. 2012. Long-term transformation and fate of manufactured ag nanoparticles in a simulated large scale freshwater emergent wetland. *Environmental Science & Technology* 46(13): 7027-7036.



- Luoma SN, Khan FR, Croteau M-N. 2014. Bioavailability and bioaccumulation of metal-based engineered nanomaterials in aquatic environments: Concepts and processes. In: Jamie RL, Eugenia V-J, editors. *Frontiers of nanoscience*: Elsevier. p 157-193.
- Macfie SM, Tarmohamed Y, Welbourn PM. 1994. Effects of cadmium, cobalt, copper, and nickel on growth of the green alga *Chlamydomonas reinhardtii*: The influences of the cell wall and pH. *Archives of Environmental Contamination and Toxicology* 27(4): 454-458.
- Mason AZ, Jenkins KD. 1995. Metal detoxification in aquatic organisms. In: Tessier A, Turner DR, editors. *Metal speciation and bioavailability in aquatic systems*. Chichester: Wiley. p 479-608.
- McTeer J, Dean AP, White KN, Pittman JK. 2014. Bioaccumulation of silver nanoparticles into *Daphnia magna* from a freshwater algal diet and the impact of phosphate availability. *Nanotoxicology* 8(3): 305-316.
- Merrifield DL, Shaw BJ, Harper GM, Saoud IP, Davies SJ, Handy RD, Henry TB. 2013. Ingestion of metal-nanoparticle contaminated food disrupts endogenous microbiota in zebrafish (*Danio rerio*). *Environmental Pollution* 174: 157-163.
- Meyer JN, Lord CA, Yang XY, Turner EA, Badireddy AR, Marinakos SM, Chilkoti A, Wiesner MR, Auffan M. 2010. Intracellular uptake and associated toxicity of silver nanoparticles in *Caenorhabditis elegans*. *Aquatic Toxicology* 100(2): 140-150.
- Meylan S, Behra R, Sigg L. 2003. Accumulation of copper and zinc in periphyton in response to dynamic variations of metal speciation in freshwater. *Environmental Science and Technology* 37(22): 5204-5212.
- Miao AJ, Luo Z, Chen CS, Chin WC, Santschi PH, Quigg A. 2010. Intracellular uptake: A possible mechanism for silver engineered nanoparticle toxicity to a freshwater alga *Ochromonas danica*. *PLOS ONE* 5(12).
- Miao AJ, Schwehr KA, Xu C, Zhang SJ, Luo ZP, Quigg A, Santschi PH. 2009. The algal toxicity of silver engineered nanoparticles and detoxification by exopolymeric substances. *Environmental Pollution* 157(11): 3034-3041.
- Minshall GW. 1978. Autotrophy in stream ecosystems. *BioScience* 28(12): 767-771.
- Mirzajani F, Ghassempour A, Aliahmadi A, Esmaeili MA. 2011. Antibacterial effect of silver nanoparticles on *Staphylococcus aureus*. *Research in Microbiology* 162(5): 542-549.
- Morones JR, Elechiguerra JL, Camacho A, Holt K, Kouri JB, Ramirez JT, Yacaman MJ. 2005. The bactericidal effect of silver nanoparticles. *Nanotechnology* 16(10): 2346-2353.
- Musee N, Oberholster PJ, Sikhivihilu L, Botha AM. 2010. The effects of engineered nanoparticles on survival, reproduction, and behaviour of freshwater snail, *Physa acuta* (Draparnaud, 1805). *Chemosphere* 81(10): 1196-1203.
- Muyzer G, De Waal EC, Uitterlinden AG. 1993. Profiling of complex microbial populations by denaturing gradient gel electrophoresis analysis of polymerase chain reaction-amplified genes coding for 16S rRNA. *Applied and Environmental Microbiology* 59(3): 695-700.

- Muyzer G, Smalla K. 1998. Application of denaturing gradient gel electrophoresis (DGGE) and temperature gradient gel electrophoresis (TGGE) in microbial ecology. *Antonie Van Leeuwenhoek* 73(1): 127-141.
- Navarro E, Baun A, Behra R, Hartmann NB, Filser J, Miao AJ, Quigg A, Santschi PH, Sigg L. 2008a. Environmental behavior and ecotoxicity of engineered nanoparticles to algae, plants, and fungi. *Ecotoxicology* 17(5): 372-386.
- Navarro E, Piccapietra F, Wagner B, Marconi F, Kaegi R, Odzak N, Sigg L, Behra R. 2008b. Toxicity of silver nanoparticles to *Chlamydomonas reinhardtii*. *Environmental Science & Technology* 42(23): 8959-8964.
- Navarro E, Robinson CT, Behra R. 2008c. Increased tolerance to ultraviolet radiation (UVR) and cotolerance to cadmium in UVR-acclimatized freshwater periphyton. *Limnology and Oceanography* 53(3): 1149-1158.
- Navarro E, Robinson CT, Wagner B, Behra R. 2007. Influence of ultraviolet radiation on UVR-absorbing compounds in freshwater algal biofilms and *Scenedesmus vacuolatus* cultures. *Journal of Toxicology and Environmental Health A* 70(9): 760-767.
- Neely RK, Wetzel RG. 1995. Simultaneous use of  $^{14}\text{C}$  and  $^3\text{H}$  to determine autotrophic production and bacterial protein production in periphyton. *Microbial Ecology* 30(3): 227-237.
- Newton KM, Puppala HL, Kitchens CL, Colvin VL, Klaine SJ. 2013. Silver nanoparticle toxicity to *Daphnia magna* is a function of dissolved silver concentration. *Environmental Toxicology and Chemistry* 32(10): 2356-2364.
- Odzak N, Kistler D, Behra R, Sigg L. 2014. Dissolution of metal and metal oxide nanoparticles in aqueous media. *Environmental Pollution* 191(0): 132-138.
- Oliver ALS, Croteau MN, Stoiber TL, Tejamaya M, Römer I, Lead JR, Luoma SN. 2014. Does water chemistry affect the dietary uptake and toxicity of silver nanoparticles by the freshwater snail *Lymnaea stagnalis*? *Environmental Pollution* 189: 87-91.
- Pal S, Tak YK, Song JM. 2007. Does the antibacterial activity of silver nanoparticles depend on the shape of the nanoparticle? A study of the gram-negative bacterium *Escherichia coli*. *Applied and Environmental Microbiology* 73(6): 1712-1720.
- Peulen TO, Wilkinson KJ. 2011. Diffusion of nanoparticles in a biofilm. *Environmental Science & Technology* 45(8): 3367-3373.
- Piccapietra F, Allué CG, Sigg L, Behra R. 2012a. Intracellular silver accumulation in *Chlamydomonas reinhardtii* upon exposure to carbonate coated silver nanoparticles and silver nitrate. *Environmental Science & Technology* 46(13): 7390-7397.
- Piccapietra F, Sigg L, Behra R. 2012b. Colloidal stability of carbonate-coated silver nanoparticles in synthetic and natural freshwater. *Environmental Science & Technology* 46(2): 818-825.
- Pillai S, Behra R, Nestler H, Suter MJ-F, Sigg L, Schirmer K. 2014. Linking toxicity and adaptive responses across the transcriptome, proteome, and phenotype of *Chlamydomonas reinhardtii* exposed to silver. *PNAS* 111(9): 3490-3495.
- Potara M, Jakab E, Damert A, Popescu O, Canpean V, Astilean S. 2011. Synergistic antibacterial activity of chitosan-silver nanocomposites on *Staphylococcus aureus*. *Nanotechnology* 22(13).

- Pradhan A, Seena S, Pascoal C, Cássio F. 2011. Can metal nanoparticles be a threat to microbial decomposers of plant litter in streams? *Microb Ecol* 62(1): 58-68.
- Prasad MNV, Drej K, Skawińska A, Strałka K. 1998. Toxicity of cadmium and copper in *Chlamydomonas reinhardtii* wild-type (wt 2137) and cell wall deficient mutant strain (cw 15). *Bulletin of Environmental Contamination and Toxicology* 60(2): 306-311.
- R Core Team. 2014. R: A language and environment for statistical computing. Vienna, Austria: R Foundation for Statistical Computing.
- Rainville LC, Carolan D, Varela AC, Doyle H, Sheehan D. 2014. Proteomic evaluation of citrate-coated silver nanoparticles toxicity in *Daphnia magna*. *Analyst* 139(7): 1678-1686.
- Ramelow GJ, Maples RS, Thompson RL. 1987. Periphyton as monitors for heavy metal pollution in the Calcasieu river estuary. *Environmental Pollution* 43(4): 247-261.
- Ratte HT. 1999. Bioaccumulation and toxicity of silver compounds: A review. *Environmental Toxicology and Chemistry* 18(1): 89-108.
- Ribeiro F, Gallego-Urrea JA, Goodhead RM, Van Gestel CAM, Moger J, Soares AMVM, Loureiro S. 2015. Uptake and elimination kinetics of silver nanoparticles and silver nitrate by *Raphidocelis subcapitata*: The influence of silver behaviour in solution. *Nanotoxicology* DOI:10.3109/17435390.2014.963724.
- Ribeiro F, Gallego-Urrea JA, Jurkschat K, Crossley A, Hassellöv M, Taylor C, Soares AMVM, Loureiro S. 2014. Silver nanoparticles and silver nitrate induce high toxicity to *Pseudokirchneriella subcapitata*, *Daphnia magna* and *Danio rerio*. *Science of the Total Environment* 466-467(0): 232-241.
- Ringwood AH, McCarthy M, Bates TC, Carroll DL. 2010. The effects of silver nanoparticles on oyster embryos. *Marine Environmental Research* 69: S49-S51.
- Ritz C, Streibig JC. 2005. Bioassay analysis using R. *Journal of Statistical Software* 12(5).
- Romaní AM, Guasch H, Muñoz I, Ruana J, Vilalta E, Schwartz T, Emtiazi F, Sabater S. 2004. Biofilm structure and function and possible implications for riverine DOC dynamics. *Microbial Ecology* 47(4): 316-328.
- Römer I, White TA, Baalousha M, Chipman K, Viant MR, Lead JR. 2011. Aggregation and dispersion of silver nanoparticles in exposure media for aquatic toxicity tests. *Journal of Chromatography A* 1218(27): 4226-4233.
- Rooney JPK. 2007. The role of thiols, dithiols, nutritional factors and interacting ligands in the toxicology of mercury. *Toxicology* 234(3): 145-156.
- Sabater S, Guasch H, Ricart M, Romaní A, Vidal G, Klünder C, Schmitt-Jansen M. 2007. Monitoring the effect of chemicals on biological communities. The biofilm as an interface. *Anal Bioanal Chem* 387(4): 1425-1434.
- Samberg ME, Orndorff PE, Monteiro-Riviere NA. 2011. Antibacterial efficacy of silver nanoparticles of different sizes, surface conditions and synthesis methods. *Nanotoxicology* 5(2): 244-253.

- Schauer M, Balagué V, Pedrós-Alió C, Massana R. 2003. Seasonal changes in the taxonomic composition of bacterioplankton in a coastal oligotrophic system. *Aquatic Microbial Ecology* 31(2): 163-174.
- Schaumann GE, Philippe A, Bundschuh M, Metreveli G, Klitzke S, Rakcheev D, Grün A, Kumahor SK, Kühn M, Baumann T, Lang F, Manz W, Schulz R, Vogel H-J. 2015. Understanding the fate and biological effects of ag- and TiO<sub>2</sub>-nanoparticles in the environment: The quest for advanced analytics and interdisciplinary concepts. *Science of the Total Environment*. DOI:10.1016/j.scitotenv.2014.10.035.
- Scheidegger C, Suter MJF, Behra R, Sigg L. 2012. Characterization of lead-phytochelatin complexes by nano-electrospray ionization mass spectrometry. *Frontiers in Microbiology* 3: 41.
- Schreiber U. 1998. Chlorophyll fluorescence: New instruments for special applications. In: Garab G, editor. *Photosynthesis: Mechanisms and effects*. Dordrecht: Kluwer Academic Publishers. p 4253-4258.
- Scott JT, Back JA, Taylor JM, King RS. 2008. Does nutrient enrichment decouple algal-bacterial production in periphyton? *Journal of the North American Benthological Society* 27(2): 332-344.
- Seitz F, Rosenfeldt RR, Storm K, Metreveli G, Schaumann GE, Schulz R, Bundschuh M. 2015. Effects of silver nanoparticle properties, media pH and dissolved organic matter on toxicity to *Daphnia magna*. *Ecotoxicology and Environmental Safety* 111(0): 263-270.
- Serra A, Corcoll N, Guasch H. 2009. Copper accumulation and toxicity in fluvial periphyton: The influence of exposure history. *Chemosphere* 74(5): 633-641.
- Sigg L, Behra R, Groh K, Isaacson C, Odzak N, Piccapietra F, Röhder L, Schug H, Yue Y, Schirmer K. 2014. Chemical aspects of nanoparticle ecotoxicology. *CHIMIA International Journal for Chemistry* 68(11): 806-811.
- Smith EM, Del Giorgio PA. 2003. Low fractions of active bacteria in natural aquatic communities? *Aquatic Microbial Ecology* 31(2): 203-208.
- Sogin ML, Gunderson JH. 1987. Structural diversity of eukaryotic small subunit ribosomal rnsa. *Annals of the New York Academy of Sciences* 503(1): 125-139.
- Soldo D, Behra R. 2000. Long-term effects of copper on the structure of freshwater periphyton communities and their tolerance to copper, zinc, nickel and silver. *Aquat Toxicol* 47(3-4): 181-189.
- Solioz M, Odermatt A. 1995. Copper and silver transport by CopB-ATPase in membrane vesicles of *Enterococcus hirae*. *Journal of Biological Chemistry* 270(16): 9217-9221.
- Sondi I, Salopek-Sondi B. 2004. Silver nanoparticles as antimicrobial agent: A case study on *E. coli* as a model for gram-negative bacteria. *Journal of Colloidal Interface Science* 275(1): 177-182.
- Sørensen T. 1948. A method of establishing groups of equal amplitude in plant sociology based on similarity of species and its application to analyses of the vegetation on Danish commons. *Kongelige Danske Videnskabernes Selskab* 5(4): 1-34.
- Sotiriou GA, Pratsinis SE. 2010. Antibacterial activity of nanosilver ions and particles. *Environmental Science and Technology* 44(14): 5649-5654.

- Stewart TJ, Behra R, Sigg L. 2015. Impact of chronic lead exposure on metal distribution and biological effects to periphyton. *Environmental Science & Technology* 49(8): 5044-5051.
- Sun TY, Gottschalk F, Hungerbühler K, Nowack B. 2014. Comprehensive probabilistic modelling of environmental emissions of engineered nanomaterials. *Environmental Pollution* 185(0): 69-76.
- Tan KS, Cheong KY. 2013. Advances of Ag, Cu, and Ag-Cu alloy nanoparticles synthesized via chemical reduction route. *Journal of Nanoparticle Research* 15: 1537.
- Tappin AD, Barriada JL, Braungardt CB, Evans EH, Patey MD, Achterberg EP. 2010. Dissolved silver in european estuarine and coastal waters. *Water Research* 44(14): 4204-4216.
- Ter Braak C, Smilauer P. 1998. CANOCO reference manual and user's guide to CANOCO for Windows: Software for canonical community ordination (version 4.5). Microcomputer Power, Ithaca, NY.
- Terhaar CJ, Ewell WS, Dziuba SP. 1977. A laboratory model for evaluating the behavior of heavy metals in an aquatic environment. *Water Research* 11(1): 101-110.
- Thalmann B, Voegelin A, Sinnet B, Morgenroth E, Kaegi R. 2014. Sulfidation kinetics of silver nanoparticles reacted with metal sulfides. *Environmental Science & Technology* 48(9): 4885-4892.
- Thuptimdang P, Limpiyakorn T, McEvoy J, Prüß BM, Khan E. 2015. Effect of silver nanoparticles on *Pseudomonas putida* biofilms at different stages of maturity. *Journal of Hazardous Materials* 290(0): 127-133.
- Tlili A, Bérard A, Roulier JL, Volat B, Montuelle B. 2010. PO<sub>4</sub><sup>3-</sup> dependence of the tolerance of autotrophic and heterotrophic biofilm communities to copper and diuron. *Aquatic Toxicology* 98(2): 165-177.
- Tlili A, Marechal M, Montuelle B, Volat B, Dorigo U, Bérard A. 2011. Use of the MicroResp™ method to assess pollution-induced community tolerance to metals for lotic biofilms. *Environmental Pollution* 159(1): 18-24.
- Topuz E, Sigg L, Talinli I. 2014. A systematic evaluation of agglomeration of Ag and TiO<sub>2</sub> nanoparticles under freshwater relevant conditions. *Environmental Pollution* 193(0): 37-44.
- Uehlinger U, König C, Reichert P. 2000. Variability of photosynthesis-irradiance curves and ecosystem respiration in a small river. *Freshwater Biology* 44(3): 493-507.
- Völker C, Boedicker C, Daubenthaler J, Oetken M, Oehlmann J. 2013. Comparative toxicity assessment of nanosilver on three *Daphnia* species in acute, chronic and multi-generation experiments. *PLOS ONE* 8(10): e75026.
- Ward JE, Kach DJ. 2009. Marine aggregates facilitate ingestion of nanoparticles by suspension-feeding bivalves. *Marine Environmental Research* 68(3): 137-142.
- Werlin R, Priester JH, Mielke RE, Krämer S, Jackson S, Stoimenov PK, Stucky GD, Cherr GN, Orias E, Holden PA. 2011. Biomagnification of cadmium selenide quantum dots in a simple experimental microbial food chain. *Nature Nanotechnology* 6(1): 65-71.
- Wetzel RG. 1963. Primary productivity of periphyton. *Nature* 197(4871): 1026-1027.

- Wigginton NS, De Titta A, Piccapietra F, Dobias J, Nesatty VJ, Suter MJF, Bernier-Latmani R. 2010. Binding of silver nanoparticles to bacterial proteins depends on surface modifications and inhibits enzymatic activity. *Environmental Science & Technology* 44(6): 2163-2168.
- Xiu Z-m, Zhang Q-b, Puppala HL, Colvin VL, Alvarez PJJ. 2012. Negligible particle-specific antibacterial activity of silver nanoparticles. *Nano Letters* 12(8): 4271-4275.
- Xiu ZM, Ma J, Alvarez PJJ. 2011. Differential effect of common ligands and molecular oxygen on antimicrobial activity of silver nanoparticles versus silver ions. *Environmental Science and Technology* 45(20): 9003-9008.
- Yoo-iam M, Chaichana R, Satapanajaru T. 2014. Toxicity, bioaccumulation and biomagnification of silver nanoparticles in green algae (*Chlorella sp.*), water flea (*Moina macrocopa*), blood worm (*Chironomus spp.*) and silver barb (*Barbonymus gonionotus*). *Chemical Speciation and Bioavailability* 26(4): 257-265.
- Zaldibar B, Rodrigues A, Lopes M, Amaral A, Marigómez I, Soto M. 2006. Freshwater molluscs from volcanic areas as model organisms to assess adaptation to metal chronic pollution. *Science of the Total Environment* 371(1-3): 168-175.
- Zhang D, Lee D-J, Pan X. 2012. Fluorescent quenching for biofilm extracellular polymeric substances (EPS) bound with Cu(II). *Journal of the Taiwan Institute of Chemical Engineers* 43(3): 450-454.
- Zhao C-M, Wang W-X. 2011. Comparison of acute and chronic toxicity of silver nanoparticles and silver nitrate to *Daphnia magna*. *Environmental Toxicology and Chemistry* 30(4): 885-892.
- Zhao C-M, Wang W-X. 2012. Size-dependent uptake of silver nanoparticles in *Daphnia magna*. *Environmental Science & Technology* 46(20): 11345-11351.
- Zhao CM, Wang WX. 2010. Biokinetic uptake and efflux of silver nanoparticles in *Daphnia magna*. *Environmental Science & Technology* 44(19): 7699-7704.
- Zubrod JP, Feckler A, Englert D, Koksharova N, Rosenfeldt RR, Seitz F, Schulz R, Bundschuh M. 2015. Inorganic fungicides as routinely applied in organic and conventional agriculture can increase palatability but reduce microbial decomposition of leaf litter. *Journal of Applied Ecology* 52(2): 310-322.

# Acknowledgements

I am most grateful to my two supervisors, Renata Behra and Kristin Schirmer, for giving me the opportunity to conduct the research comprised in this thesis. I really appreciate all your hard work, support and encouragement, which has been crucial both for the completion of this thesis and for my development as a scientist. I am thankful to Profs. Mirco Bundschuh, Vera I. Slaveykova, Rizlan Bernier-Latmani, and Urs von Gunten, for kindly accepting to be members of my committee and taking the time to evaluate this thesis.

I would like to express my gratitude to Ahmed Tlili, for the continuous support and helpful discussions, as well as for the French translation of the summary of this thesis. I am very grateful to Mark O. Gessner, for making time for discussions, and all the helpful feedback and insight. I also appreciate all the discussions and advice from Laura Sigg, Marc Suter, Smitha Pillai, Yang Yue and Xiaomei Li.

Thanks to my colleagues working with periphyton, Alexandra Kroll, Thea Stewart and Linn Sgier, for all the support on the colonization system, as well as to all the people who helped me to scrape periphyton during the experiments. I am also grateful to Jukka Jokela, for suggesting a snail species suitable for our setup, and to Ilaria Mignola, Kirsten Klappert and Anja Buerkli for the help and advice for the starting of the snail batch culture.

A big thank you to David Kistler, for all the ICP-MS measurements and his constant good humor. I am also very thankful to Muris Korkaric, for being a great colleague and all the help with setting up the HPLC protocol, and to Anže Županič, for the analysis of non-monotonic concentration-responses in R.

I would like to thank all my colleagues at the department of Environmental Toxicology (Utox) at Eawag for creating such a stimulating and familiar environment. In particular, a big thank you goes to my officemates from BU-E08: Katrin Tanneberger, Carl Isaacson, Emel Topuz, Anni Nyman, Anke Hofacker, Julita Stadnicka-Michalak, Isabel Oliveira, Ahmed Tlili, and Hannah Schug. Thank you for making our office so lively and all the laughs.

I am thankful to the Swiss National Science Foundation for the financial support, and for creating an amazing network of researchers working in different fields of nanotechnology through the National Research Programme 64 "Opportunities and Risks of Nanomaterials".

My gratitude goes to my family, for always being supportive, even when it meant that I would be far away. *Muchas gracias a mi familia por todo vuestro apoyo, incluso cuando haya significado que vaya a estar lejos.* A special thank you goes to Anders, for being amazingly supportive and encouraging, and to Sini the cat, for all the shared study hours during the past eight years.





# Curriculum Vitae

**Carmen Omayra Gil Allué**

Born on August 21, 1986, in Huesca, Spain.

- 2011 - 2015     **Doctoral Program in Civil and Environmental Engineering**  
École Polytechnique Fédérale de Lausanne, Switzerland.  
Eawag: Swiss Federal Institute of Aquatic Science and Technology, Switzerland.  
Thesis title: Silver nanoparticle effects on simple stream food webs and ecosystem processes: Periphyton-grazer system.
- 2009 - 2011     **M.Sc. in General Toxicology and Environmental Health Risk Assessment**  
University of Eastern Finland.  
Eawag: Swiss Federal Institute of Aquatic Science and Technology, Switzerland.  
Thesis title: Uptake and toxicity of engineered silver nanoparticles to a cell wall free mutant of *Chlamydomonas reinhardtii*.
- 2009             **Research Assistant**  
University of Eastern Finland and University of Oulu, Finland.
- 2004 - 2009     **Degree in Environmental Science**  
Autonomous University of Madrid, Spain.
- 1997 - 2004     **High school**  
I.E.S. San Alberto Magno, Sabiñánigo, Spain.